The University of Nottingham

UNITED KINGDOM · CHINA · MALAYSIA

On Design and Simulation of Passive Damping Solutions for Milling of Thin-walled Parts

Kiran V S S Kolluru

M.Tech

Thesis submitted to the University of Nottingham for the degree of Doctor of Philosophy

Department of Mechanical, Materials, and Manufacturing Engineering

April 2014

Abstract

Machining of thin wall structures is a challenging area due to the problems such as chatter and forced vibrations that arise due to low stiffness of such structures. Up to now, most of the research was driven by need to improve productivity in manufacturing of aircraft components such as airframe panels; hence, straight thin walls such as cantilever structures were considered for research in machining dynamics. However, thin wall casings and particularly thin wall assemblies that are encountered in jet engine casings are not well studied. Not only their dynamics is quite different from that of straight thin walls, they present a different set of challenges for fixturing to minimise machining vibrations such as presence of multiple internal parts (e.g. vanes, plumbing lines, etc.).

Hence, there is a two-fold need of research: (i) to understand the effect of dynamics of thin wall casings on interaction of tool and workpiece and (ii) to design and validate damping solutions to minimise machining vibrations in such structures.

In this work, both the above objectives are addressed. Initially a coupled dynamic interaction of tool and workpiece is studied through experimental analysis of machining vibration signal. This study was carried out both on a straight thin wall cantilever and on a thin wall casing to present the effect of variation of dynamics on dynamic coupling between tool and workpiece. Dynamic response tests were carried out on individual elements such as tool and workpiece and then the machining

vibration signal was analysed in frequency and time-frequency domain to see which of the elements are dominant during the machining process. Such an analysis was not performed earlier and hence the effective coupled dynamic interaction was not studied. In this work, interesting observations such as participation of tool's bending and torsional mode and their dependence on depth of cut were noticed.

For providing fixturing solutions to minimise machining vibrations, initially tuned mass dampers were studied. In literature they were employed on rigid workpieces, but not on thin wall structures. Tuned dampers with increased mass ratio were studied to see their effect in minimising vibrations. Subsequently, two novel surface damping solutions - viscoelastic based surface damper and torsion spring fixture - were proposed and validated experimentally. The design philosophy behind both these solutions is to improve mass and stiffness of the casing in addition to imparting damping to it. Experimental validations of both the concepts were carried out in terms of root mean square value of the vibration signal and also the effect of damping solution on coupled dynamic interaction. Finite element modelling was carried out to predict the dynamic response without and with proposed solutions. Experimental validation of the responses through impact hammer testing showed the maximum error in prediction is 9%.

The current study provides a scientific understanding of dynamic interaction between tool and thin wall workpiece and shows how this knowledge can then be used to identify a suitable damping solution.

Publications originating from the thesis

The research in this thesis has contributed in part or full for the following publications:

[1] **K. Kolluru** and D. Axinte, "Coupled interaction of dynamic responses of tool and workpiece in thin wall milling," *J. Mater. Process. Technol.*, vol. 213, pp. 1565–1574, 2013.

[2] **K. V. Kolluru**, D. A. Axinte, M. H. Raffles, and A. A. Becker, "Vibration suppression and coupled interaction study in milling of thin wall casings in presence of tuned mass dampers," *Proc. Inst. Mech. Eng. Part B J. Eng. Manuf.*, Nov. 2013.

[3] **K. Kolluru**, D. Axinte, and A. Becker, "A solution for minimising vibrations in milling of thin walled casings by applying dampers to workpiece surface," *CIRP Ann. - Manuf. Technol.*, vol. 62, no. 1, pp. 415–418, Jan. 2013.

[4] M. H. Raffles, **K. Kolluru**, D. Axinte, and H. Llewellyn-Powell, "Assessment of adhesive fixture system under static and dynamic loading conditions," *Proc. Inst. Mech. Eng. Part B J. Eng. Manuf.*, vol. 227, no. 2, pp. 267–280, Feb. 2013.

[5] D. Axinte, P. Butler-Smith, C. Akgun, and **K. Kolluru**, "On the influence of single grit micro-geometry on grinding behavior of ductile and brittle materials," *Int. J. Mach. Tools Manuf.*, vol. 74, pp. 12–18, Nov. 2013.

Patent:

[1] **K. Kolluru**, S. Lowth, D. Axinte, and M. Raffles, "A reconfigurable fixture for damping circular and non-circular thin wall components," Filed by Rolls-Royce, 2014.

Acknowledgements

My parents are real inspiration for me to do this PhD. So all the credit of effort I had put into this work goes to them and their loving support.

First of all, I would like to sincerely thank the most important person who made me to realise this goal of PhD - my principal supervisor Prof Dragos Axinte. He supported me in all matters, right from technical inputs and discussions, publishing scientific papers, to funding issues. Without his motivation and dedicated support, this work would not have been successful. I would also like to thank my co-supervisors Dr Mark Raffles and Prof Adib Becker for reviewing my work and participating in technical discussions and thank Prof Becker for providing NAFEMS publications.

I would like to thank my industrial supervisor and UTC coordinator from Rolls-Royce, Mr Peter Winton, who is always supportive and had put me in contact with various experts from Rolls-Royce to clarify my doubts.

I thank Rolls-Royce and EPSRC for providing funding for this research under Dorothy Hodgkin Postgraduate Award scholarship.

I would like to thank UTC Manufacturing Lab Technical Staff, Mr Stuart Branston, Mr Mark Daine, and Mr Geoff Bexon for supporting experimental activities in this work.

Doing research for 3 years in non-native country is a challenge and I thank my friends SivaSrinivas and Sailesh for giving me some good time off work. I also appreciate friendly support provided by all MCM group members and staff.

Table of contents

List of Figures

List of Tables

1 Introduction

1.1 Background

Aerospace manufacturing is gaining prominence since last few years with the increase in air traffic all over the world and particularly in developing countries. A recent survey [1] shows that in the next twenty years the air traffic growth is poised to increase by 4.7% annually, as shown in Figure 1-1. This directly translates to projected requirement of 28,200 aircraft (including both passenger and freight) by 2031. This presents an opportunity to both the aircraft and engine manufacturers to rise up to this challenge through improved and efficient processes and operations management.

In the engine manufacturers three of the most important players are: General Electric, Rolls-Royce, and Pratt & Whitney. The above mentioned volume requirements for aircraft corresponds to an order book for Rolls-Royce with their production of engines to be doubled in the next 10 years [2]. In addition to meeting these volume requirements of the engines the companies also have to offer a product variety catering to different sectors of the aircraft industry. To meet these challenges of productivity and innovation, Rolls-Royce is focussing to reduce the non-value added manufacturing time and minimising the part rejections.

One of the common manufacturing problems which results in significant scrap or rework is the machining chatter. It is widely known that most of

the jet engine structures are thin wall casings. During finish machining operations, these casings are prone to significant vibrations leading to chatter marks. These chatter marks not only result in poor surface finish, thus compromising fatigue life of the component [3]–[5], but also results in reduced machining accuracy, reduced cutting tool life, increased wear of machine tool spindle bearings [6]. To improve the fatigue life of the component, the chatter marks are generally removed post-machining through hand finishing operations till the machining surfaces meet the specified functional requirements. However for critical applications such as jet engine components, the machining parameters are reduced to avoid formation of such chatter marks. In either case this results in reduced productivity and increases the delivery lead time of the component for downstream engine assembly operations.

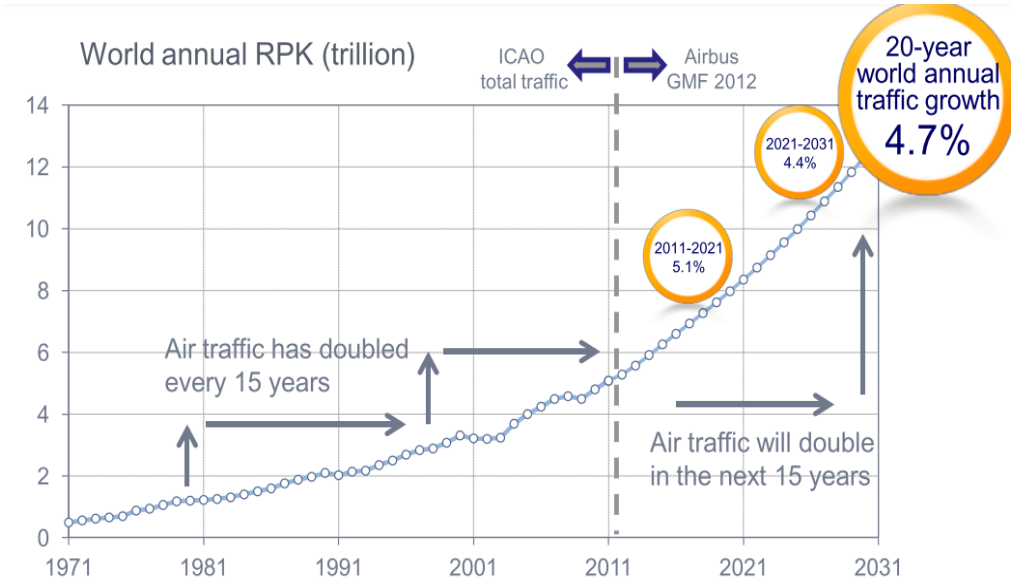

Figure 1-1 Air traffic growth as per Airbus Global Market Forecast [1]

Considering its importance towards part quality and productivity chatter was studied by many researchers and different mechanisms were proposed in understanding it such as regenerative chatter and mode coupling [7]. Methodologies were proposed to find chatter free machining parameters such as spindle speed and depth of cut using well known stability charts. A typical stability chart is shown in Figure 1-2. These charts depict the variation of axial depth of cut with respect to the spindle speed. The underlying concept of these charts is that the machining is stable and hence more depth of cut can be given at certain spindle speeds which are close to the cutting tooth frequency. Matching of the spindle speed with that of the cutting tooth frequency ensures uniform chip thickness and hence avoids chatter. Though these charts were not very accurate in predicting the chatter free parameters, due to various reasons such as process damping, dependence of cutting constants on depth of cut and feed, and variation in dynamic response due to spindle rotation, they give reasonable estimates to start with. Some commercial software such as CUTPRO® and MetalMax® are available which can predict such stability charts given the inputs of cutting mechanics (cutting constants, tool geometry, etc.) and dynamics of machine tool system in the form of tool tip dynamic response.

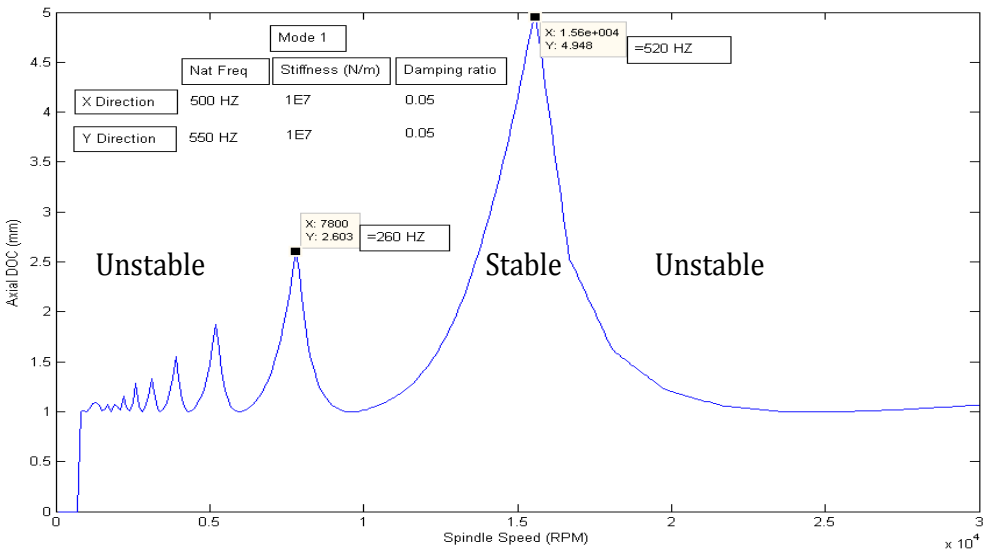

Figure 1-2 Stability charts showing stable and unstable machining zones

Machining of thin wall workpieces brings in an additional factor of workpiece dynamics into these predictions. The difficulty in considering the workpiece dynamics is its variation along the whole machining zone and also its variation due to continuous material removal during machining. To account for these variations some researchers have suggested measuring responses at different locations of the workpiece and also at different stages of machining. The end result is shown in the form of 3D stability charts with the third axis corresponding to either position on the workpiece or the stages of machining. Obviously this is a very tedious task and prone to significant approximations. Moreover this methodology can be applied only for simple geometries such as thin cantilever. For complex structures such as thin wall casing having intermittent machining operations this procedure is difficult to apply. It is for these reasons that chatter avoidance or vibration minimisation while machining thin wall workpieces is mostly addressed through fixturing

solutions. Traditionally the fixturing solutions that were researched have taken the route of damping the workpiece to minimise the vibrations. While most of the damping solutions researched were focussed on machine-tool system vibrations rather than workpiece, the recent increase in light weight structures along with the feasibility to machine them in single piece using High Speed Machining is making damping of workpiece vibrations more relevant. As far as damping thin wall workpieces is concerned, only research into particle dampers and piezoelectric damping was reported on simple straight cantilever workpieces. While these straight cantilever geometries have appeal towards real life structures such as airframe parts (e.g: fuselage panels, ribs, etc.) other class of thin wall structures such as jet engine casings which have closed cylindrical geometry were not researched. As explained previously the increase in the number of jet engines over next 20 years requires an improvement in productivity while maintaining quality. This necessitates an in-depth understanding of the machining dynamics of such structures while also evaluating suitable damping solutions for mitigating vibrations during machining.

1.2 Problem definition

Damping of machining vibrations is crucial not only to improve surface finish of workpiece and thereby part life but also to increase life of cutting tools and machine tool spindle. The importance of workpiece surface quality is more relevant in critical applications such as jet engine structures. Previous studies have come out with various machining

strategies for thin wall structures such as alternate step machining etc. to maintain and make use of part rigidity while machining. These are useful while machining individual components. But most of the jet engine casings need assembly operations through welding (electron beam welding, for example) which cause weld induced distortion. To enable accurate alignment of parts for downstream assembly operations, the mating datum features must be re-machined to remove this weld distortion. And generally small amount of finish stock is left on these features for this purpose. In this situation there is no sufficient material available for following the above strategies and moreover the thin shells which are welded are prone to significant vibration. Considering that the assembly is in the final stages of manufacturing, significant value addition has already taken place and any damage occurring to the assembly in the form of chatter or other vibration induced dimensional error will be very costly and may result in scrapping of the whole assembly. One example for this is shown in Figure 1-3 which shows a Front Bearing Housing (FBH) of Trent 900 engine of Rolls-Royce. As can be seen from figure the top Rear Outer Casing (ROC) is electron beam welded to Ring of Vanes along the periphery. The bosses on ROC have a finish allowance to be removed post welding. While machining these bosses the whole assembly vibrates and hence leads to poor surface finish.

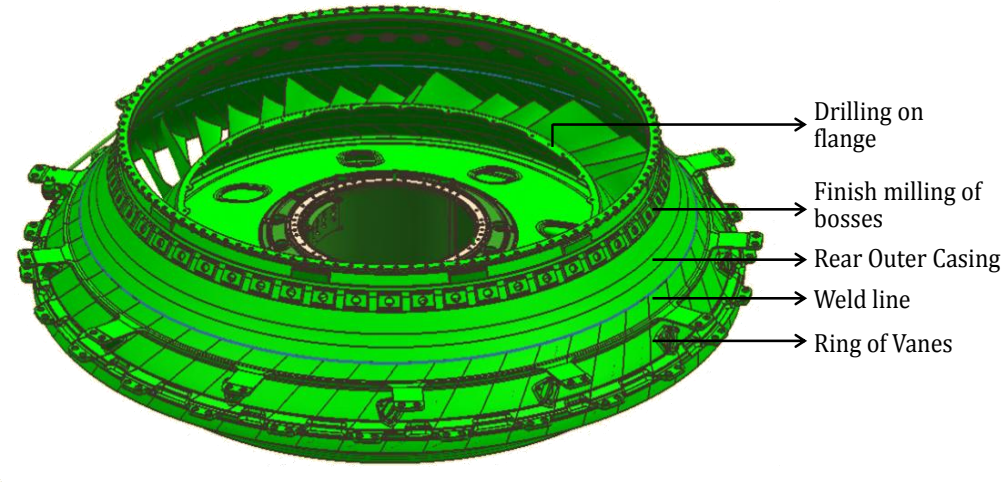

Figure 1-3 Front Bearing Housing assembly of Trent 900 and needed finish machining operations

One of the major constraints in these kinds of requirements is the necessity for adequate space, after mounting the fixture, to allow for multiple machining operations in same setup. For example in Figure 1-3, the FBH assembly needs drilling operation on the central flange along with the finish milling of bosses. This means the central hub cannot be covered while deploying the damping fixture or solution.

While this FBH is only one example there are similar such casings in jet engine, for example, high pressure / intermediate pressure casings, combustion casings, and intercase structures all of which have similar requirements and constraints. Hence in addition to evaluating a suitable damping solution for these types of structures, a thorough understanding of the involved dynamic interaction is essential. Very little work was reported on the interaction between tool and workpiece dynamic responses in thin wall milling. This knowledge is useful in understanding not only the dominant frequency component (tool or workpiece) in the

measured responses but also in deducing conclusions on dynamic interaction mechanism of damping solution and in evaluating its effectiveness.

1.3 Aims and objectives

1.3.1 Aim of the work

This research is directed to understand and explain the scientific issues related to coupled interaction of dynamic response of tool and workpiece and how it varies with different types of workpiece geometries. This work also tries to utilise this knowledge in evaluating the variation in this dynamic interaction with the mounting of damping solution on workpiece. A finite element model of workpiece along with the proposed damping solution is developed to predict the dynamic response under impact kind of loading - a first step in developing a fully coupled dynamic model for machining simulations.

1.3.2 Objectives of the research

1. Understand the coupled dynamic interaction between tool and thin wall workpiece. The variation in such a coupled interaction for straight (open) geometries and circular (closed) geometries is studied. This study will highlight the dominant modes that are participating in the machining vibration.
2. Design and evaluate tuned mass dampers for the dominant modes found in the coupled interaction study. Effectiveness of dampers over different machining parameters will also be studied. This

study enables to evaluate the sufficiency of tuned mass dampers while at the same time presents the coupled dynamic interaction variation due to the mounted tuned dampers.

3. Design and evaluate surface damping solution to minimise the machining vibration. The effectiveness of damping as well as the coupled dynamic interaction in the presence of surface damper will be studied
4. Model the above studied solutions in finite element and predict the dynamic response and compare it against experimental tap testing response. This will not only provide a model for further optimisation studies of proposed and other surface damping solutions, but also acts as a base model for incorporating coupled dynamic interaction between tool and workpiece.

1.3.3 Structure of the thesis

Chapter 2 presents a detailed literature review on the machining dynamics focussing more on the thin wall machining. Various passive and active damping solutions studied by previous researchers and the methodologies they used to evaluate them were reviewed in detail. The identified research gaps were then highlighted.

Chapter 3 presents the experimental set up and research methodology used in all the experiments in this research work. This includes a detail description of the machine tool and tooling used, sensor measurement chain employed, and data acquisition system. Finally this chapter describes the methodology used to evaluate coupled dynamic interaction

between tool and workpiece. While Chapter 3 is specifically devoted to explain this concept and the novel findings thereof, a specific explanation of methodology is given in this chapter as it is commonly used to define the effectiveness of various damping solutions proposed

Chapter 4 details the studies conducted to identify the coupled dynamic response interaction between tool and workpiece. The methodology and the measurement chain utilised to study this coupled interaction are explained. While the main focus of this work is on damping vibrations in thin wall casings, to understand the differences in dynamic response, initial experiments were conducted on a straight thin wall and the results presented. Then the experiments on test casing are explained along with an explanation for the observed variations in coupled response.

Chapter 5 presents finite element (FE) modelling of the test casing chosen to study the damping solutions. The FE predicted natural frequencies and harmonic response are then compared against the experimentally measured dynamic response on test casing and also mode shape comparison carried out through modal testing. Thus the accuracy of the FE modelled casing was evaluated.

Chapter 6 presents the rationale behind designing and testing the tuned mass dampers and the experiments carried out with them on the test casing. The quantified effectiveness of the dampers in minimising the vibration is presented with results. The variation in coupled interaction and observed consequences of this are then highlighted. FE modelling of

test casing with tuned dampers and prediction of the associated dynamic response and its experimental validation is also covered.

Chapter 7 highlights the necessity of surface dampers for thin wall casings and then presents a surface damping solution that was envisaged for minimising the machining vibrations. Experiments carried out with the proposed surface damping solution and its effectiveness are described. FE modelling of proposed surface damping solution along with the necessary characterisation of damping materials is explained. The predicted and measured dynamic responses are then compared and possible reasons for the observed variation are briefed.

Chapter 8 presents an innovative fixturing concept for surface damping, using torsion springs, and compared the measured dynamic response with the initially proposed surface damping solution. This study then highlights the importance of mass and stiffness addition in minimising vibration in thin wall machining.

Finally, **Chapter 9** presents the major conclusions and final remarks of this research work. It also highlights possible future directions in which this work can be extended and associated benefits of such a research.

1.3.4 Highlights and significant contributions of the thesis

This thesis possesses some key findings with regard to dynamic interaction between tool and thin wall workpiece and surface damping of thin wall casings. Following are the highlights of these findings.

1. The machining vibration in a thin wall workpiece is significantly dominated by cutting tool's modes. This is an important and novel finding and shows the dominance of forced vibration on a thin wall workpiece.
2. The type of tool's mode that couples with workpiece and becomes dominant during machining depends on the geometry of the workpiece. It is observed that for a straight geometry workpiece such as cantilever thin wall the tool bending mode is dominant; whereas for closed geometry workpiece such as cylindrical casing it is the torsional mode of the tool that is dominant.
3. It was observed that there is a relation between depth of cut and the modes that are participating in the machining vibration. Workpiece fundamental mode is found to participate along with tool's mode at lower depth of cut while tool's mode alone is dominant at higher depth of cut.
4. Tuned mass dampers that are tuned for workpiece fundamental mode are found to be effective in damping the targeted mode and also nearby workpiece modes with higher mass ratio tuned damper blocks. However due to inadequate surface area coverage, variation in workpiece vibration was noticed across the machining zone leading to thickness variation of machined workpiece wall.
5. The proposed surface damping solution with added stiffness and mass along with damping resulted in better reduction in vibration. This indicates the importance of improving mass and stiffness in addition to damping particularly in a forced vibration situation

such as thin wall machining where the tool's modes are dominant. This finding was further reinforced by observed dynamic response of another surface damping design - torsion spring fixture – which has more mass and stiffness contribution than damping and was found to be more effective than the first proposed solution.

Thus the work undertaken in this research highlighted the importance of tool-workpiece coupled interaction and also brought to attention the principles to be considered while designing a surface damping solution for thin wall casings.

2 Literature review

2.1 Introduction

Minimising the machining vibrations has been traditionally addressed through two approaches: analytical study of process to select optimum machining parameters and designing fixturing solutions. The first approach is through process mechanics and dynamics point of view where the machining parameters (feed, speed, depth of cut) are selected such that chatter is avoided. This approach is extensively researched and many algorithms developed in these researches are available in the form of commercial software such as CutPro® [8] and MetalMax® [9]. These software gained popularity in aerospace industries and inspired many SMEs to adopt High Speed Machining technology and improve productivity tremendously. While these algorithms are very useful for predicting stable cutting parameters in rigid workpieces, implementing them for machining low stiffness workpieces poses following problems:

1. Measuring dynamic response of workpiece accurately
2. Consideration of changing workpiece dynamics due to machining

Moreover, the research in this approach is mostly directed at simple structures such as thin wall. This is mainly to address productivity improvements in machining of aerospace aluminium structures such as fuselage panels, bulkheads, etc. However, thin wall machining also presents challenges in structures such as jet engine casings where the thin walled cylindrical features are common. Milling of thin walled cylindrical

structures is little researched, possibly due to the fact that turning is employed in most of the operations, which generally does not present machining dynamics problems except at very high cutting speeds. While simple cylindrical casings are generally machined by turning, finish machining of complex assemblies (to remove weld distortion, for example) and generation of prismatic features on casings requires milling operation. With the popularity of mill-turn centres increasing to reduce set up time and also to maintain relative geometric feature accuracy, milling on cylindrical casings is becoming more common. Milling is inherently an intermittent machining operation where cutting tooth impacts the workpiece periodically causing the dynamics of tool and workpiece to play a major role. Hence an understanding of dynamic interaction of tool and workpiece is more relevant in minimising the machining vibration.

Another challenge in thin wall machining is to minimise part deflection and thereby reduce the surface profile error. This aspect is addressed by proposing innovative machining strategies for thin wall and thin floor and also by simulating the milling process and proposing error compensation strategies. Process simulation and subsequent error compensation is a very useful tool during the process planning stage for choosing optimum machining parameters. However, this area is not matured enough for industrial application.

The second approach for addressing machining vibration problem is through designing appropriate fixturing solutions. Two main reasons that can be cited for adopting this approach are:

1. Significant deflection of workpiece during machining
2. Difficult to machine workpiece material such as titanium or superalloys (Inconel, etc.)

Generally aluminium structural components permit usage of higher machining speeds where the benefits of machining dynamics can be made use of – by generating stability lobes which indicate the selective spindle speeds where higher depths of cut can be given. In addition to higher depths of cut, higher spindle speeds allows faster feed rates which also add to improvement in productivity. However, for difficult to machine materials such as titanium or superalloys the cutting zone temperature limits the cutting speeds. At lower cutting speeds the available bandwidth of stability lobes is very narrow and the prediction is not accurate enough due to process damping effects. This makes it difficult to improve productivity by giving higher depths of cut without vibration. Fixturing solutions are applied in such cases. They can come as traditional mechanical fixtures or as scientifically designed damping solutions. While in the former, some innovative mechanical fixturing concepts are patented, the latter involves studying of piezoelectric damping, particle dampers, tuned mass dampers, etc. With this background, the literature pertaining to following areas will be reviewed and highlight the relevant previous contributions:

1. Process dynamics based chatter prediction with focus on thin wall geometry

2. Simulation and error compensation strategies in thin wall machining
3. Fixturing solutions for thin wall machining: (a) Mechanical fixtures (b) Damping solutions
4. Studies on dynamic interaction between workpiece and tool in machining

As the focus of this work is on studying the dynamic interaction of tool and workpiece and proposing appropriate damping solutions, the literature in the last two sections will be reviewed in detail. Finally, the identified research gaps will be presented along with the industrial relevance of such a research.

2.2 Process dynamics based chatter prediction in thin wall milling

Most of the research in chatter prediction was carried out on thin wall plates owing to its importance in airframe structures and electrode making in die for mould/die industry. However the interest in thin wall cylinders has driven research in thin wall cylinder turning. The literature in these two areas is described in the following two sections.

2.2.1 Milling of thin wall plates

Tobias and Fishwick [10] proposed initial chatter stability theory with the concept of dynamically varying chip thickness (regenerative chatter) in orthogonal cutting. Regenerative chatter theory creates a relationship between spindle speed and the critical chip width or depth of cut. This

relationship is then plotted in the form of a stability lobe diagram as shown in Figure 1-2 which shows the spindle speeds at which more depth of cut can be given thereby improving material removal rate (MRR). One of the major driving forces behind generating these stability lobes is the possibility of implementing High Speed Machining (HSM) in thin wall machining. And with the implementation of HSM, many thin wall assemblies which were fabricated previously by riveting sheet metal structures can be machined as integrally stiffened structures. Tlusty and Polacek [11] proposed oriented transfer function in the direction of resultant cutting force for dynamic forces and displacements. Both these theories yield inaccurate results for oblique cutting where the cutting edge is inclined with respect to the direction of cutting. Moreover this theory was developed based on linear stability assumption, which ignores factors such as tool jumping the cut, process damping, and nonlinear cutting constant due to varying cutting force direction. Sridhar et al. [12] made a comprehensive model of milling dynamics and proposed time-varying directional dynamic milling coefficients and then used numerical procedures for evaluating stability limits. Minis and Yanushevsky [13], [14] applied stability concepts of periodic systems for evaluating the stability of milling model proposed by Sridhar et al. [12].

Budak and Altintas [15], [16] developed analytical formulation in frequency domain for predicting milling stability considering both endmill and workpiece as multi-DOF systems, as shown in Figure 2-1. This is the first work on thin wall milling where the workpiece immersion

boundaries are updated due to static workpiece deflections. The stability algorithm essentially takes the cutting coefficients and transfer functions in X & Y directions for endmill and workpiece at different nodes along axial depth and formulates the problem as an eigenvalue equation and performs stability analysis to find out stable spindle speeds and corresponding axial or radial depth of cuts. Considering that the stability solution is developed as an eigenvalue problem, the computation time is much less as compared to previous time domain simulations. In addition to this the ability to predict chatter frequency makes this model widely employed in commercial software.

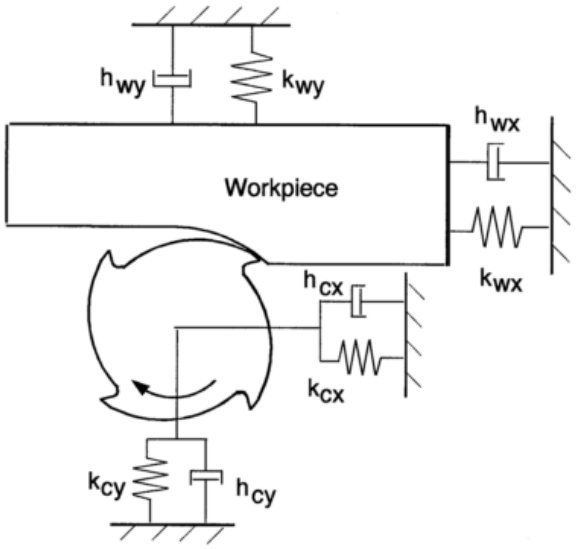

Figure 2-1 Two-DOF milling model of tool & workpiece for stability prediction[15]

Though the above frequency domain approach predicts reasonably accurate stability lobes, its accuracy reduces as the thin wall machining progresses. This is mainly due to two factors: variation in dynamic response of thin wall at various locations (for e.g. compliance at the top of

thin wall is more than at the bottom) and change in dynamic response of the thin wall due to material being removed. These two factors do not pose significant problem in machining of bulk material where the variation in dynamic response will be minimal. To address this problem, Bravo et al. [17] proposed generating 3D stability charts where the third axis corresponds to the intermittent steps of machining, as shown in Figure 2-2. In fact, this concept of 3D stability charts was proposed earlier by Schmitz et al. [18] with the third axis representing different tool overhangs. From Figure 2-2 it can be seen that such a concept of 3D stability charts for intermittent machining steps is not only tedious to construct and approximate, but the whole methodology is difficult to replicate in complex thin wall assemblies to be machined. Moreover, in many applications the vibrating part need not be the part being machined. For example, a part or assembly might have a thin wall panel that vibrates during machining. In such situation the stability lobes will not be of use as the tool tip point faces a stiffer structure to be machined whereas the forced vibration due to thin panel on assembly might be more.

Wall from 150 x 50 x **4.8** mm to 150 x 50 x **0.8** mm

	0 Step	3 Step	6 Step	14 Step
Mode 1	1225 Hz	1550 Hz	1525 Hz	425 Hz
Mode 2	1650 Hz	1925 Hz	1650 Hz	675 Hz
Mode 3	2625 Hz	2875 Hz	1950 Hz	800 Hz
Mode 4	-	-	2150Hz	1025 Hz
	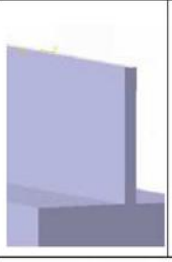	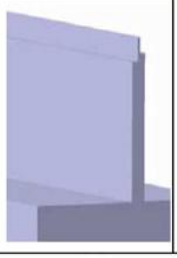	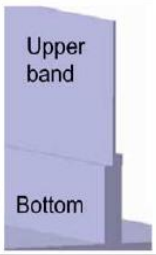	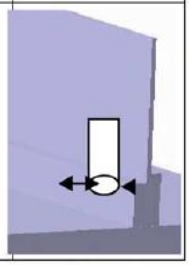

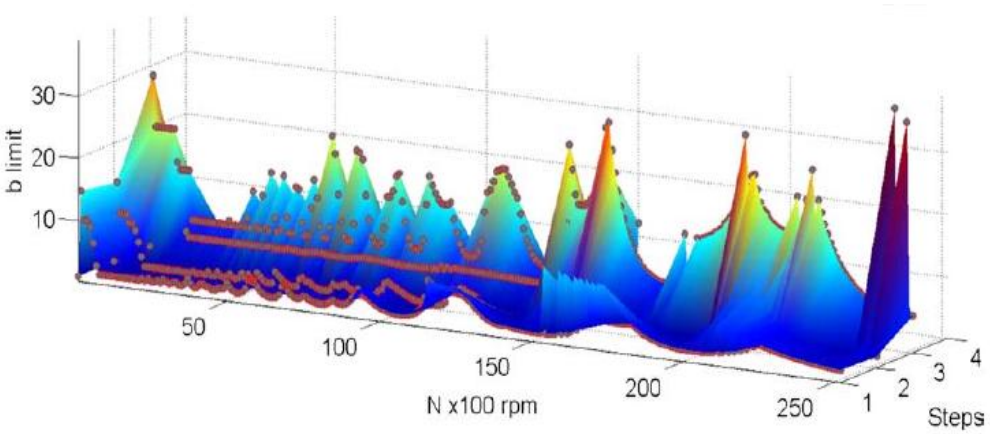

Figure 2-2 3D stability charts considering different stages of thin wall milling [17]

2.2.2 Turning of thin wall cylinders

Chang et al [19] for the first time reported chatter characteristics of thin wall cylindrical workpiece in turning. They initially presented the dynamic characteristics of thin wall cylinder reporting that the ratio of the inner diameter of shell to the thickness has a significant influence on chatter behaviour. When this ratio is smaller (less than 5) the beam mode of cylinder dominates and when higher, shell mode dominates. These beam

and shell modes, as presented in [19], are shown in Figure 2-3. They also reported that the occurrence of chatter vibration of shell mode is more likely as the ratio increases and that this chatter frequency of shell mode decreases as the cutting progresses owing to decrease in stiffness due to material removal.

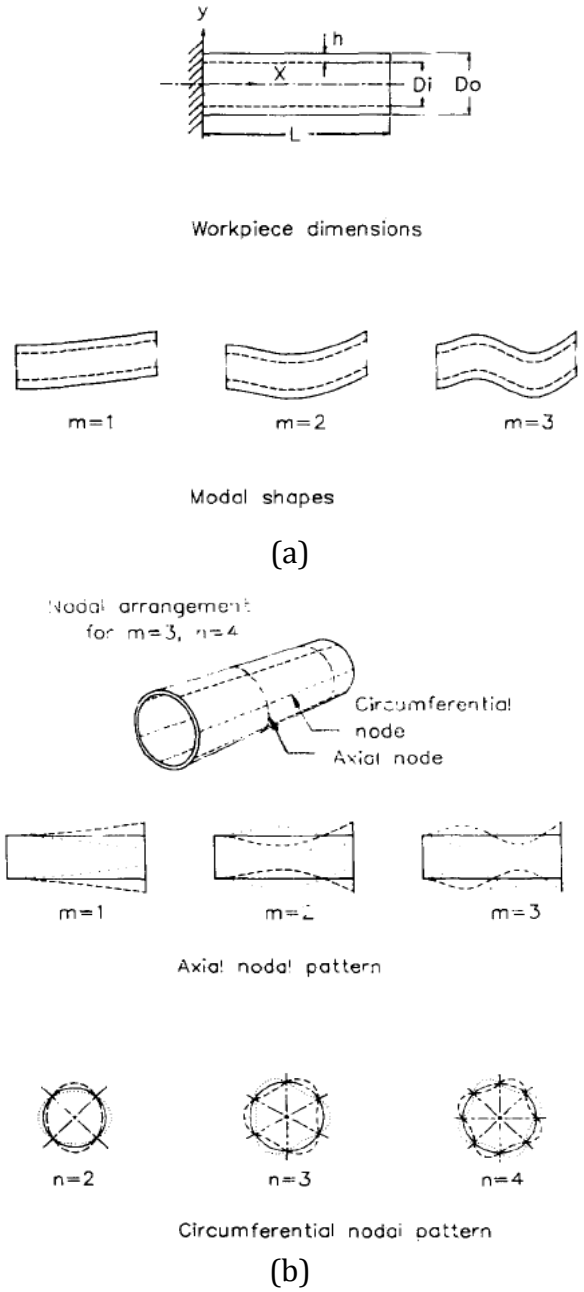

Figure 2-3 (a) Beam and (b) shell mode shapes for thin wall cylinder [19]

Based on the above findings of dynamic characteristics, Lai and Chang [20] observed that the chatter behaviour of a three-jaw clamped thin wall cylinder is complex not only due to variation of stiffness and damping coefficients along the length but also change in the vibration direction angle according to relative position of cutting tool to the chucking jaw. This causes a parametric vibration along the periphery of the cylinder causing the stable cutting depth of three-jaw clamped thin wall cylinder to become very small.

Mehdi et al [21], [22] presented dynamic behaviour of thin walled cylinder during turning for which they reported a numerical simulation. One of their interesting findings is that the natural frequencies of shell are highly influenced by its diameter (60% influence) as compared to its thickness (4%). Hence they suggested that hypothesis of thick walled workpieces as a source of stiffness in a manufacturing system must be revised. Using the developed numerical simulation they predicted the time response of vibrating thin cylinder and its corresponding FFT by applying cutting excitation forces, but not by explicit modelling of tool and its dynamics. This has an important relevance as would be explained in next section. Figure 2-4 shows the time response and its FFT for roughing and finishing operations; shows the presence of workpiece modes in the vibration spectrum with sharper peaks in the finishing spectrum owing to less damping. To evaluate the stability of the turning process Nyquist diagrams were used. Though Part 2 of this paper [22] reports experimental validation, no comparison was made between the results of developed

numerical simulation and experimental results. The authors have also inserted a rubber damping ring inside the thin wall cylinder to show the improvement in terms of vibration reduction. However the damped dynamic response of thin wall cylinder due to the rubber ring which was also modelled as proportional viscous damping was not compared against the experimental response. Such a validation might not be successful considering the fact that a simple proportional viscous damping model cannot truly represent viscoelastic behaviour of rubber which is usually modelled through Standard Linear Solid (or Zener) model.

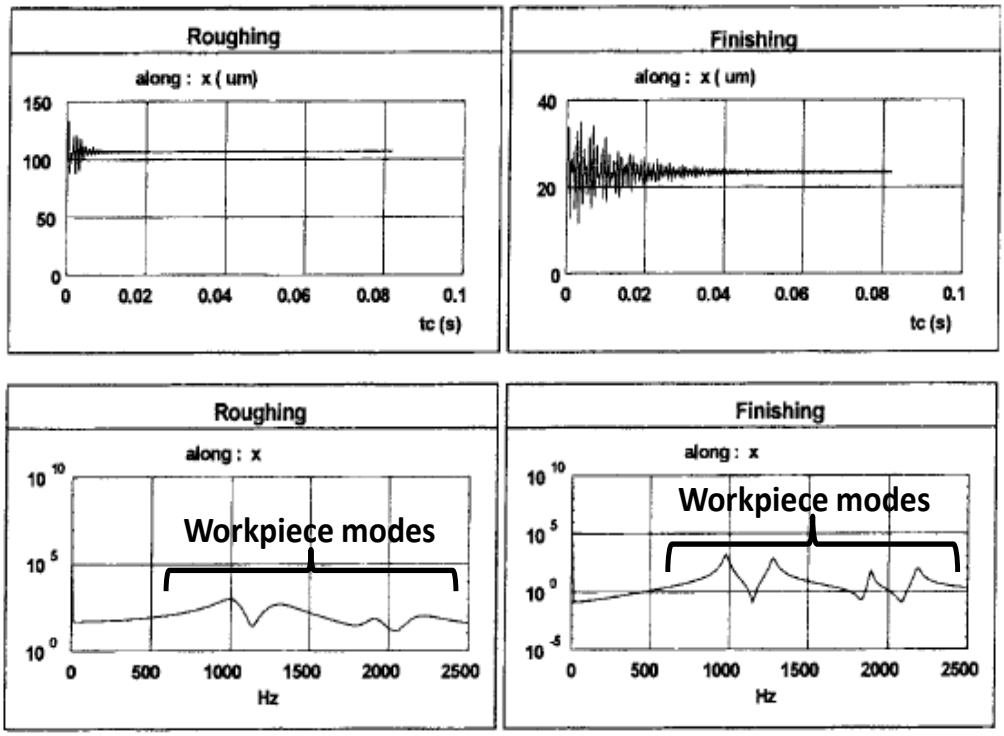

Figure 2-4 Thin wall cylinder vibration response in time and frequency domains for roughing and finishing operations [21]

The above mentioned three works [19]–[22] are the only reported research works in machining of thin wall cylinders and all these works

considered only turning process. Moreover in their numerical simulation they have not considered the dynamics of tool.

2.3 Simulation and error compensation strategies in thin wall milling

Further research in thin wall machining researched into finite element prediction of deflection of thin wall, tool and workpiece systems with similar dynamic response, process planning strategies, error compensation strategies and numerical prediction of workpiece response. One of the important inputs required for simulation and compensation of deflection of thin wall is the process force model. Researchers have developed different mechanistic models and the accurate the model the better the deflection predictions. Hence one of the key considerations in improving the accuracy of force model is accounting for varying chip thickness due to workpiece deflection in thin wall machining. Kline and Devor [23] predicted the deflection of workpiece for the first time using cutting force model. They used finite element model was used to model the plate workpiece. However their force model is static i.e. the dynamics of the cutting process is not taken into account for force prediction.

Budak and Altintas [24] presented an analytical cutting force model and workpiece surface generation model which considers partial separation of tool and workpiece due to the deflection of the latter. They modelled tool as cantilevered elastic beam and plate workpiece as a meshed finite element model. The surface generation model predicts the static form error of the machined thin wall. Their model also calculates the variation

in feed rate required along the plate to keep the error within the specified tolerance. Lim and Menq [25] and Feng and Menq [26] proposed a model for prediction of surface errors using ball end mill considering different cutting strategies, regenerative feedback of cutting system deflection for chip thickness calculation. Ning et al [27] analysed the deformation caused in the thin wall due to machining force using commercial finite element software. Though obvious, they showed that the machined thin wall will have higher thickness at the top as compared to bottom and also the thinner wall has more variation than that of thicker walls. They have not incorporated any machining force model in their work and assumed an approximate value of 500N as cutting force with different distributions (uniform, ladder type profile distribution, etc.). Similar analysis was used by Herranz et al. [28] to predict deflection of cantilever thin wall and relieve the shank of endmill to avoid its rubbing against thin wall.

Considering the limitations of analytical models in accurately predicting the surface generated due to workpiece deflection, Ratchev et al [29] have developed a virtual environment for simulation and prediction of deflection. It is part of an adaptive machining planning environment for modelling, prediction, and selection of process and tool path parameters for rapid machining of complex low-rigidity high-accuracy parts. Their simulation methodology, shown in Figure 2-5, includes genetically modified neural networks for force prediction and finite element analysis for modelling of part deflection. A voxel-based model is used for modelling

material removal process from deflected parts. The deflection results were used for off-line compensation of surface errors.

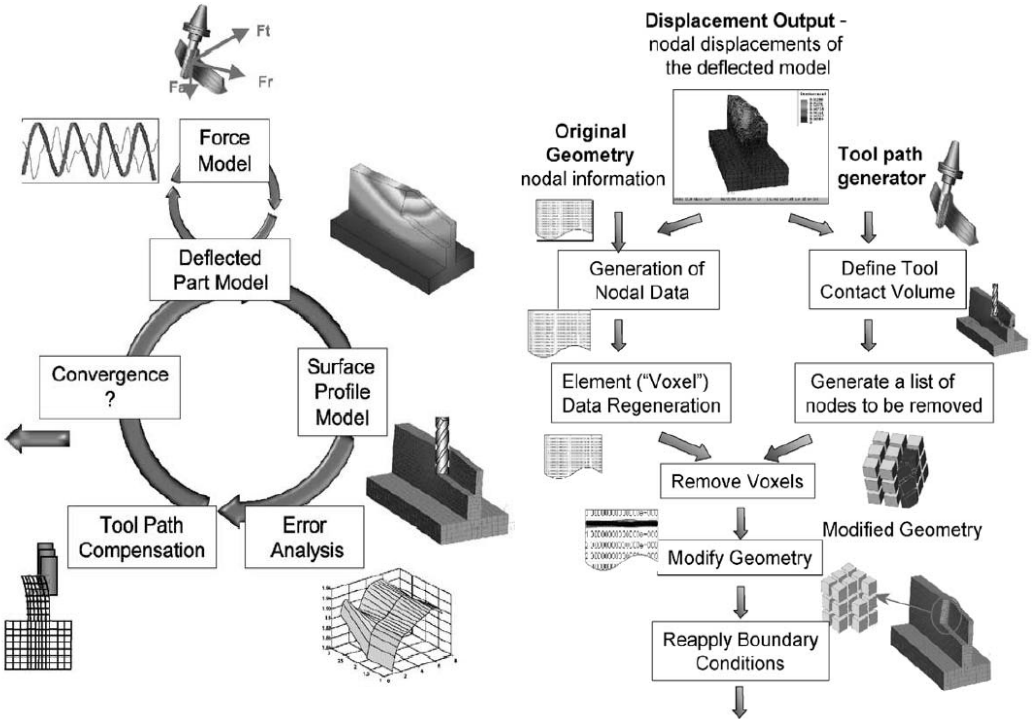

(a) (b)

Figure 2-5 (a) Deflection prediction and compensation methodology (b) Voxel based modelling for error prediction and compensation [29]

Ratchev et al [30] also proposed an advanced machining error compensation strategy considering force induced errors in machining of thin wall structures. The machining errors are predicted using an analytical force model which also takes into account deflection of flexible workpiece. The toolpath is then optimised by compensating for the predicted surface error. In another work [31] they have also reported integration of commercial FEA package Abaqus with analytical force model to iteratively update FE model for multi-step simulation and predict force-induced part deflection. Wan et al [32] proposed strategies to

control the force-induced surface dimensional errors in milling of thin wall structures. Similar to Budak and Altintas work [24] they have chosen feed per tooth for optimisation. And also radial depth of cut was selected for simultaneous optimisation of surface error, as shown in Figure 2-6. Similar to previous works, mechanistic model was used for cutting force estimation and FE model of workpiece was used for deflection estimation. Thus it can be seen that all the research focussed on surface form error minimisation of simple cantilever thin walls using mechanistic models or genetic algorithms for cutting force prediction and subsequent deflection calculations through FE and compensating it by varying feed rate and depth of cut.

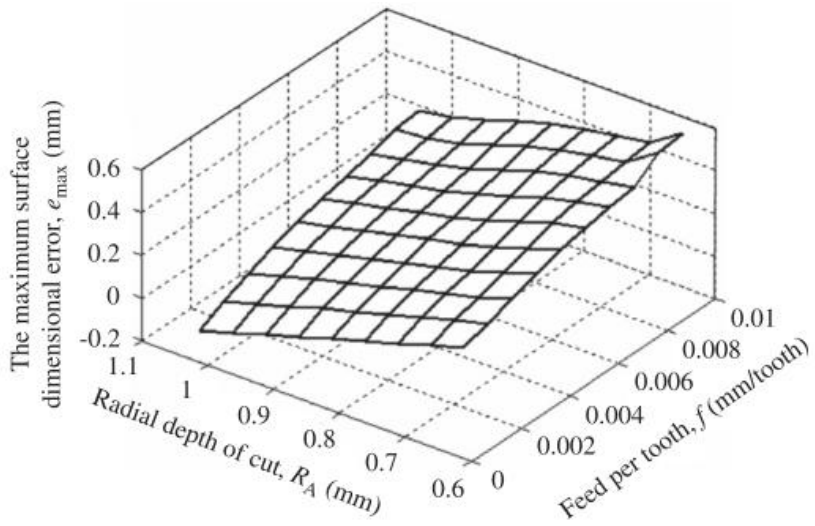

Figure 2-6 Maximum surface error variation with feed & radial depth of cut [32]

2.4 Fixturing solutions for thin wall machining

As explained previously fixturing solutions can be of two types – standard dedicated mechanical fixtures and scientifically designed non-

conventional fixtures such as piezoelectric dampers, particle dampers, and tuned mass dampers. These two types will be reviewed in the following sections. Also the research literature on the scientific analysis of mechanical fixturing will be presented.

2.4.1 Mechanical fixturing for circular thin wall casings

Mechanical fixturing relevant to circular thin wall structures only will be reviewed and the problems with their design will be highlighted for usage in complex thin wall assemblies with multiple internal features such as Front Bearing Housing (FBH) assembly as shown in Figure 1-3. Before reviewing various mechanical fixtures it is pertinent to list the requirements to be met by a fixture for such complex assemblies:

1. Provide significant damping to the thin wall structure of assembly so that machining induced vibration is damped
2. Adequate central space to allow multiple machining operations in the same setup
3. Light weight so as not to damage the other parts of the assembly and also do not cause deflection of thin wall casing to which fixture is attached

With these requirements in view, various relevant fixtures available as patents or in general literature will be presented.

2.4.1.1 Ringspann Fixture [33]

The German company Ringspann are known within fixturing community for their expertise in clamping circular components. They hold a number of patents based on use of flexure clamp solution. As shown in Figure 2-7 a flat tapered circular ring is the basis for Ringspann system. Upon applying the actuating force axially the ring outer diameter increases if the inner diameter is restricted by mandrel or conversely inner diameter reduces if outer diameter is supported. The axial actuating force is amplified 5 to 10 times radially to clamp the workpiece through frictional connection. The applications of Ringspann system typically range in clamping in short lengths or thin wall components that are susceptible to deformation. As can be noticed the major disadvantages of such a fixture are that it is heavy, and needs a central mandrel to exert external force. Also the flexure can accommodate only small amounts of component deviation, typically less than 10mm. All these factors make this kind of a fixture unsuitable for FBH type of application.

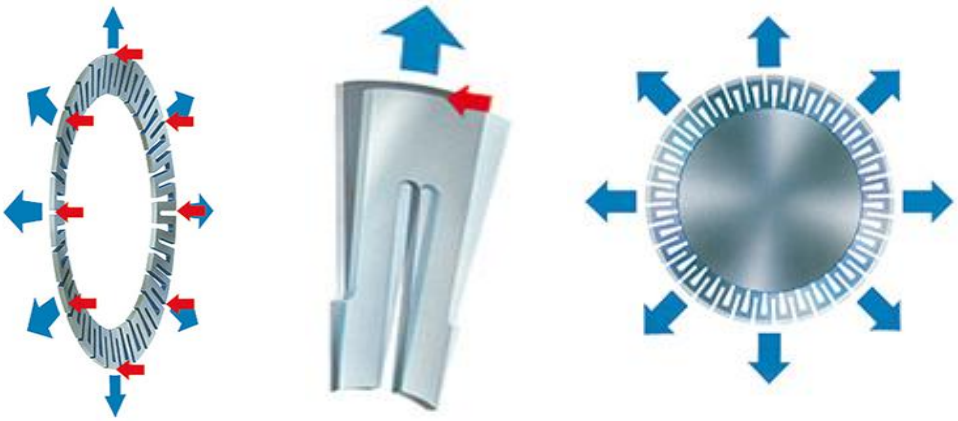

(a)

(b)

Figure 2-7 Ringspann Fixture Principle (a) application in holding a turbine component (b) [33]

2.4.1.2 Inflatable diaphragm [34]

An inflatable rubber diaphragm was proposed to damp the machining vibrations in thin-walled shell / cylindrical components. As shown in Figure 2-8 the inflatable diaphragms are supported against a mandrel either for external machining or internal machining configuration. This concept is currently being used for machining of Rolls-Royce combustion casings which are open internally without any vanes or plumbing lines. However this concept suffers from following disadvantages:

- It can be applied only for hollow casings (when applied internally) or a smooth surface without ribs and bosses (when applied externally). Hence this solution cannot be used for complex thin wall assemblies with internal features such as vanes and plumbing lines exist.

- Usage of such a concept necessitates multiple fixturing setups to machine a thin walled part if multiple operations are needed in single machining setup due to hindrance to tool movement.

- There is a need for separate cylinder or arbour and inflatable tubes for different diameter casings which makes it non-reconfigurable and hence expensive to use for various casing configurations.

- It cannot be effectively used for non-circular shapes where the contact area of rubber diaphragm with the thin-walled part reduces to small patches. Even with regular shells of revolution, the contact area is limited to local patches thereby not providing damping over full surface.

- Finally the setup is heavy and needs significant time to set it in place and pump the inflatable diaphragms

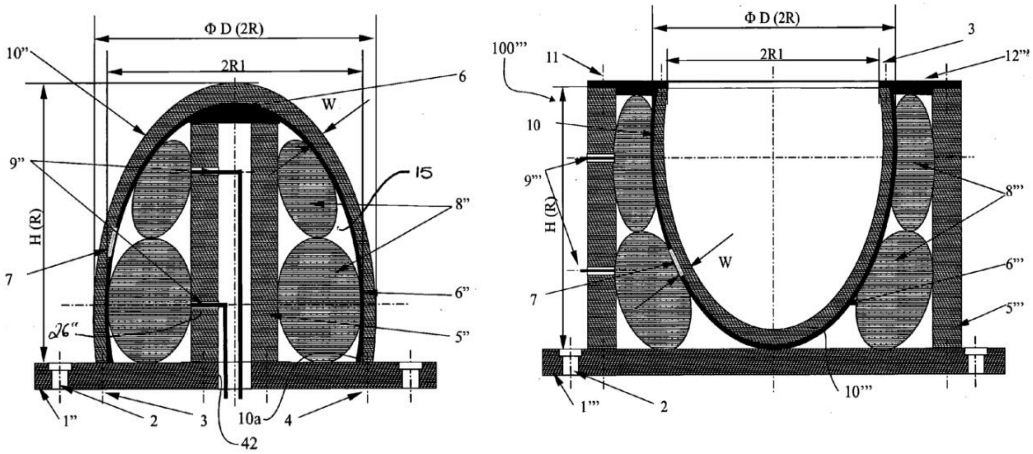

(a) (b)

Figure 2-8 Inflatable rubber diaphragm to damp vibrations in (a) external machining and (b) internal machining

2.4.1.3 Hydraulically or pneumatically actuated fixtures

In response to a requirement of damping fixture for similar open combustion casing, shown in Figure 2-8, previous researchers at University of Nottingham have designed a fixture with hydraulically actuating pads [35] as shown in Figure 2-9. Similar to previously mentioned fixtures, this concept suffers from same problems as being heavy, not feasible for usage in applications needing central access, etc. Moreover this fixture is very complex for industrial usage and its set up time offsets any time advantage gained through its use. Also using such a fixture for internal machining (i.e. damping from external side) needs total redesigning.

Similar concept of hydraulic actuation but with expandable collets is also proposed by Hydra-Lock corporation as shown in Figure 2-10 [36]. While this concept was proposed and seems ideal for holding small thin walled parts, it can be scaled for larger casings. However it has similar drawbacks

as explained for the other above-mentioned concepts: applicable only for hollow casings, non-reconfigurable over wide range of casings, difficulty and time-consuming in setting up the fixture, non-suitability for non-circular casings.

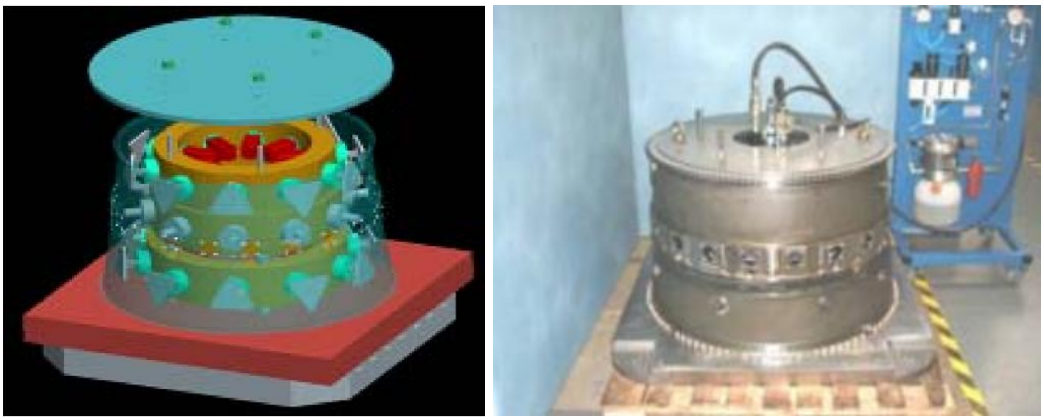

Figure 2-9 Combustion casing with hydraulically actuating pads fixture [35]

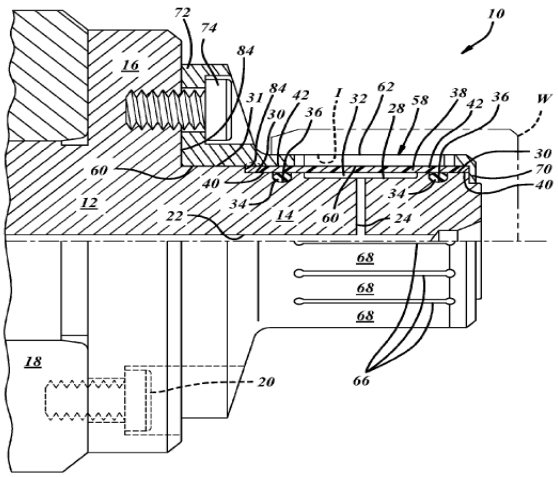

Figure 2-10 Fluid actuated workholder with a collet driven by a soft and thin bladder [36]

These are the major mechanical fixturing designs existing for clamping and damping thin wall casings from machining vibrations. As can be seen

all these concepts have more or less similar drawbacks that make them not useful for complex thin wall assemblies (e.g. Front Bearing Housing) where internal access is primary requirement apart from being light weight. In this context, the damping solutions researched for thin wall machining applications might be a better option and they are reviewed in the following section.

2.4.2 Scientific analysis of mechanical fixturing

One of the initial researches in the fixture based solutions for minimising vibration in thin wall machining is reported by Daimon et al [37]. They reported that for workpieces with wall thickness of $1/100^{th}$ to $1/200^{th}$ of maximum dimension (aspect ratio of thin wall), the possible rate of metal removal is often limited by the onset of machining vibration. And by improving the workpiece rigidity a high feed rate is possible in milling plate- and/or box-like castings and weldments. The number of workpiece support points in a fixture is determined from the maximum compliance on the workpiece at unsupported points and ensuring that compliance at any point on structure is not more than 0.1μm/N. In a similar work Yeh and Liou [38] reported development of software tool to predict optimum number of support points to minimise static compliance of workpiece due to fixture contact. They suggested the concept of modelling the workpiece-fixture contact with virtual spring elements which takes into account the surface finish, contact stiffness, etc. and used FEM to model workpiece and fixture systems. They showed that it is possible to monitor the contact

conditions based on fixture system's dynamic response frequencies and validated this through FE and experimental method.

Li and Melkote [39] presented an optimisation method to optimise the fixture layout and clamping force accounting for workpiece dynamics during machining. The objective minimises the maximum positional error at machining point. The dynamic model is based on Newton-Euler equations of motion, with each fixture-workpiece contact modelled as an elastic half-space subjected to distributed normal and tangential loads. They showed that the maximum magnitude of positional error vector during machining was reduced by 58%. They also reported that the final result is insensitive to initial fixture layout and clamping forces. Tan et al [40] proposed a model for fixture design for thin walled parts which can get easily deformed at higher clamping forces. They used force closure, optimisation, and finite element methods to modelling, analysis and verification of the fixturing configurations. While the optimal clamping positions are determined by force closure, the minimum clamping forces required to balance cutting forces are determined by optimisation. And the finite element method predicts workpiece displacement and deformation and also the force on locators which are experimentally verified through an embedded sensor.

Considering the sensitivity of workpiece deformation and reaction force predictions, Satyanarayana and Melkote [41] studied the effect of various FE boundary conditions and workpiece compliance on workpiece deformation and reaction force predictions. They considered spherical-

planar (clamp-workpiece) and planar-planar (locator-workpiece) contact geometries. The FE boundary conditions they tried are basically whether to use node-node contact or surface-surface contact to model the above contacts and what should be mesh density at contact zone. Based on their findings they gave certain modelling and meshing guidelines and showed that using those guidelines yielded an error within 5% as compared to experimental predicted workpiece deformation. Ratchev et al [42] have studied the effect of various contact profiles for a range of fixturing elements and workpieces using springs and damper elements in FE to represent fixture-workpiece contact points, as shown in Figure 2-11. By employing such a method they can control the stiffness and damping of the elements to generate various contact (deformation) profiles. They have also studied effects of imperfect fixturing conditions on these contact profiles and validated the experimentally observed contact profiles with that of Hertzian contact theory. They reported that Hertzian contact theory produces relatively accurate results at low levels of applied forces (500-700N for steel workpiece and 250N for that of aluminium). They showed satisfactory experimental results with proposed simulation methodology for a real life component – a complex nozzle model.

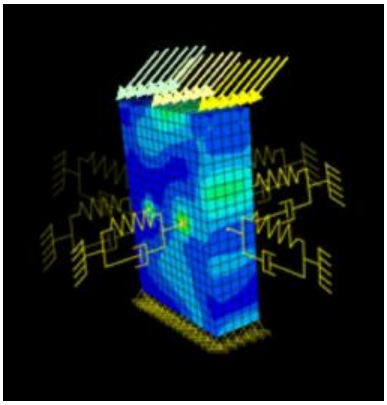

Figure 2-11 Workpiece with fixture contacts represented as springs and dampers [42]

Liu et al [43] proposed optimisation of the locator positions to minimise the surface error in peripheral milling of thin walled workpiece. They developed a finite element model which takes cutting forces as input and also takes into account the thickness variations of workpiece. They highlighted the importance of accurate cutting force model to calculate surface errors and optimise locator positions. Boyle et al [44] and Wang et al [45] presented a detailed review of computer aided fixture design approaches, research trends and new research areas where efforts need to be focussed.

Thus the scientific study of mechanical fixtures focused more on modelling clamping elements (as springs or spring-dampers), fixture workpiece contact modelling in finite element and its idealisation using Hertz theory. All these researches feed into ultimate objective of having a computer aided fixture design approach where the fixture can be modelled and analysed for its static and dynamic response thus predicting and controlling the fixture behaviour in the operation.

2.4.3 Damping solutions for minimising vibrations in thin wall machining

In addition to the dedicated mechanical fixturing solutions many researchers have focussed on improving the damping of structure (machine tool system or workpiece) to absorb the machining vibrations. Damping the machine tool system vibrations here encompasses one or more of all the components of machine tool system – machine tool structure, tool holder, tool, etc. And workpiece damping covers the workpiece and fixture used to hold the workpiece. While damping the machine tool system vibrations is extensively researched, workpiece damping is relatively less researched. These two areas will be covered in the following two sections.

2.4.3.1 Damping of machine tool system component vibrations

Damping of vibrations is targeted at the most flexible mode of the whole machine-tool holder-tool system. Generally it is the tool or toolholder which is most flexible. So traditionally damping of machining vibrations was focussed mostly on turning and boring toolholders or machine tool spindles. Sometimes depending on the specific problem at hand, tuned dampers are designed and mounted targeting particular component of machine tool. But in general tools or toolholders are the main components chosen for damping the vibrations due to their slenderness and hence higher compliance in vibration. Dampers for machine tool structures are presented as early as 1950s [46]. However considering the higher cutting speeds being used, since late 90s, which excite the dominant frequencies

of machine tool system such as that of tool or toolholder, damping these elements has become recent research interest to mitigate chatter.

Tarng et al [47] studied a piezoelectric inertia actuator, acting as a tuned vibration absorber, mounted on the cutting tool to suppress chatter vibration in turning operations. They showed that vibration absorber can modify the dynamic response of the cutting tool and hence improve the cutting stability. In their findings, they showed the necessity of matching (or tuning) the natural frequency of vibration absorber to that of the cutting tool and also the need for having a larger damping ratio for the vibration absorber. The piezoelectric inertia actuator was tuned by adjusting the size of the inertia mass. The schematic of their experimental set up and variation in dynamic response without and with the actuator are shown in Figure 2-12. They reported a six times increase in cutting stability (measured by machining vibration acceleration magnitude) by using the piezoelectric inertia actuator. Similar work was reported by the same research group in Lee et al [48].

Alwarsamy et al [49] proposed placing a ultra-thin rubber-brass laminate between insert and toolholder to minimise chatter vibrations during turning. They placed a vibration pick up near to tool and measured amplitude of vibration and also measured surface roughness of machined component. They carried out an experimental study using design of experiments with different cutting speed, feed and depth of cut. They reported up to 50% decrease in surface roughness with the use of damping rubber-brass laminate.

Boring is one of the processes where damping is extensively researched and applied to minimise tool-induced chatter vibrations due to its importance as a finish machining operation aimed at obtaining better positional tolerance of holes. Many designs were patented [50]–[52]incorporating different kinds of tuned passive dampers inside the boring bars. One popular and commercially available damped boring bar from Sandvik is shown in Figure 2-13 [53]. They have an in-built dampening device with fluid which counteracts the machining vibrations.

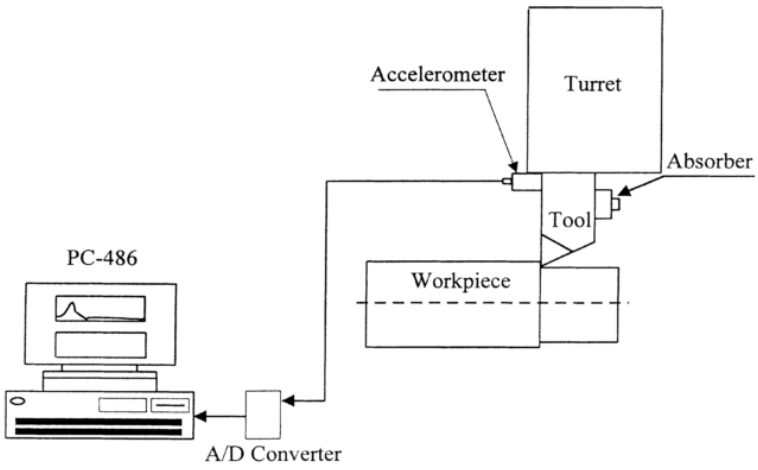

(a)

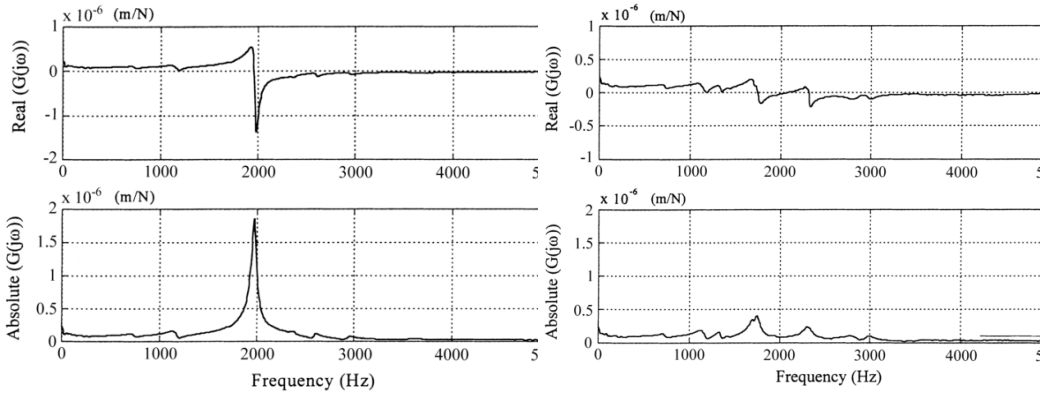

(b) (c)

Figure 2-12 Piezoelectric actuator as vibration absorber mounted on turning tool (b) Dynamic response without absorber (c) with absorber

Figure 2-13 Damped boring bar: Silent tool® by Sandvik [53]

Moradi et al [54] modelled the boring bar as a cantilever Euler-Bernoulli beam and the tuneable vibration absorber as mass-spring-dashpot system while considering the mass of spring also. They developed an algorithm to find out the optimum specifications of the absorber such as spring stiffness, absorber mass and its position. They evaluated the chatter stability at all the dominant modes of the frequency response function and showed that at higher frequency modes the critical widths of cut (i.e. limiting depth of cut in stability lobes diagram) are larger and leading to more material removal rate. While they have not experimentally validated their model, the simulation results showed significant reduction in vibration after application of optimum absorber. Moradi et al [55] in a recent work made an interesting observation that the tool wear and process damping in milling act as tuned vibration absorbers and hence increase the stable depth of cut. In addition they also modelled a tuned vibration absorber in 2-dof system milling model as shown in Figure 2-14 (a) and predicted the stable depths of cut with and without the absorber,

shown in Figure 2-14 (b). Similar to the previous work, these analytical predictions were not experimentally validated.

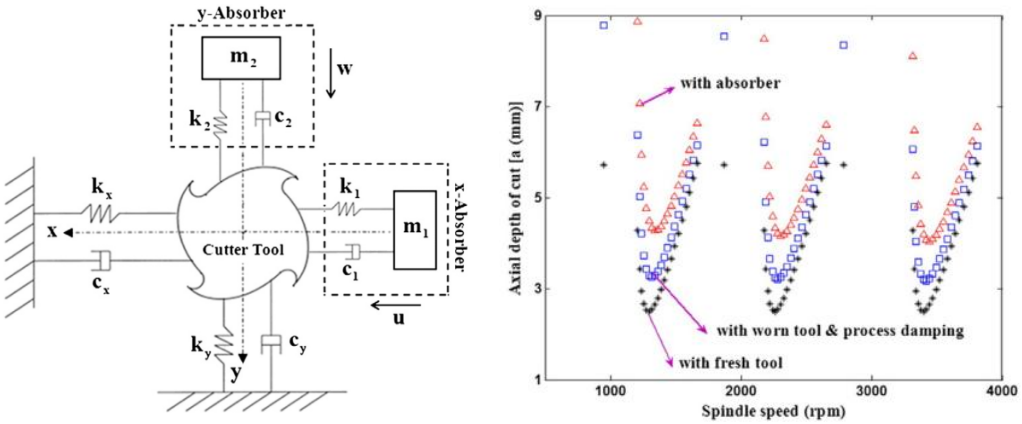

Figure 2-14 (a) 2-Dof endmill with two tuned vibration absorbers (b) Stability lobes showing improvement in stability without and with absorbers [55]

Instead of active tuning of vibration absorber through piezoelectric inertia actuator as presented above by Tarng et al [47] which doesn't incorporate explicit damping, tuned mass dampers with passive damping material such as viscoelastic material are quite popular in industry. Before presenting the research on tuned mass dampers application to machining vibration control, the distinction between a vibration absorber and a tuned mass damper is explained here. A tuned vibration absorber (TVA) is essentially a simple mass tuned for the targeted frequency and mounted through a bolt or some other mechanical means. The stiffness and damping applicable in this case are only from material of the tuned mass and the joint applied (such as structural damping due to bolt, etc.). No external damping is provided. The schematic of vibration absorber and the dynamic response of structure with such an absorber are shown in Figure 2-15 (a). As can be noticed, with the application of vibration

absorber, the targeted frequency peak is split into two equal peaks on either side of target frequency. While this will reduce the vibration at the targeted frequency the side lobe vibration is not desirable. Though in practice the material damping of tuned mass will not make the peaks look so sharp, still an explicit addition of damping is needed. A tuned mass damper (TMD) is similar to TVA but with added damping in the form of viscoelastic damping material. The schematic and dynamic response of structure with TMD is shown in Figure 2-15 (b). The reduction of heights of peak depends on optimum selection of the damper loss factor which varies between 0 and 1. The optimum loss factor suppresses both the peaks with a shallow trough in between. It is for this reason where complete minimisation of vibration near targeted resonant mode is required, an explicit damping is added.

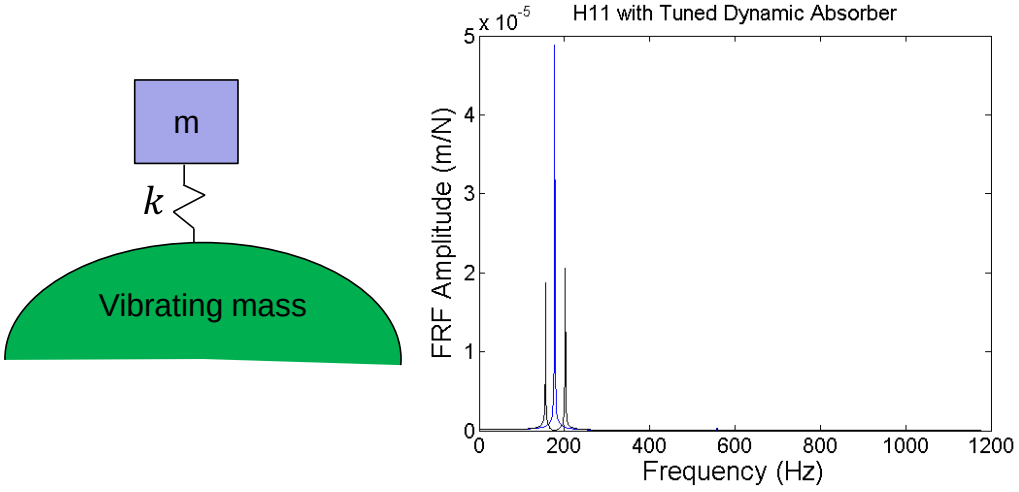

(a)

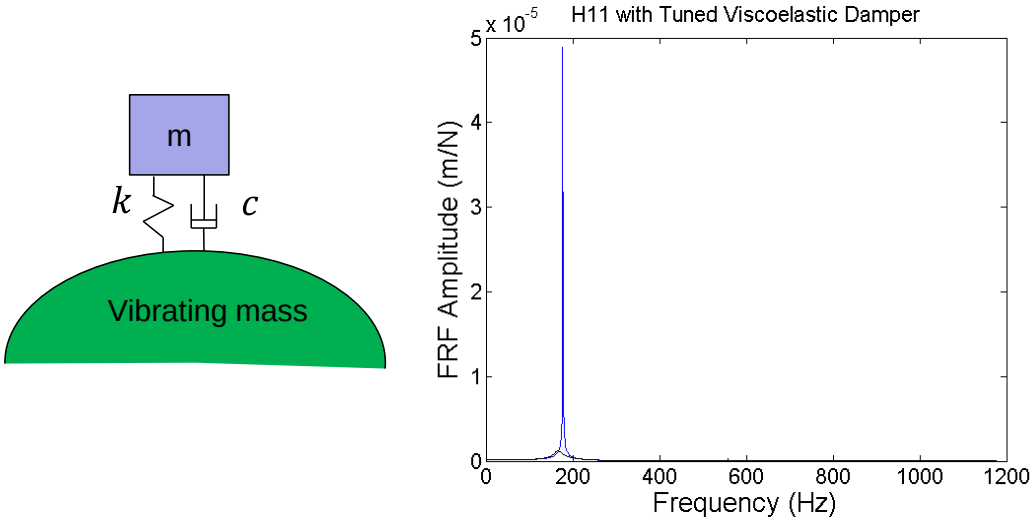

(b)

Figure 2-15 (a) Tuned vibration absorber schematic and its dynamic response (b) Tuned mass damper with loss factor 0.6 and its dynamic response

This method of tuning TMD by choosing the loss factor so that peaks of frequency response function (FRF) magnitude are minimised is traditionally proposed by Den Hartog [56]. However in regenerative chatter phenomenon, the limiting depth of cut depends on the negative real part of the FRF, instead of magnitude. This can be seen from the expression for limiting depth of cut for a single degree of freedom system such as turning:

$$b_{lim} = \frac{-1}{2*k_s*Re(G)}$$ Equation 2-1

where K_s indicates cutting coefficient and Re(G) indicates real part of FRF

So considering that the real part of the FRF is relevant Sims [57] proposed an alternative method for tuning – equal troughs in real part (see Figure 2-16). The difference in this approach as compared to Den Hartog's method of equal peaks in magnitude and the corresponding improvement in the stability margin can be seen in Figure 2-16 adopted from [57].

Yang et al [58] studied optimisation of tuned mass damper for chatter suppression in turning. They targeted a flexible mode from the fixture of a lathe, as shown in Figure 2-17 (a). The tuning methodology employed by them, though similar to that of equal troughs in real part approach, is different in its implementation. They formulated maximising the chatter stability as an optimisation problem and employed a numerical approach (steepest descent method) and obtained optimum frequency and damping ratio of tuned mass damper. Some of their important findings are: 1. Equal peaks tuning method can achieve maximum stiffness of the target mode comparing to equal troughs of real part tuning method. 2. They showed a 27% increase in critical depth of cut as compared to equal peaks of magnitude tuning method. 3. Fundamental difference of two tunings is that the optimum frequency ratio for equal peaks is lower than unity, whereas it is greater than unity for tuning of equal troughs of real part.

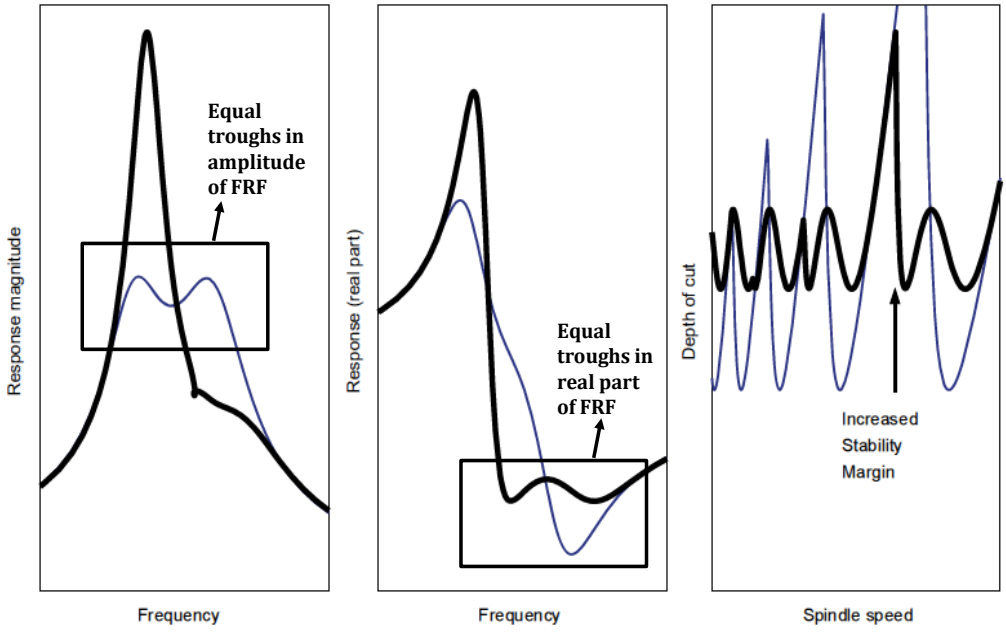

(a) (b) (c)

Figure 2-16 Optimal absorber tuning (a) response magnitude (b) real part of the response (c) stability lobes. Classical tuning ————, Equal troughs in real part ——— [57]

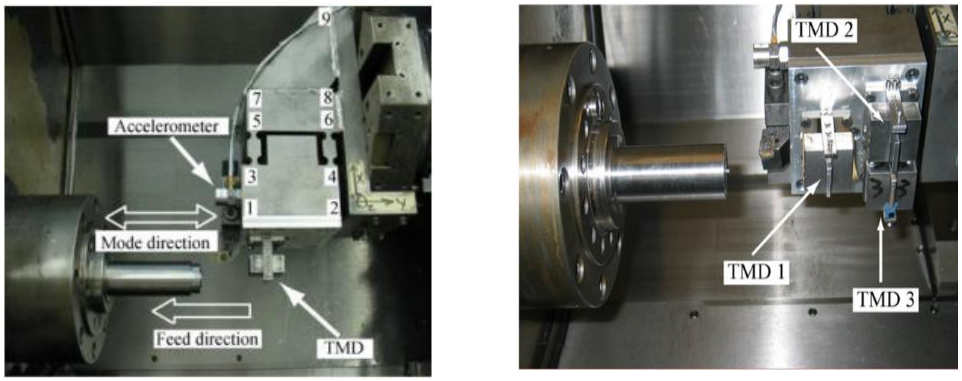

(a) (b)

Figure 2-17 (a) Single tuned mass damper mounted on tool fixture of lathe [58] (b) Multiple tuned mass dampers [59]

For the same tool fixture of lathe, Yang et al [59] also studied incorporating multiple tuned mass dampers to suppress machine tool chatter, shown in Figure 2-17 (b). The principle of their tuning the multiple dampers is similar to what Sims [57] has proposed (equal troughs of real part, as explained above), but applied for multiple TMDs

through an optimisation strategy with chatter stability law as objective function. Minimising the real part of frequency response is then implemented. As with any other application such as automotive and aerospace they considered the weight restriction as a limiting factor while designing multiple dampers and hence limited the total mass of all the TMDs as 5%. They reported that when multiple TMDs are used natural frequencies of TMDs spread above and below the targeted natural mode of structure, which can be intuitively understood considering the fact the natural frequency of structure varies with addition of every mass. In their work, all the multiple TMDs are targeted to damp one single mode and they commented that the modes which became more flexible after damping targeted mode need to be damped by designing new TMDs for those modes.

So it can be seen that most of the machine tool system component vibrations are minimised through vibration absorbers or tuned mass dampers – mounted either on machine tool structure or on toolholder. In all the above cases the tool and toolholder are stationary allowing the dampers to be mounted. In the case of boring where eccentric rotation exists the damper is built inside. In rotating tools such as milling and drilling, mounting such dampers is not possible and any tool originated chatter has to be addressed through process mechanics approach – i.e. using stability charts.

2.4.3.2 Damping of workpiece system vibrations

Thin wall workpiece machining or compliance in workpiece holding fixture can result in workpiece chatter. It is here few researchers attempted using different damping solutions – active damping such as piezoelectric damping, and passive dampers such as particle damping, and tuned mass dampers.

Zhang and Sims [60] applied piezoelectric patch on a horizontal cantilever, shown in Figure 2-18, to minimise the workpiece chatter. A positive position feedback control strategy was used to actuate the piezoelectric patch mounted on the cantilever and demonstrated seven-fold improvement in the limiting stable depth of cut. They highlighted two important drawbacks of such a solution: attachment of transducers and influence of coolant on transducer. The bonding of piezoelectric material to workpiece and its subsequent removal is difficult and needs chemical treatment of the workpiece. Also during machining the transducers were sealed to avoid contamination with coolant. In real machining environment this might pose a problem and an insulation material would have to be sourced.

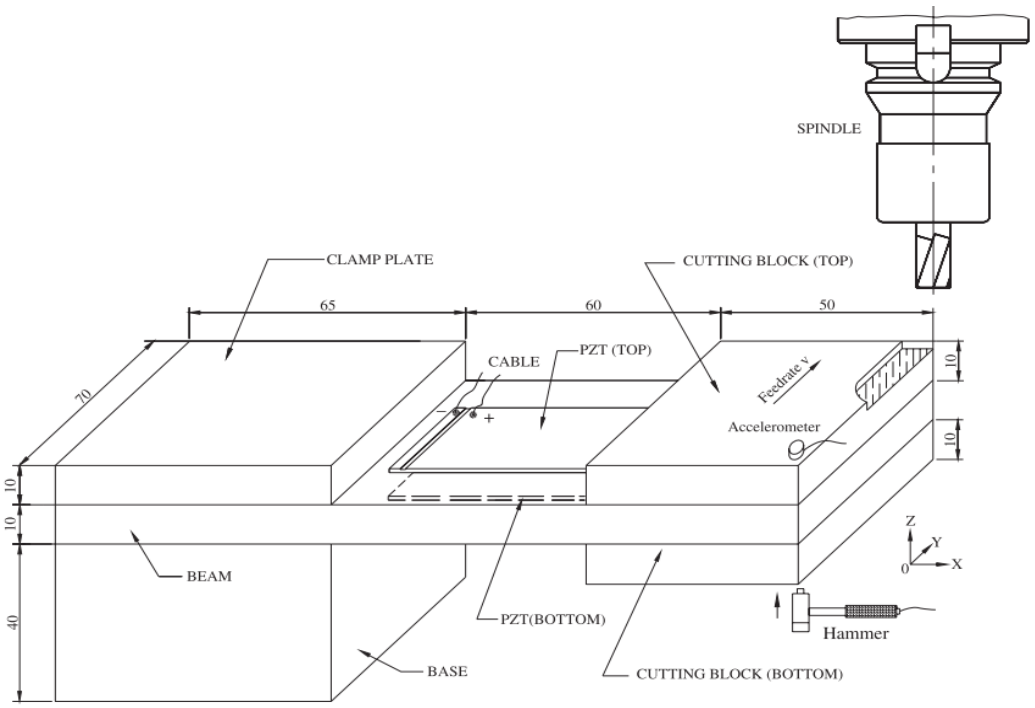

Figure 2-18 Piezoelectric damping of cantilever thin wall in milling [60]

Sims et al [61] studied using particle dampers for workpiece chatter mitigation. They used granular particles contained within a single housing as particle dampers. They have studied effect of parameters like particle damper cavity size and clearance, mass ratio (ratio of mass of granular particles to effective mass of structure), number of particles, and particle size. And to study the effect of vibration amplitude on damping, they used an electromagnetic shaker to excite the structure. They have shown that the particle damper significantly improves the chatter stability (by 8 times) but reported that the stability predictions for damped workpiece are not accurate due to the non-linear effects in damper. Also similar to the piezoelectric damping patches, they reported the difficulties in mounting the particle damper and its debonding during initial engagement of tool with workpiece. But one important conclusion they made is that the

particle damper is effective over wider bandwidth unlike tuned vibration absorbers which are targeted to a specific frequency.

Rashid and Nicolescu [62] studied tuned viscoelastic dampers (TVD) for vibration control in milling of solid workpieces, not thin walled workpieces. They designed the dampers for a torsional mode of workpiece which is dominant in both X- and Y- directions, as shown in Figure 2-19. The viscoelastic material they used for damping is commercially available tape 3M® ISD112. The thickness of the viscoelastic tape was calculated for tuning the targeted frequency for a given weight of tuned mass (5% of vibrating mass). The design of this damper can be called semi-analytical as they used analytical modelling methodology with experimental FRF data to find out which mode to be tuned. Application of TVD reduced the vibration acceleration by 20dB for targeted mode while also being effective on modes away from the targeted mode (3dB in with one TVD and 7dB with four TVDs).

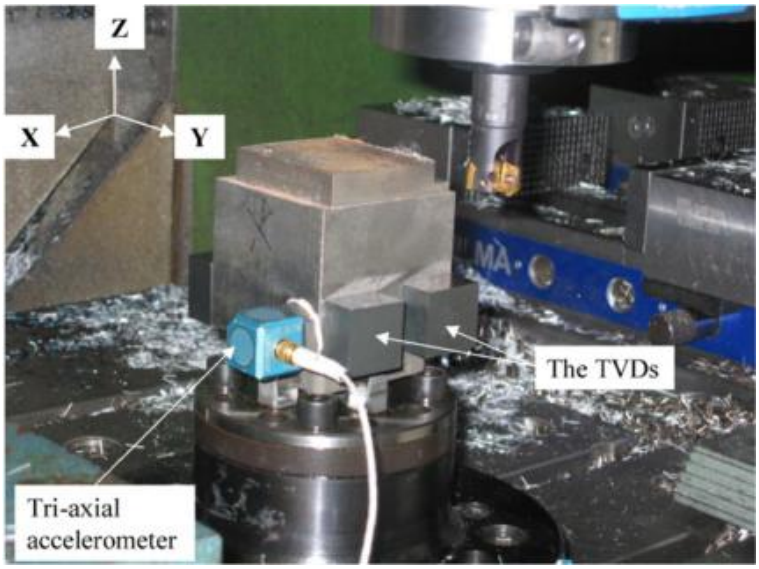

(a)

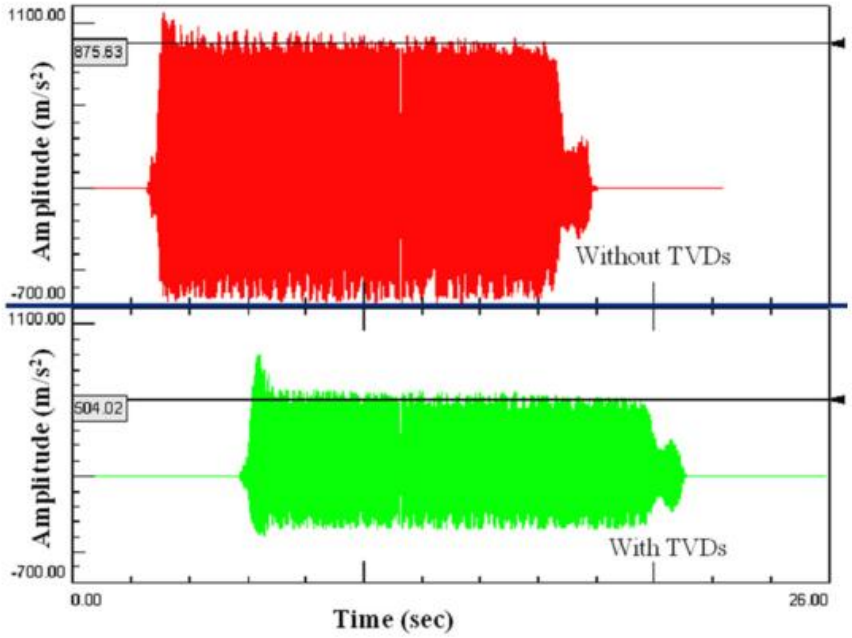

(b)

Figure 2-19 (a) Tuned viscoelastic dampers mounted on solid workpiece (b) comparison of vibration signal without and with dampers [62]

Rashid and Nicolescu [63] proposed active vibration control in palletised workholding system through sensors and actuators. The sensors measure the vibration of workpiece mounted on the pallet. The measured vibration after necessary signal processing such as amplification and digitisation are

filtered and fed to control actuators which counteract the chuck vibration. They developed an adaptive control algorithm for this active vibration control. As a result of the vibration control, a qualitative reduction in tool wear and improvement in surface finish was reported. Some modifications such as reduction in operating voltage of actuators, integration of hardware and software in compact unit were suggested.

Thus a limited work is reported on damping the workpiece vibrations – either passive or active. And no work on damping vibrations of thin wall casings was reported. Thin wall casings, though inherently stiffer due to closed geometry, are prone to significant forced vibrations which can result in poor surface finish and associated tool wear. Hence damping such kind of structures is of significant interest – both from industrial and research points of view.

2.5 Dynamic interaction between workpiece and tool in machining

Considering that damping solutions need to be studied for thin wall cylindrical structures, an understanding of their dynamic response in the presence of forced vibrations of tool is essential. Such a response is termed as 'coupled dynamic response' in this work. In this section, the available literature on such a coupled response will be presented. The phenomena of dynamic interaction between tool and straight thin wall is researched to some extent by Davies and Balachandran [64]. They studied the vibrations measured on a thin wall plate, shown in Figure 2-20 (a), using various analysis tools such as time series, power spectra, and phase

portraits. They reported that the tooth cutting frequency and its harmonics are noticed in the power spectrum and that these harmonic peaks are modulated over a wide frequency band where a workpiece mode exists, shown in Figure 2-20 (b). The broadband peak between 375Hz and 500Hz corresponds to first mode frequency of the workpiece. The prominent appearance of tooth engagement frequency with increasing radial depth of cut was also highlighted using auto bi-spectra. However, they did not make any mention about tool's natural frequency in the acquired vibration spectrum. This could be possibly due to the fact that the authors have low-pass filtered their acquired signal at 5000Hz. It might be possible that their tool first mode might be more than this frequency and hence authors failed to notice it. Also, while the time series and phase portrait plots show the tool workpiece interaction and workpiece free vibration, no study was reported on the actual tool-workpiece interaction during and after the cut which can offer an insight into the evolution of tool and workpiece frequencies as the thin wall is being machined and also the extent to which each of this dominates the spectrum. The authors have also tried to analytically model the coupled interaction using single degree-of-freedom mass-spring-damper system. While the predictions are qualitatively similar, the predicted periodic motion of tool impacting the workpiece is not seen in the experimental power spectrum. The authors attributed this to effect of changing workpiece surface (regeneration) which was not modelled.

Other than this work there is no research literature available on studies of coupled interaction of tool and workpiece – either straight thin wall or a casing.

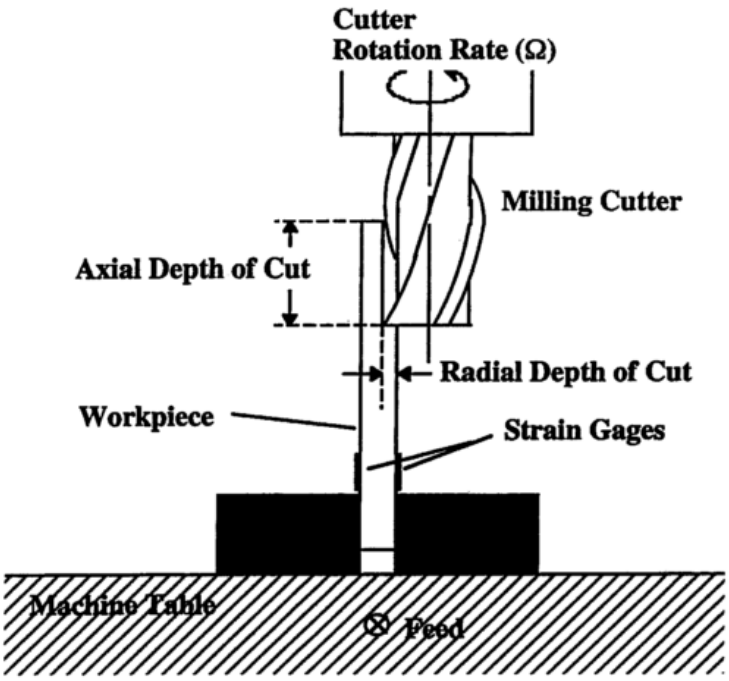

(a)

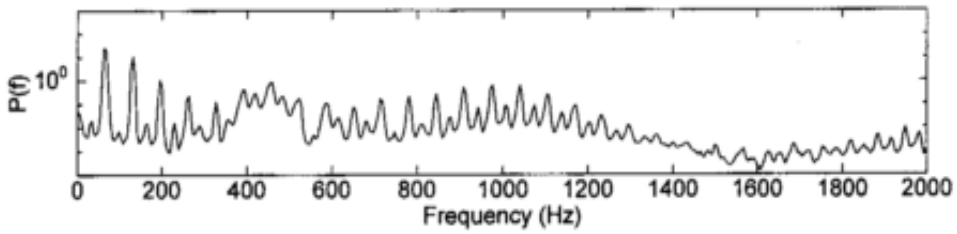

(b)

Figure 2-20 (a) Experimental set up for measuring dynamic interaction between tool and a thin wall in milling (b) Modulation of cutting tooth frequency harmonics at workpiece frequencies [64]

While studying the dynamic interaction of tool and workpiece, the monitoring and analysis of different machining signals is an integral part. Many research papers exist on this literature, however a comprehensive review on advanced monitoring of machining operations was given in Teti et al. [65]. This paper covers in detail all the various types of sensors and sensor systems that were employed to analyse machining signals and also explains various signal processing methodologies and statistical features that can be extracted from time and frequency domains. It highlights the importance of sensor fusion where a combination of sensory data from different sources is utilised for getting more accurate and more complete result. A reconfigurable monitoring system, as shown in Figure 2-21 [65], is presented for sensor fusion which involves different sensory sources such as cutting force, vibration, acoustic emission, motor current, audible sound and optical sensors.

Figure 2-21 Reconfigurable monitoring system for sensor fusion [65]

Such a sensor fusion concept was demonstrated for tool wear measurement [66] and residual stress measurement [67]. Marinescu and Axinte [68] have also demonstrated the usage of such sensor fusion (AE + force) coupled with AE signal analysis in time-frequency domain to identify workpiece surface malfunctions in milling with multiple teeth cutting simultaneously. They showed that identification of number of teeth in cut in milling can be shown by time-frequency analysis of AE signal. Moreover detection of surface anomalies such as folded laps that are generated by damaged cutting edges were successfully identified. Segreto et al. [69] presented application of advanced signal processing technique, Principal Component Analysis, on cutting force signal to classify various chip forms.

The above signal analysis techniques were employed on cutting force, vibration and AE signals to identify tool wear, residual stress, chip form and formation of workpiece surface anomalies. No work was reported on using these techniques to identify the coupled dynamic interaction between tool and workpiece.

2.6 Summary of literature review and research gaps

In this chapter, a comprehensive literature review of relevant research and development is presented on machining thin walls and various solutions to minimise machining vibration. As presented in the previous sections, minimising the vibrations in thin wall machining is addressed from various perspectives: studying process mechanics & dynamics (stability lobes), mechanical fixturing, and providing passive or active

damping solutions. While the process dynamics based algorithms are very useful in predicting chatter free process parameters for rigid workpieces, they become less accurate for thin wall structures due to difficulties in measuring the workpiece dynamic response at different stages of machining. Moreover the dynamic response varies as the machining progresses due to material removal. It is these major factors which necessitate resorting to mechanical fixturing to minimise the vibrations in thin walled structures. Research into modelling of the mechanical fixturing focussed on workpiece deformation due to clamping force and its optimum value by using springs and dampers to represent locating and clamping elements. The machining forces to be used in the model to calculate workpiece deformation are predicted using mechanistic cutting force models. Though much research has been done on these aspects and some researchers have presented virtual environment, there is no commercial software available using these findings for industrial fixture design. In addition to regular mechanical fixturing, unconventional methods of minimising vibrations such as piezoelectric damping, particle dampers and tuned mass dampers were also researched. While the former two were attempted only on thin walls, tuned dampers were studied only on rigid solid block. Moreover no detailed work is reported on understanding dynamic interaction of tool and workpiece in thin walled casings.

From the above summary of literature review following research gaps can be identified which are presented as academic challenges and the corresponding industrial benefits that would result in.

Academic challenge 1 - There is presently little understanding on the dynamic interaction of tool and workpiece in cylindrical thin wall casings and how does this differ from straight thin wall.

Industrial benefit 1 – Understanding of coupled tool-workpiece dynamics helps in modelling impact dynamics in milling correctly and this can then be incorporated in any commercial software which gives an idea as to which modes are participating during the machining so that they can be damped.

Academic challenge 2 - Damping of large surface areas of complex assemblies for machining applications is totally unaddressed in research literature. The solutions which were proposed such as tuned dampers, piezoelectric damper, can be used on small local patches but are quite impractical to apply on a whole large surface area.

Industrial benefit 2 - As shown in some of the patents presented in previous sections, simple structures such as hollow casing were damped to minimise machining vibration. But for complex assemblies typical in jet engine structures (e.g. Front Bearing Housing discussed earlier) no damping solution is proposed. A surface damping solution covering whole thin wall surface of casings is hence highly desirable from industrial application point of view.

Academic challenge 3 - No work was previously reported on application of tuned mass dampers on large thin wall casings. While it is widely known that a properly designed tuned damper will subdue the targeted mode, the effect of multiple tuned dampers with higher mass ratio, mounted across whole surface area, is not reported. This is probably due to the fact that most of the applications have constraints in terms of maximum mass that can be mounted. But considering machining of thin wall structures is a ground based stationary application and an area where forced vibrations are dominant (apart from regenerative chatter, if it exists), mass addition will improve inertia forces and hence such a study is important and relevant.

Industrial benefit 3 – While locally mounted tuned dampers are not as effective as a surface damper, an understanding of the tuned dampers with higher mass ratio helps in its usage on medium surface area casings in minimising vibration.

Academic challenge 4 - No work was reported on FE analysis of damping solutions for manufacturing applications – be it either active or passive damping. Considering the emergence of computer aided fixture design in the recent years, such a study will highlight necessary methodology and modelling issues to be addressed.

Industrial benefit 4 – This provides a tool to simulate the proposed damping solution at the fixture design stage itself thereby avoiding the vibration damping problem as troubleshooting.

The above four areas are very broad each in itself and in this work research has been focussed on addressing them while at the same time provide practical relevance to the findings from such research.

3 Experimental setup and research methodology

3.1 Introduction

In the previous chapter, the research gaps confirm the need for evaluating the coupled dynamic response interaction of tool and workpiece and also to design and evaluate a surface damper for thin wall casings. In this chapter, the general methodology followed in studying these objectives is presented: such as experimental set up, measurement chain utilised, data acquisition system and software, signal processing methodology, tooling used, etc. These units will be explained for both evaluation of interaction of coupled response and surface dampers. The coupled response interaction experiments were conducted both on straight thin wall and thin wall casing to verify the difference in interaction. However the dampers were evaluated only for thin wall casings, which is the major interest in this research. As the casing tested is bigger in size representing an industrial component, a bigger dynamometer and a vertical milling machine were used. Whereas tests on the straight thin wall cantilever were conducted on a horizontal milling machine with a smaller dynamometer. Following sections present the experimental set up and measurement chain for both the features. The signal analysis methodology employed is same for both the features. For evaluating the dampers, along with machining validation experiments, finite element (FE) analysis was conducted for comparing the dynamic responses with and without

dampers. A detailed description of FE methodology is presented in Chapter 5.

3.2 Experimental set up for coupled interaction study on thin wall straight cantilever

Recent machining studies [70] on straight thin walls suggested machining with higher finish stock and employing alternate step machining strategies, as shown in Figure 3-1. This provides necessary stiffness to thin wall during machining reducing the deflection and workpiece induced chatter. However such a strategy is not feasible in finish machining of thin wall casings where very little stock is left on one side of casing to correct for process errors such as weld-induced distortion. This is usually 2-3mm for the casings of interest to industrial sponsor. Hence in this research a thin wall straight cantilever of 3mm thickness, made of aluminium, was chosen to study coupled dynamic interaction. The experiment was carried out on a Makino A55E horizontal milling machine, shown in Figure 3-2, specifications of which are given in Table 3-1.

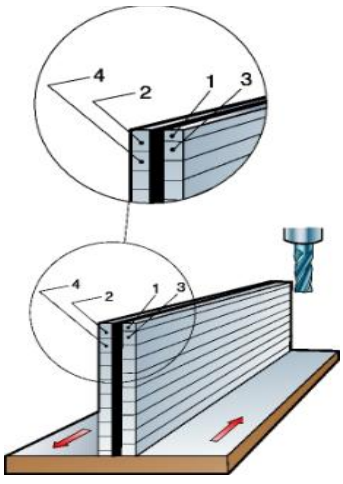

Figure 3-1 Step machining strategy for thin wall

3.2.1 Cutting force measurement

The workpiece cutting forces are measured using a dynamometer (Kistler 9272) such that the radial cutting force is aligned along Z-direction of the dynamometer (shown in Figure 3-3). This dynamometer has 4-channels: F_x, F_y, F_z, and M_z. The characteristics of the dynamometer are given in Table 3-2. As can be seen in Figure 3-3 the cantilever workpiece is designed in such a way that always a constant overhang of length of 25mm can be maintained for all the experiments.

Figure 3-2 5-axis Makino A55E machining centre

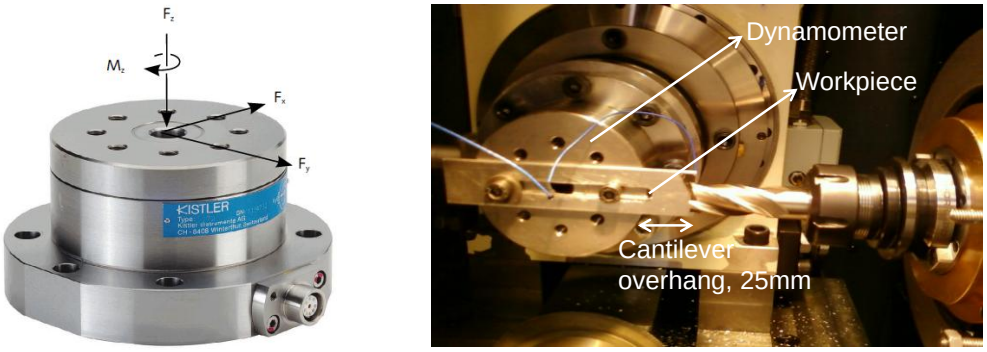

(a) (b)

Figure 3-3 (a) Dynamometer for measuring forces on thin wall (b) Experimental setup for measuring cutting force and acceleration

3.2.2 Vibration measurement

An accelerometer is attached on the back side of the workpiece, shown in Figure 3-4 for the cantilever trials, to measure the vibrations arising due to machining. Mounting the accelerometer on the workpiece exactly behind the region where the tool contacts the workpiece enables the coupled dynamic response of the entry, contact and exit of the cutting edge to be studied using the acceleration signal in the time domain. PCB 352C23 accelerometer was chosen due to its light weight (0.2gms) and hence will not add significant mass to the thin wall workpiece. The characteristics of PCB 352C23 accelerometer are given in Table 3-3.

Table 3-1 Specifications of Makino horizontal milling machine

Manufacturer	MAKINO
Model	A55E
Control	CNC / DNC / Tape DNC
Max. spindle speed	18.000 min^{-1}
Spindle taper hole	7/24 No.40 (BT40)
Spindle power	22kW
Travel X/Y/Z-axis	560x560x560 mm
Travel A-axis	180 deg
Travel B-axis	360 deg
Maximum workpiece size	630 mm dia. x 1,000 mm
Maximum feed-rate (X/Y)	50m/min
Maximum feed-rate (Z)	94 m/min
Max. coolant pressure	70 bar
Controller	FANUC OM

Table 3-2 Kistler 9272 dynamometer characteristics

Measuring range	X/Y-direction	-5…5	kN
	Z-direction	-5…20	kN
	Torque (M_z)	-200…200	Nm
Sensitivity	X/Y-direction	-7.8	pC/N
	Z-direction	-3.5	pC/N
	Torque (M_z)	-160	pC/Nm

Table 3-3 PCB 352C23 accelerometer characteristics

Sensitivity	0.5	mV/(m/s^2)
Measurement range	±9810	m/s^2
Frequency range (±5%)	2.0 to 10000	Hz
Resonant Frequency	≥70	kHz
Weight	0.2	gm

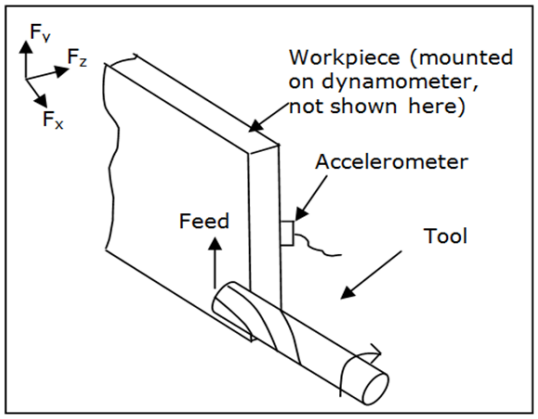

Figure 3-4 Experimental setup for measuring vibration while machining thin wall straight cantilever

3.2.3 Data acquisition system and software

The dynamometer and accelerometer were connected through signal conditioners to a data acquisition (DAQ) system. Various types of DAQ systems can be used to capture the sensorial data: either PC based (using USB, PCI or PCI express standards) or industrial (using PXI, CAN, DeviceNET standards). The PC based DAQ systems should be used more for low-cost, off-line monitoring applications, where the sensorial data is required to be analysed for studying various frequency components.

The present DAQ system is composed of:

- Hardware:
  - Connexion boxes (i.e. SCB-68 and BNC-2110)
  - Data transfer cables (SH68-68EP cables)
  - DAQ boards (NI PCI-6115 and NI PCI-MIO-16E) that uses the PCI connection to transfer the acquired data to the hard disk
  - RTSI cable between the two DAQ boards needed for synchronous acquisitioning of data.
- Software
  - In-house developed software for continuous synchronous DAQ using data triggering, dedicated buffering and data streaming.

The DAQ system employed uses two PCI boards for acquisitioning the sensorial data. The NI PCI 6115 is used to acquire up to 4 channels of high-frequency sensorial data, all the channels having their own analogue-to-digital converter (ADC), the board has a capability to be used between 1 and 4MS/s (mega-samples per second). This board is employed for capturing vibration data as more number of points is required to get sufficient resolution in the FFT of signal for one revolution of tool. National Instruments PCI-MIO-16E is used to acquire signals at 50 kHz sampling rate. The PCI MIO-16-E is used for logging the low-frequency response data of max. 16 channels with overall 200 kS/s sampling rate capability. However, having only one ADC for all of the channels, the bandwidth is shared amongst the number of channels used at one time

(e.g. if all of the channels are used at the same time than the bandwidth is limited to 200/16=12.5 kS/s). Both of the boards had 12-bit resolution for their analogue inputs. The low frequency board is used to acquire cutting force data as this is only used to correlate the one tool revolution of vibration data and no processing is done on it. In-house software developed in LabVIEW was used for data acquisition. The main characteristics of this software are detailed as follows:

- Capability of pre-viewing the channel data. The data is pre-viewed either in time-domain or frequency domain.
- The program is fully independent of the cutting process. It can be used for milling, drilling, turning, tapping and other manufacturing processes saving their cutting parameters and data settings into text files, if the user wishes to do so.
- Capability of data logging using 16 channels for low-frequency boards and 4 channels for high-frequency ones.
- Capability of pre-viewing the acquisitioned data after the experimental trial has been conducted. Without this option the user has to use other software (e.g. MATLAB, Diadem) to check the sensorial signals.
- Conversion from binary to ASCII using 12-bit resolution.
- Possibility of using the low-frequency, high-frequency boards or both at the same time.
- Simplified signal pre-view version.

3.2.4 Cutting tool

During the various experimental trials conducted in this research work, two types of milling tools were used: HSS tool for aluminium workpieces (for straight cantilever experiments) and inserted tool with coated carbides inserts for nickel based superalloy (for circular casing experiments). The HSS tool used in this coupled dynamic response experiments is Ø20mm HSS 4-flute milling cutter. A tool overhang of 70mm was used in the experiments for the HSS tool.

3.3 Experimental set up for coupled interaction study on thin wall cylinder

This experiment was conducted to study variation in coupled interaction for closed geometries such as ring type casings as compared to open geometry structures such as thin wall cantilever. The experiment was carried out on a thin wall closed geometry such as a ring type casing, which has a close resemblance to an industrial component, with a thin wall of thickness 2.5mm and height 95mm and outer diameter 365mm. The casing, which is made of a Nickel based superalloy, Waspaloy™, is shown in Figure 3-5. While the measurement procedure remained same, the measuring instruments and machine tool were changed to suit the requirements of the thin wall casing.

3.3.1 Cutting force measurement

To accommodate the bigger casing, a large dynamometer Kistler 9255B was chosen as it is designed for heavy duty applications. As the mounting

holes of casing and that of dynamometer do not match, a fixture plate was designed to enable mounting of casing. The fixture plate is a 420mm square plate made of mild steel and ground to a flatness of 0.1mm. This ensures the cutting forces are accurately transferred to the dynamometer. The characteristics of 9255B dynamometer are given in Table 3-4.

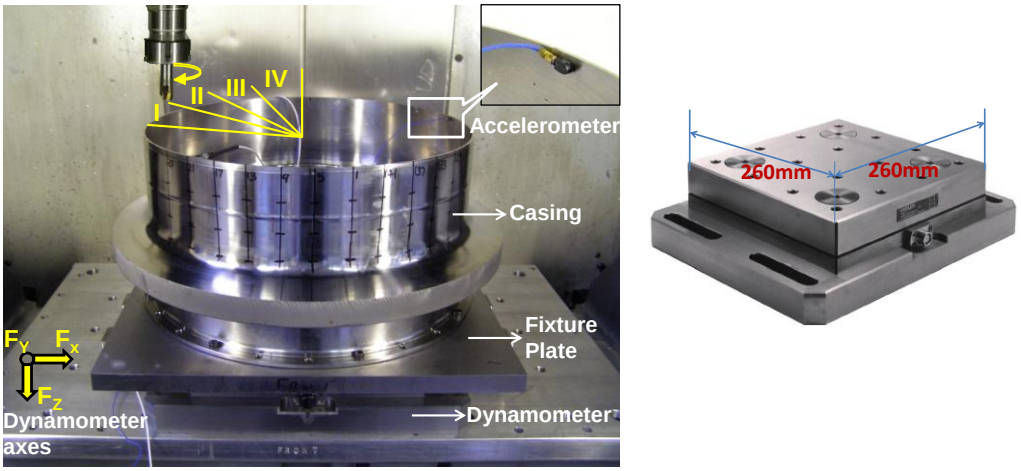

(a) (b)

Figure 3-5. (a) Casing used for coupled dynamic response study (b) dynamometer

Table 3-4 Kistler 9255B dynamometer characteristics

Measuring range	X/Y-direction	-20…20	kN
	Z-direction	-10…40	kN
Sensitivity	X/Y-direction	-8	pC/N
	Z-direction	-3.7	pC/N

3.3.2 Vibration measurement

In addition to the PCB 352C23 accelerometer that was used in thin cantilever experiment, another low sensitivity accelerometer PCB 353B14

was used to capture the data on casing at two sections while machining. As the vibration data is acquired at 1e6 Hz, acquiring data for whole quarter section of casing results in huge data file which is difficult for post processing analysis tasks. Hence the quarter section of casing was machined in four sectors as shown in Figure 3-5. The accelerometer is mounted in the middle of each sector being machined. The characteristics of PCB 353B14 are given in Table 3-5.

3.3.3 Cutting tool

The cutting tool used to machine the thin wall cylinder was a 2-flute Ø16mm inserted tool held in a collet chuck. Inserts suitable for machining superalloys (grade GC2040) were used. They are essentially coated carbides with layers of Ti(C,N)/Al_2O_3/TiN for improved wear resistance and low coefficient of friction. Due to the complex dynamic characteristics of a ring type casing with multitude of closely spaced modes, the effect of variation of tool natural frequencies on coupled interaction was also studied using three different tool overhangs: 45mm, 58mm and 65mm.

Table 3-5 PCB 353B14 accelerometer characteristics

Sensitivity	0.51	mV/(m/s^2)
Measurement range	±9810	m/s^2
Frequency range (±5%)	1.0 to 10000	Hz
Resonant Frequency	≥70	kHz
Weight	1.8	gm

3.3.4 Machine tool

To accommodate for the heavy casing and dynamometer a vertical milling machine had to be used for machining operations. A Hermle C800U 5-axis machining centre, shown in Figure 3-6 was used, specifications of which are given in Table 3-6.

Figure 3-6 Hermle C800U machine tool

Table 3-6 Specifications of Hermle milling machine

Manufacturer	Hermle
Model	C800U
Control	CNC / DNC / Tape DNC
Max. spindle speed	15.000 min^{-1}
Spindle taper hole	ISO40
Spindle power	10.5kW
Travel X/Y/Z-axis	800x600x500 mm
C-axis	360^{o}
A-axis	$+/-90^{o}$
Maximum feed-rate (rapid)	35m/min
Max. coolant pressure	70 bar
Controller	Heidenhein TNC430

3.4 Signal analysis methodology for coupled interaction evaluation

To determine the coupled interaction of tool and workpiece, the below four major steps are followed.

1. Determination of dynamic response of tool and workpiece: The natural frequencies of the tool-toolholder system and workpiece with fixture are to be evaluated to identify the modes which are actively participating in machining vibration. This evaluation is done in this research using impact hammer testing and using accelerometers for measuring response. While other methods of excitation such as shaker can be used, it becomes significantly difficult to mount the stinger of shaker on a helical fluted cutting tool. Moreover on a big structure such as a thin wall casing, attaching a stinger adds to mass loading due to force transducer. As non-contact methods of vibration response measurement are very expensive, a low-weight (0.2gms) miniature accelerometer was chosen to minimise any mass loading effect due to accelerometer. Figure 3-7 shows the measurement setup for measuring dynamic response. The frequency response function (FRF) from the impact hammer test gives the dominant natural frequencies of the system measured. A typical FRF acquired on a tool with amplitude-phase representation is shown in Figure 3-8.

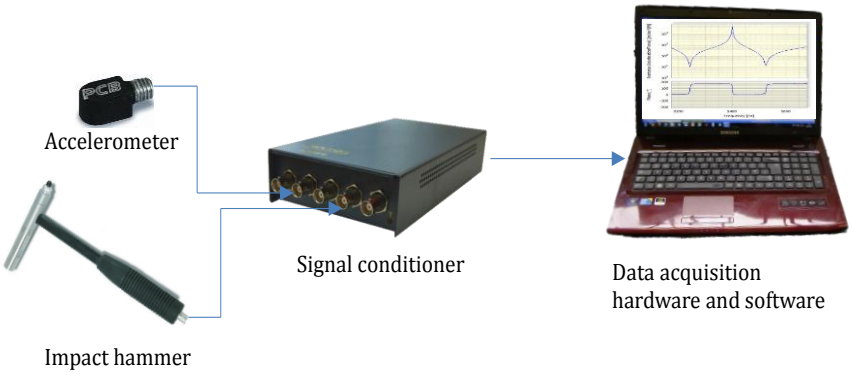

Figure 3-7 Measurement chain utilised for measuring dynamic response of tool and workpiece

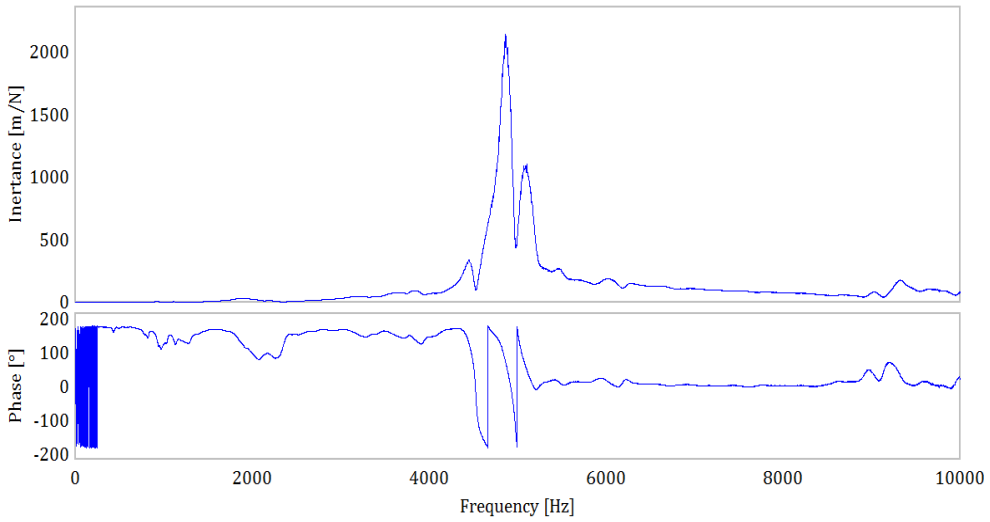

Figure 3-8 Sample Frequency Response Function acquired on a tool

2. Synchronous acquisition of cutting force and vibration signal: The cutting force and vibration signals need to be acquired synchronously to enable the evaluation of vibration signal corresponding to each excitation of cutting tooth of the tool. The workpiece was mounted on dynamometer to measure the cutting forces and the workpiece vibration during machining was measured by mounting the accelerometers. The measurement chain, as shown schematically in Figure 3-9, consists of

sensors (accelerometer and dynamometer), signal processing unit, data acquisition unit, and a computer with in-house developed LabView based data acquisition software. Typical machining vibration signal acquired on a casing during milling operation is shown in Figure 3-10.

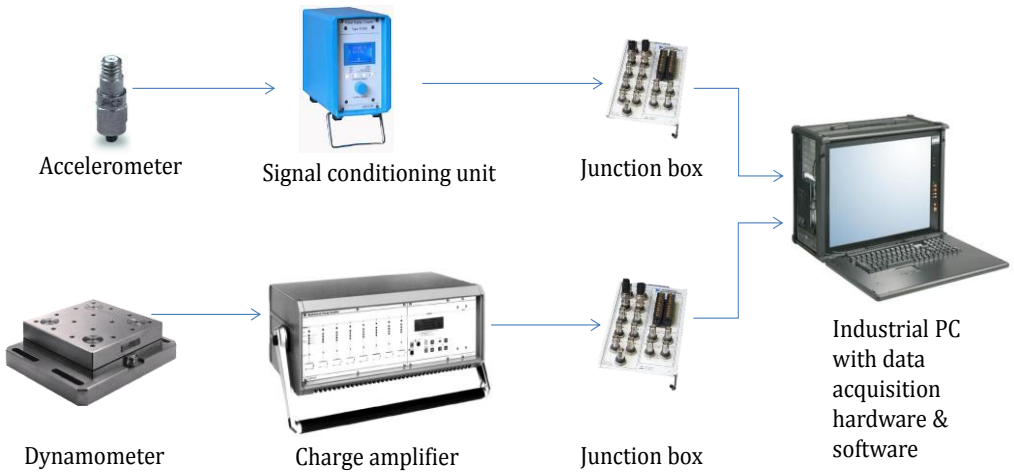

Figure 3-9 Measurement chain utilised for acquiring data to study coupled interaction

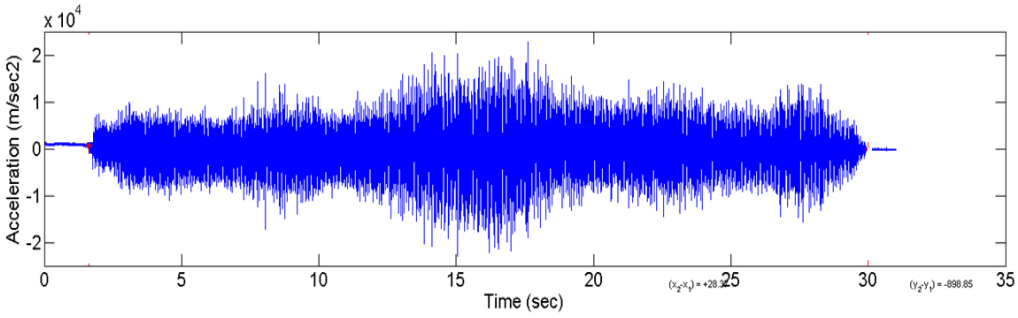

Figure 3-10 Milling vibration signal acquired using accelerometer

3. Analyse the vibration signal for multiple tool revolutions in frequency domain: The vibration signal thus acquired is analysed over multiple revolutions of tool in frequency domain using Fast Fourier Transform (FFT). Such an analysis will show the cutting tooth frequency and its harmonics along with any significance of tool and workpiece modes.

4. Analyse the vibration signal for one tool revolution in time-frequency domain: Sectioning the vibration signal for one tool revolution at equal time intervals, shown in Figure 3-11, and finding the frequency content of each section enables understanding of how the tool-workpiece coupling varies with contact pressure between tool and workpiece. MATLAB built-in function for Short Time Fourier Transform (STFT) is used for this analysis. For a structure where significant number of closely spaced modes exist, such as in thin wall casings, similar functionality of STFT is carried out using 3D FFT waterfall plots. This involves applying FFT for each section of the vibration signal.

Using the above methodology, the coupled dynamic interaction between tool and thin wall circular casing was studied. However, before studying a closed geometry structure such as thin wall casing, an open geometry structure such as a straight cantilever thin wall was studied. The reason for this is two-fold:

- To study how the coupled interaction is influenced by variation of the structural geometry
- To study if workpiece or tool modes are predominant in machining vibration and in which operating conditions they are dominant

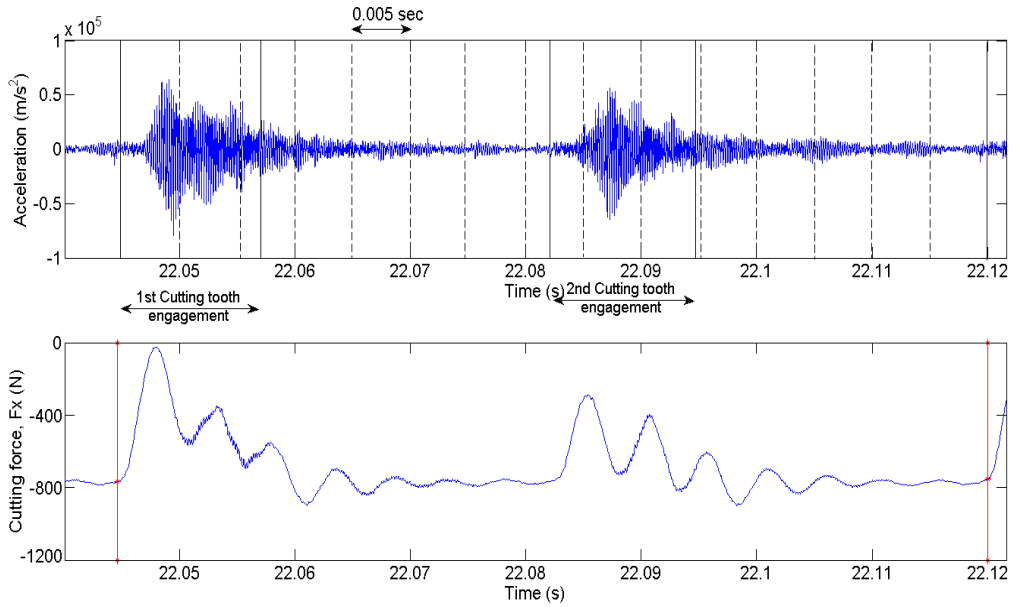

Figure 3-11 Synchronous acquisition of vibration and cutting force signals to evaluate coupled interaction of tool and workpiece

3.5 Finite element analysis methodology

The FE method is a numerical technique that involves subdividing a large problem into many smaller segments (elements) and finding the solution for the equations of each element. The behaviour of each element is determined by its displacement and the material law described for it. The equations for the whole model are solved for the known initial and boundary conditions from the original problem to provide a numerical solution for the overall problem. The FE methodology followed in the current research has four major stages, each of which has two analysis steps.

3.5.1 Analysis steps

3.5.1.1 Modal analysis

Once the FE model of the structure to be analysed is generated and meshing completed, the first type of analysis that is to be carried out is to find the natural frequencies of the structure. Knowledge of natural frequencies is not only useful in understanding the behaviour of structure (e.g. presence of repeated frequencies, density of modes, etc.) but also in finding the frequency range over which the response has to be evaluated (as explained in next section). Another advantage of modal analysis is that it provides the mode shape pattern which is useful in understanding the importance of a particular mode for the considered loading. Other output from the analysis that can be useful during analysis is generalised mass. This represents the percentage of the total mass of the structure participating in a particular mode. The summation of generalised mass can be taken as an indicator for the sufficiency of the number of extracted modes. If the total sum is close to 100% of the structural mass, then all the possible mode shapes are extracted.

3.5.1.2 Harmonic analysis

The frequency response of the structure over a certain frequency range is evaluated by harmonic analysis. In this, the response (acceleration or velocity or displacement) of any node for a given force excitation is evaluated. The given force is applied harmonically over the range of frequencies and the response measured. The frequency response as predicted in FE can be used to find the effect of added mass, damping and

stiffness. The frequency response curve is validated through experimental frequency response curve obtained through impact hammer testing.

3.5.2 Stages of FE analysis in current research

The major stages in FE analysis followed in this research are as follows:

1. Validation of viscoelastic properties and FE modelling methodology
2. Analysis of undamped casing
3. Analysis of casing with tuned mass dampers
4. Analysis of casing with surface damper

Stages 1 and 2 are explained in chapter 5; stages 3 and 4 are explained in chapters 6 and 7 respectively.

3.6 Conclusions

This chapter presents the experimental set up used in this research such as measuring chain employed, data acquisition system used, machine tools and cutting tools used. In addition the methodologies for analysing machining vibration signal to determine coupled dynamic interaction and finite element analysis of various damping solutions are presented. These methodologies are used in all the remaining chapters as an evaluation procedure for coupled dynamic interaction and damping effectiveness.

4 Coupled dynamic interaction of tool-workpiece

4.1 Introduction

In milling due to the intermittent nature of cutting process, the dynamics of the workpiece are excited through an impact excitation from the cutting tool. In the whole machine tool – tool holder – tool – workpiece – fixture system, it is the weakest link of these that will be easily excited, mean to say that the component in the above system which has lowest stiffness is responsible for major vibrations. This is the common perception that exists among the machining dynamicists. While this is true it can be appreciated that the milling operation is a coupled phenomenon between tool and workpiece and the combined dynamic interaction is of significant importance. The knowledge of impact dynamics can be applied for prediction and controlling the vibrations in milling and complements the analytical models for predicting stable machining parameters. However, while the former is applicable to general forced vibration analysis, the latter is significant only in the occurrence of regenerative chatter. As reviewed in Chapter 2, Davies and Balachandran [64] studied the frequency spectrum of thin wall vibration signal on a macro scale (meaning for several revolutions of cutter) and reported that the cutting tooth frequency harmonics are modulated at workpiece natural frequencies and the role of tool dynamics is not addressed. However, the actual coupling of dynamics of tool and workpiece is significant. As shown in Figure 4-1, while machining it is not the dynamics of tool or workpiece

alone that will be prominent, but a 'coupled' interaction between these two. The tool and workpiece dynamics are affected not only by their individual dynamic characteristics, but by their clamping interaction such as toolholder, workpiece clamping fixture, etc. Hence the whole system must be considered for analysis and study which all modes participate in the machining spectrum. This particular aspect of coupled dynamic interaction is not researched earlier and will be explained in this chapter. Initially a detailed analysis of the machining vibration signal is presented to understand the coupled interaction during and after the tool contact with the workpiece and also how this varies for different structural geometries. The next section presents the signal analysis methodology to determine the coupled interaction of tool with workpiece. Subsequently the analysis results will be presented for straight thin wall and a circular thin wall casing.

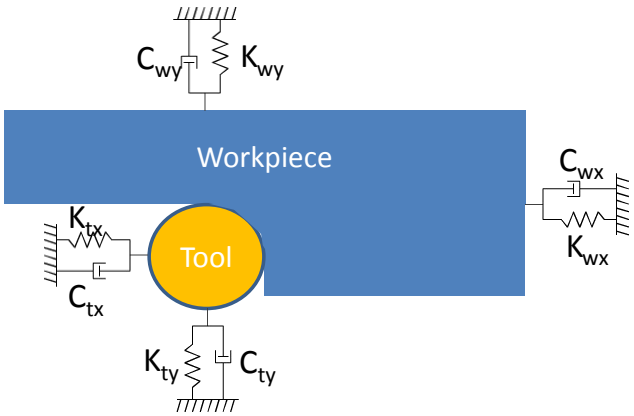

K_t, C_t – Tool stiffness and damping
K_w, C_w – Workpiece stiffness and damping

Figure 4-1. Concept of coupling of tool and workpiece dynamics

4.2 Signal analysis for coupled interaction evaluation

The analysis steps for determining the coupled interaction between workpiece and tool are explained in section 3.4. In brief they are:

1. Determination of dynamic response of tool and workpiece as separate entities

2. Synchronous acquisition of cutting force and vibration signals during machining

3. Analyse the machining vibration signal for multiple tool revolutions in frequency domain

4. Analyse the machining vibration signal for one tool revolution in time-frequency domain

Using the above methodology, the coupled dynamic interaction between tool and thin wall circular casing was studied.

In the following sections, the experimental results for coupled dynamic interaction are discussed initially for a straight thin wall and then for a circular thin wall casing.

4.2.1 Experimental results on thin wall straight cantilever

Extensive experimental trials have been carried out over wide range of axial (a_p=0.5 - 2mm) and radial (a_e=0.5 - 2mm) depths of cut while maintaining a constant cutting speed of 125m/min (spindle speed – 2000 rpm) and feed of 0.1mm/tooth. All the experiments were conducted in stable (chatter-free) machining zone. That is, the coupled interaction

between tool and workpiece is studied in purely forced vibration situation due to excitation of tool. For the comparison with previous literature (Davies and Balachandran [64]) on impact dynamics of thin wall cantilever type structures, only results of a_p=2mm and a_e=1.0mm and 1.5mm are detailed here.

Within the experimented range of radial depths of cut (a_e = 0.5 to 1.5mm), only one tooth out of four is in contact during machining at any given time and hence, there is a period when no teeth are in contact with the workpiece. This provides the opportunity to study the coupled response with and without a cutting edge in contact with the workpiece. The synchronous acquisition of acceleration and cutting force signals helps in correlating the acceleration signals for each cutting edge of the tool during its rotation. The cutting force signals were filtered and subsequently analysed in the time domain to identify the per tooth force profile. The acquired acceleration signal was then analysed in time and time-frequency domains (section 3.4), corresponding to one tooth profile, to find out the coupled interaction between tool and straight cantilever.

As explained in section 3.4, initially the dynamic response of the tool and workpiece are evaluated using impact hammer testing and mounting miniature accelerometer on the tool and thin wall workpiece. The measured dynamic responses (Frequency Response Functions) are shown in Figure 4-2. It can be seen from Figure 4-2(a) that the FRF acquired on the tool has multiple modes – of which 2980Hz corresponds to the tool cantilever mode (identified through cantilever 1st mode frequency

through Finite Element Analysis). Other modes in the FRF (g_{t1}, g_{t2}, g_{t4} – g_{t6}) correspond to other parts in the machine tool system such as tool holder, spindle, etc.

Similarly in Figure 4-2(b), the dominant frequency of g_{w1}=1130 Hz corresponds to the cantilever mode of the workpiece. It can also be observed that the workpiece is more flexible than its other system modes such as dynamometer, etc. (e.g. g_{w2} – g_{w5}) by more than an order of magnitude. Also comparing the tool and workpiece responses, it can be noticed that workpiece is more flexible than tool by more than 40 times.

The acceleration signals acquired during milling of thin wall cantilever are analysed both in frequency domain (for multiple revolutions of tool) and time-frequency domain (for single revolution of tool). The filtered cutting force, F_z was used for correlation with the acceleration signal (a_z) so that the vibration corresponding to one cutting tooth engagement and subsequent free vibration of the workpiece can be analysed.

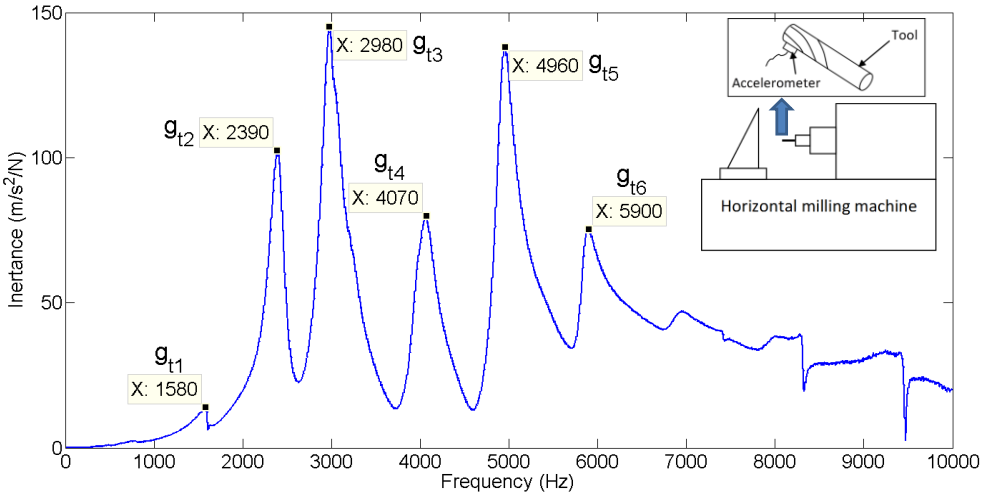

(a)

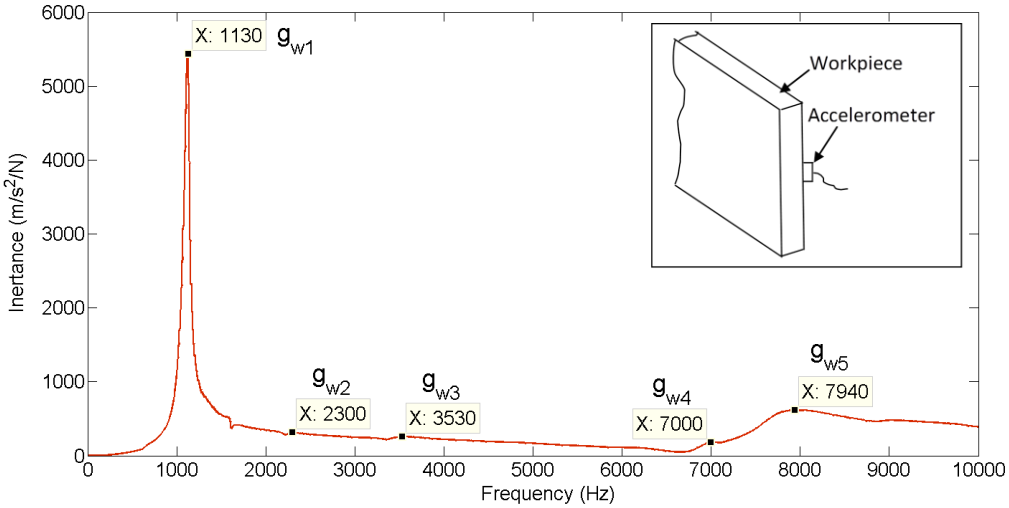

(b)

Figure 4-2. Drive point frequency response of (a) tool and (b) straight cantilever workpiece

Figure 4-3 shows the vibration and cutting force for one complete rotation of tool from which it can be noticed that the vibration due to impact of every tooth has subsided to a reasonable extent by the time next tooth comes in contact. A FFT, Figure 4-4, of the acceleration signal over many tool rotations shows the presence of harmonics of the cutting tooth frequency (133Hz). While a slight increase in amplitude around the

workpiece cantilever frequency (1130Hz, g_{w1}) can be noticed, the amplitude around the tool's system frequencies such as spindle, toolholder and tool (1580Hz, 2390Hz, 2980Hz - g_{t1}, g_{t2} & g_{t3} respectively) is significantly high. This is different from the previously reported findings of Davies and Balachandran [64] in thin wall machining where they showed that the tooth harmonics are only modulated at workpiece frequencies. Thus this finding indicates that in machining of thin wall plate type workpiece, the influence of cutting tool system frequencies is greater and hence need to be considered. The FFT was carried out at various time sections of the acquired acceleration signal and also for varying radial depths of cut (a_e, 0.5 to 1.5mm) and it is found that always tool system frequencies dominated the spectrum in spite of workpiece being significantly flexible than tool.

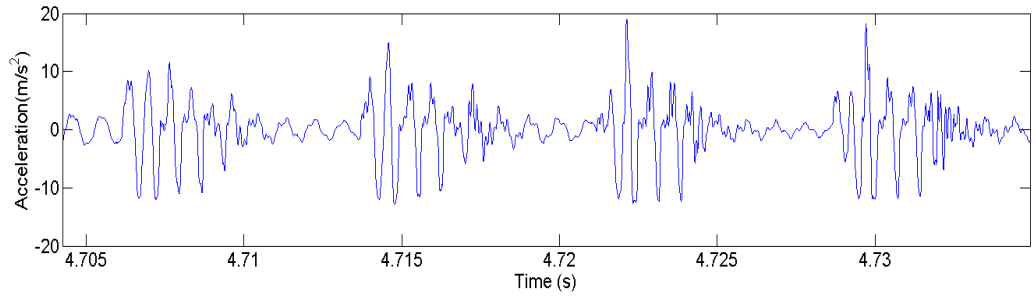

(a)

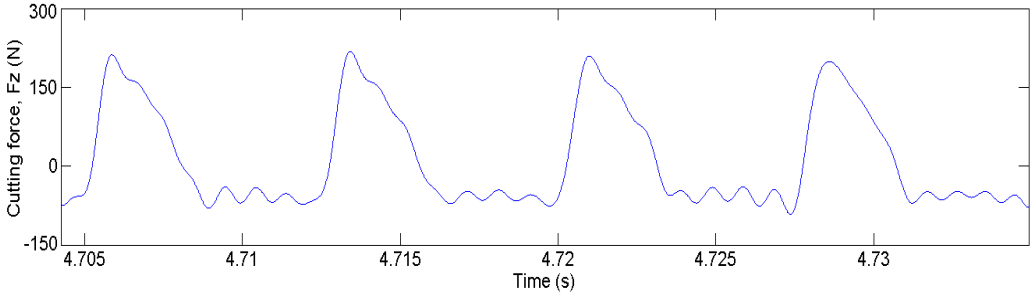

(b)

Figure 4-3. Acceleration signal (a) and filtered cutting force (b) for one revolution of the tool

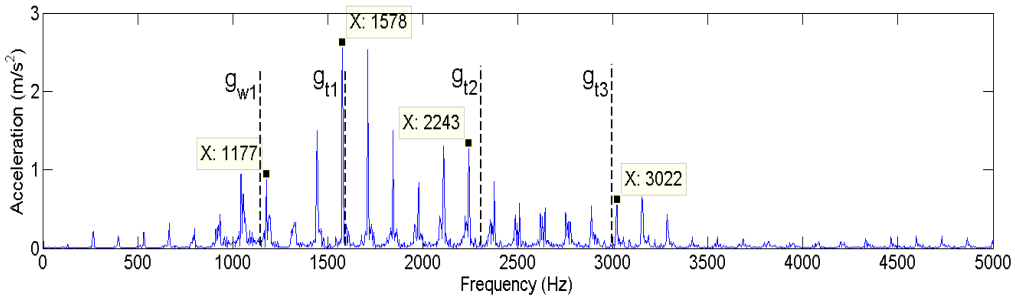

Figure 4-4. FFT of acceleration signal for a_p=2mm, a_e=1mm

In order to analyse the evolution of this frequency content with the engagement and exit of the tool, a time-frequency analysis (STFT) was carried out on the acceleration signal corresponding to one tooth engagement and successive free period of the workpiece. STFT essentially takes FFT over small time data sequentially, applying (Hamming as default) window on each section of data. As amplitude of the data, i.e. colour indication in spectrogram, logarithm of the power spectral density as calculated by MATLAB® spectrogram function is plotted. Figure 4-5 shows a STFT plot for one tooth contact and successive free vibration of the workpiece. Window overlap of 20% is employed. The tool, workpiece and other workpiece system frequencies are marked on the plot. Following observations can be made:

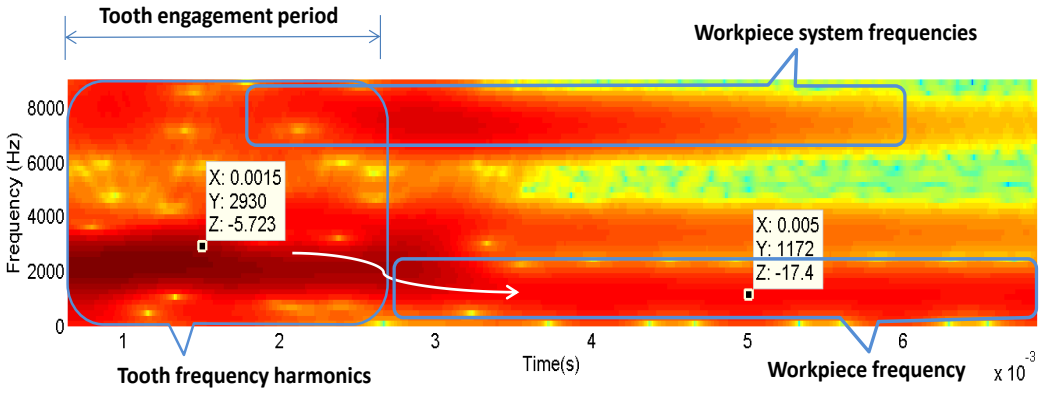

Figure 4-5. STFT plot of acceleration for one tooth contact on straight cantilever (a_p=2mm, a_e=1mm)

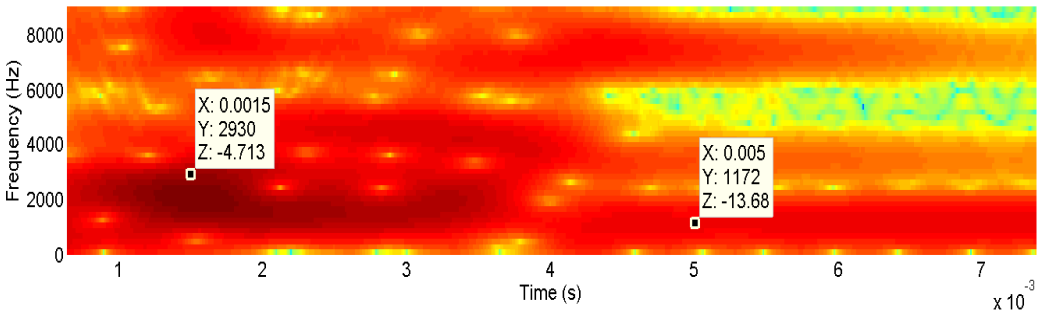

Figure 4-6. STFT plot of acceleration for one tooth contact on straight cantilever (a_p=2mm, a_e=1.5mm)

1. Though the accelerometer is mounted on the workpiece, as long as a cutting tooth is in contact with the workpiece, the harmonics surrounding the cutting tool frequency and other machine tool system frequencies such as that of the toolholder and spindle dominate the frequency spectrum. The lower thickness of the workpiece and the contact pressure between the tool and workpiece during cutting could be the cause for the appearance of tool frequency in the machining spectrum.

2. As the cutting tooth of the tool is disengaged, the group of harmonics surrounding the workpiece frequency (g_{w1}) and the workpiece system frequencies (g_{w4}, g_{w5}) appear in the spectrum. That is, after the disengagement of one cutting tooth and until the second cutting tooth comes into contact, the workpiece and its system vibrate at their natural frequency; this can be clearly observed from Figure 4-5. Also due to the higher stiffness of other parts in the workpiece system such as the dynamometer, etc. their vibration subsides quickly when compared to free vibration of the

workpiece, which continues until the next cutting tooth comes in contact.

3. To study if this behaviour persists with the variation in depth of cut, the acceleration signal acquired at other depths of cut was analysed and a sample result for 1.5mm depth of cut is presented in Figure 4-6. The amplitude of the signal is indicated by Z value marked on the figures. As can be seen a pattern similar to that in Figure 4-5 is observed where the tool's natural frequency dominates during the period of cut and workpiece vibration dominates after the tool leaves the cut. If the pitch between two cutting teeth is reduced, then the cutting tool frequency would dominate most of the machining spectrum.

These observations reinforce the previous finding that tool and other machine tool system frequencies need to be carefully considered when evaluating the dynamic response in thin wall plate milling.

4.2.2 Experimental results on thin wall casing

The thin wall casing as described in section 3.3 was used for coupled dynamic response studies. Peripheral milling operations were carried out along the circumference of the casing, with a wide range of depths of cut (a_p = 0.5 - 2mm, a_e = 0.5 - 2mm) while maintaining a constant cutting speed and feed rate of 40m/min (spindle speed = 800 RPM) and 0.1mm/tooth. Though this particular casing is more suited to a turning operation on the thin wall, a milling operation was chosen to simulate the machining of a real industrial component. These kinds of operations are

now a day widely common due to introduction of multi-tasking machining centres which can perform mill-turn operations in single setup. Similar to that of thin straight cantilever, individual dynamic responses were acquired for both tool and workpiece in the actual machining set up condition. Figure 4-7 (a) and (b) show the drive point frequency response of the tool and casing respectively. The tool FRF has dominant tool modes (f_{t1} – f_{t5}); of which 3092 Hz (f_{t2}) and 14044 Hz (f_{t4}) correspond to the tool's bending and torsional modes that were confirmed in their nature and values by FE simulation tool (here not presented). It is pertinent to note that these high frequencies of 14kHz are measured with same accelerometers (PCB 353B14 and 352C23) which has specified frequency limit up to 10kHz. This is possible because the resonant frequency of accelerometer is 70kHz and hence useful frequency limit can be up to $1/3^{rd}$ of this. Moreover, the accelerometer specification states that linearity up to 10kHz is 5% and up to 25kHz is 10%. This variation is considered acceptable for the present measurements. For the ring type casing, while many drive point responses were acquired for the casing, only one is shown here (Figure 4-7(b)) as an example. It can be seen that the casing exhibits a high modal density with significant number of modes within the measured range of <16 kHz, 1387 Hz (f_{w1}) being the workpiece fundamental mode. Also the casing is about 10 times more flexible than the tool thus, leading to a strong tendency of the workpiece to vibrate.

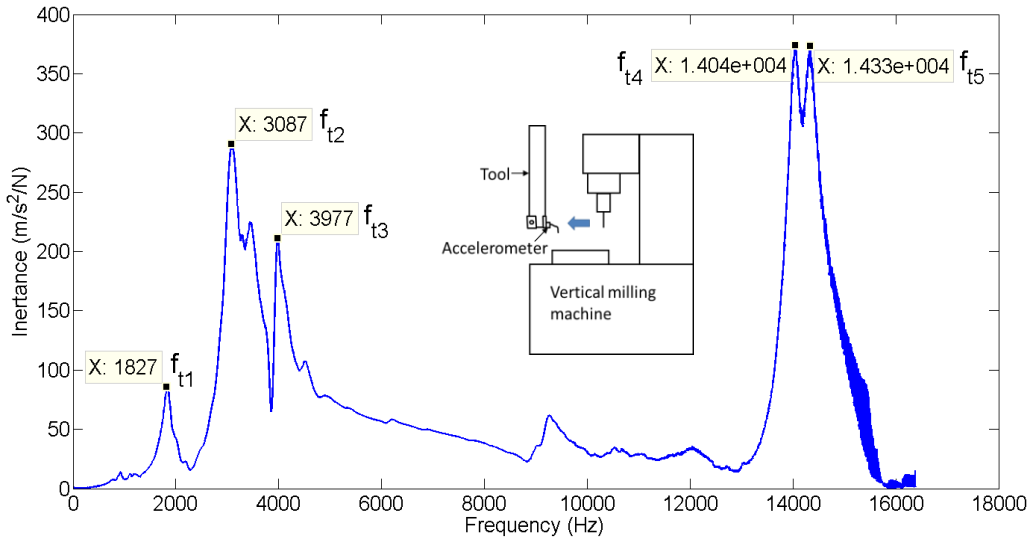

(a)

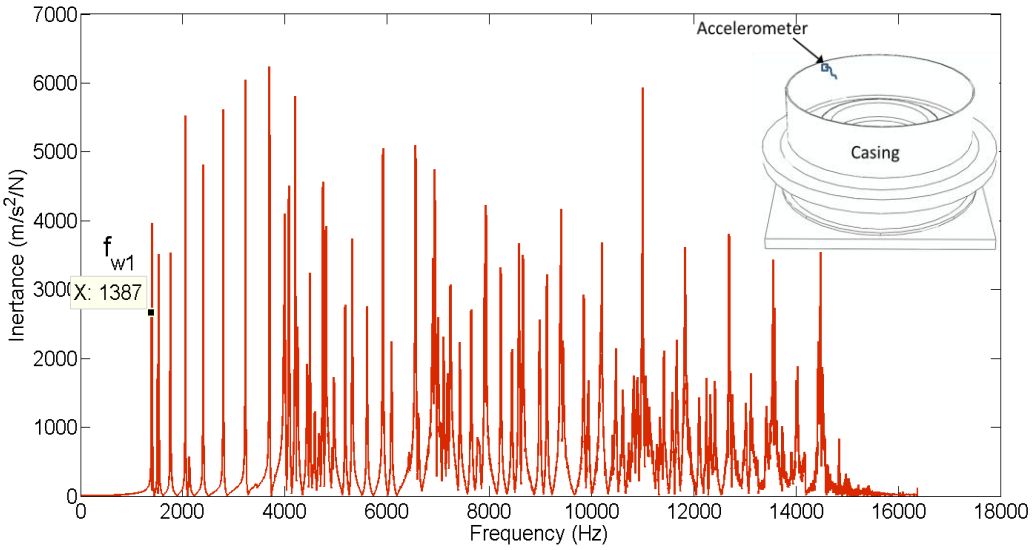

(b)

Figure 4-7. Drive point frequency response of (a) tool and (b) thin wall cylinder workpiece

The cutting force profile for one full rotation of the tool and the corresponding acceleration signal measured on casing are shown in Figure 4-8. FFT of the acceleration signal at the accelerometer, (Figure 4-9), shows a dominant modulation of harmonics of cutting tooth frequency (26Hz) around cutting tool torsional mode (f_{t4}) and also to some extent at the workpiece fundamental frequency (f_{w1}). The pattern

observed is similar to that of thin wall plate, however with the exception that out of whole machine tool system frequencies the cutting tool frequency is significantly dominant at higher axial and radial depths of cut (e.g. a_p=2, a_e=1mm).

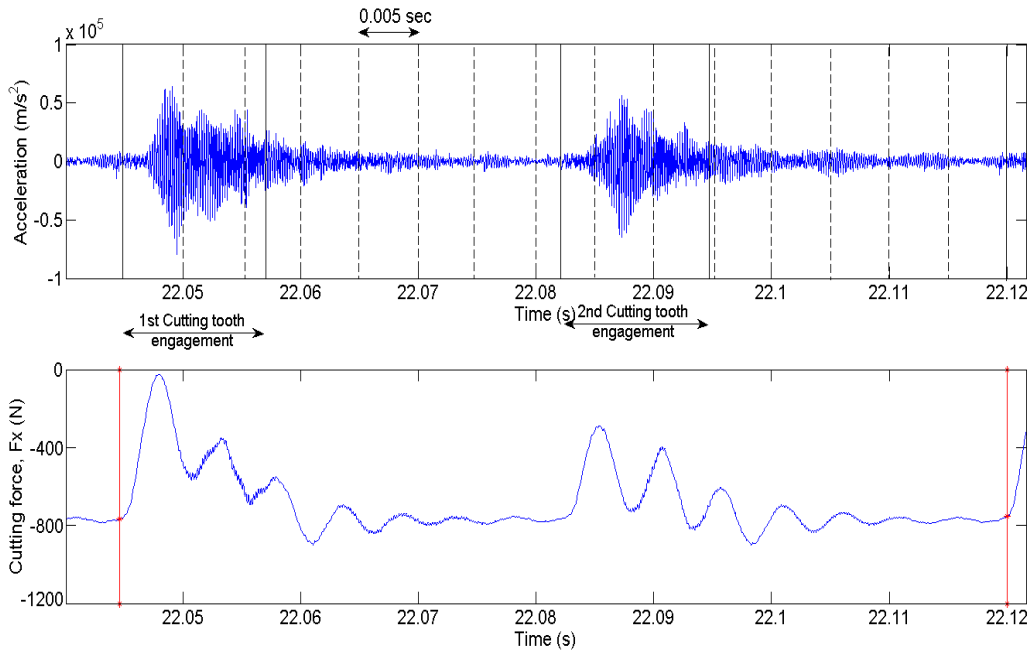

Figure 4-8. Acceleration and cutting force signals on casing for one revolution of tool, a_p=2mm, a_e=1mm

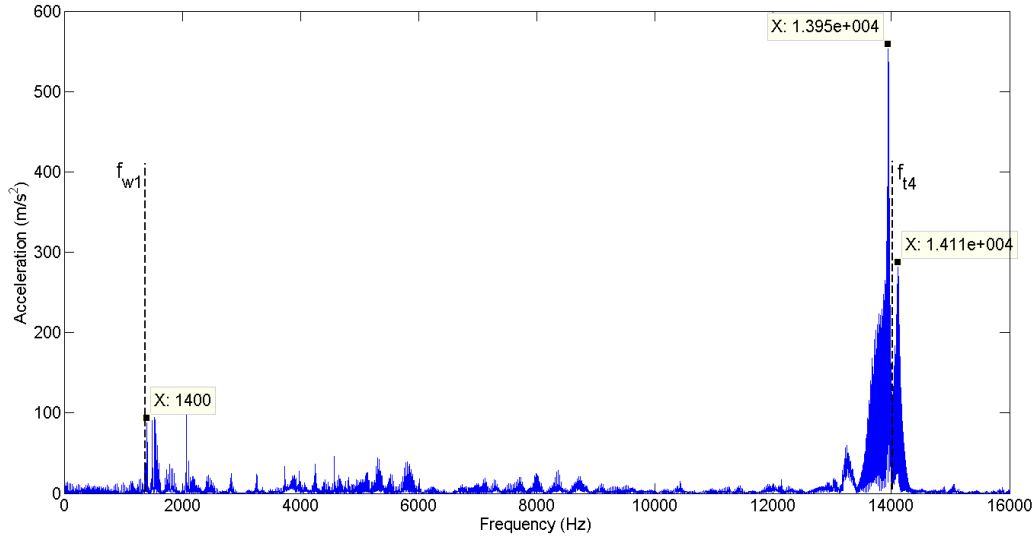

Figure 4-9. FFT of acceleration signal for multiple tool revolutions for a_p=2mm, a_e=1mm

Analysis of the per tooth acceleration data during machining of thin wall casing using STFT was performed and was difficult to analyse as the frequency range of modes present is large (1400Hz – 14000Hz) and also due to trade-off in clarity in time resolution with that of frequency. Hence frequency analysis was performed using FFT. But it is known that time data is lost while doing FFT, that is, the evolution of frequencies with time cannot be identified. To circumvent this problem, FFT is done at various sections of the acceleration data, as shown in Figure 4-8. To obtain sufficient data points for doing FFT, the data is acquired at a higher sampling rate of 10^6 samples per second.

The Fast Fourier Transform is carried out on the acceleration signal at various sections during contact of the tooth with the workpiece and during the successive non-contact period. Figure 4-10(a) shows the evolution of various frequency components as FFT is carried out on the sections shown in Figure 4-8. Before taking FFT, Hann window is applied on each section data and 20% overlap is used. It can be seen that the tool torsional mode, f_{t4} (shown in Figure 4-7(a)), was observed in spectra irrespective of whether the tool is in contact with the casing. The tool mode is dominant until the next cutting tooth engages with the workpiece. This indicates a strong coupling between tool and thin wall casing. It can be seen that due to the presence of small run-out in the tool, the second cutting edge took a lesser depth of cut and hence the acceleration amplitude is less. This also points out that if the depth of cut is less, the workpiece mode starts appearing in the spectrum as shown in the Figure

4-10(a). Figure 4-10(b) shows a similar FFT plot for lower axial (a_p) and radial (a_e) depths of cut – 0.5X0.5mm where it can be noticed that for a lower depth of cut the tool dominant mode is present only during the cutting tooth contact period and the workpiece mode dominates during the tooth non-contact period – an observation similar to that of the thin cantilever plate.

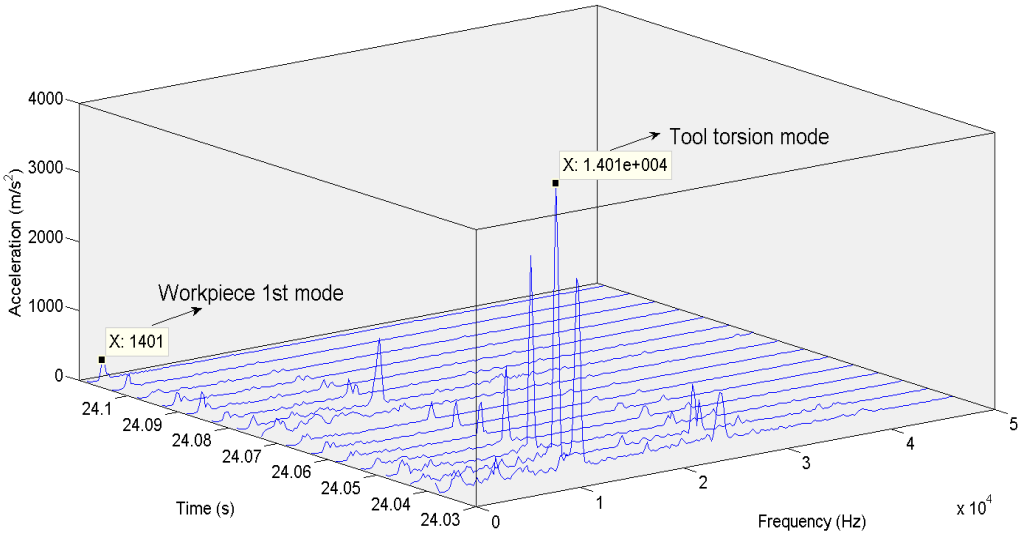

(a)

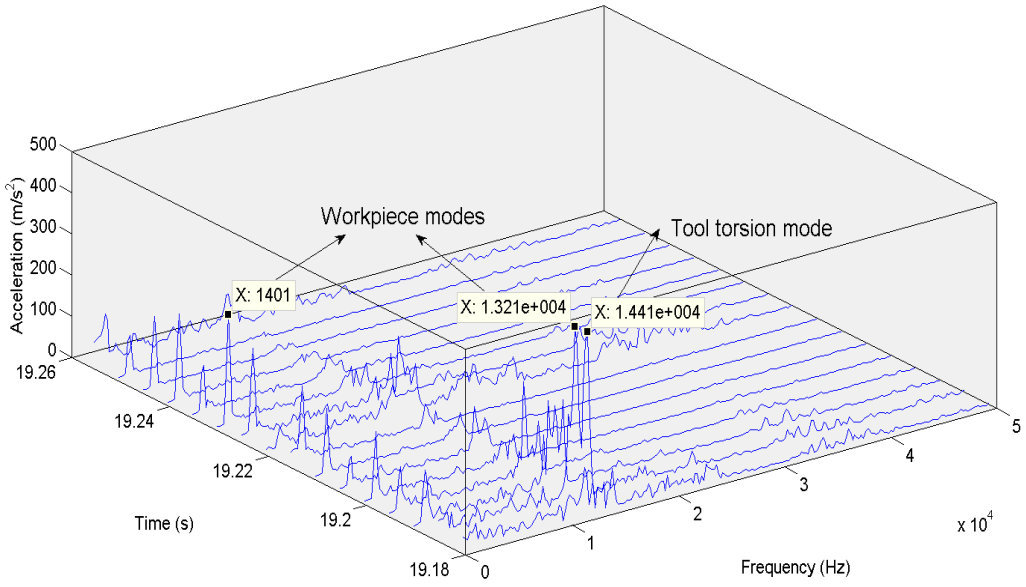

(b)

Figure 4-10. FFT waterfall plot at various 0.005 second sections of acceleration signal (a) a_p=2mm, a_e=1mm (b) a_p=0.5mm, a_e=0.5mm

Hence it can be observed that, there are two major distinctions in the coupled interaction between a closed geometry structure such as ring type casing and an open geometry structure such as thin wall cantilever.

- The depth of cut (both radial and axial) has much significant influence on the impact dynamics for a closed geometry as compared to an open geometry structure. The former exhibits complete dominance of tool mode at higher depths of cut and at lower depths of cut a mix of tool mode during engagement and workpiece mode during free vibration are seen. The open geometry structure on the other hand always exhibits both tool and workpiece modes of relative magnitude in a spectrum, at any depth of cut. As shown in Figure 4-5, for a thin wall cantilever even at depths of cut of a_p=2mm, a_e=1mm, the pattern of tool mode during contact and workpiece mode during non-contact are evident. This could be due to the inherent stiffness offered by the casing due to its closed geometry unlike cantilever which is relatively less stiff due to its open geometry.
- In closed geometry structure (thin wall casing) the torsional mode of tool is coupled at all depths of cut unlike in thin wall plate where the bending mode is coupled. This is again due to inherent stiffness in tangential direction of casing and hence exciting the torsional mode of tool with sufficient energy.

The above-mentioned results were also verified for different tool overhangs, e.g. 46mm and 65mm and hence different tool natural

frequencies. The dominant mode that appeared in the spectrum always corresponded to the tool torsional mode for a higher depth of cut and to both tool torsional and workpiece modes for a lower depth of cut.

4.3 Conclusions

This chapter presents the experimental identification of coupled interaction of tool and workpiece dynamic responses during machining of thin wall structures. In the research literature available till now, there is no reporting on the coupled interaction of tool and workpiece – either for thin wall or solid rigid parts. Only one research paper mentioned that cutting tooth harmonics are modulated at workpiece frequencies. However, in this work, through analysis of machining vibration signal in frequency domain it is shown that in addition to workpiece frequencies, tool frequencies also dominantly modulate the cutting tooth harmonics. And that this depends significantly on the depth of cut employed. Higher depths of cut modulate the cutting tooth harmonics more with tool frequency and lower depths of cut modulate it with both tool and workpiece frequencies. Another significant finding in this work is the type of coupling between a thin wall workpiece and tool. For an open geometry structure such as straight cantilever thin wall, the bending mode of the tool couples with that of the workpiece. Whereas for a closed geometry structure such as a thin wall casing the torsional mode of the tool couples with that of the workpiece. These findings are of importance while developing an analytical or numerical model of the milling impact dynamics on a thin wall structure.

5 Finite element modelling of test casing and its experimental validation

5.1 Introduction

Mounting the dampers on a thin wall structure modifies its dynamic response – by modifying its damping, stiffness or mass depending on its specific contribution to each of these parameters. In manufacturing applications it is the end effect due to modification of these parameters that is of major interest. For example, reduction in vibration during machining or absence of chatter, etc. might be parameters of interest. However, an understanding of the effect of the mounted damping solution on the dynamic response variation of the structure is useful not only for better understanding of the mechanism of damping but for developing a simulation tool which can predict the effectiveness of damping.

A numerical finite element simulation was developed to achieve these two objectives. In chapter 4 it is seen that while machining a thin wall casing with an endmill, the tool mode and workpiece mode participate in the machining vibration. At higher depths of cut, the dominance of the tool mode is significant and at lower depths of cut, the workpiece fundamental mode is dominant. Hence, in finishing operations which have typically lower depths of cut, the workpiece fundamental mode would be dominant, although tool mode presence can be observed. To simulate the same effect, one has to model the thin wall workpiece and the tool to capture the dynamics of both the systems. However, considering that most of the thin wall applications require finishing operations, present research focusses

on modelling the thin wall workpiece alone. For developing a complete dynamic system of machining one can, in future, extend this model by modelling the dynamics of tool also.

The basic steps followed in the FE analysis are explained in section 3.5.1. The following sections present the FE modelling of the thin wall casing, evaluation of its dynamic properties (natural frequencies and mode shapes), and experimental validation of the FE results through impact hammer testing. The FE predicted harmonic response is compared with experimentally measured frequency response function (FRF). Thus the accuracy of the FE model of the casing used in this research is validated.

5.2 FE modelling of test casing

5.2.1 Detailed modelling of casing

The test casing as described in section 3.3 is modelled using the commercial finite element software Abaqus®. The casing was modelled as a solid of revolution (shown in Figure 4-7) and the fixture plate as an extruded solid. The reason for modelling the fixture plate is to see if any of the fixture modes are dominant as compared to the casing thin wall modes. The casing was assigned material properties of a Nickel based superalloy – Waspaloy™ and the fixture plate was assigned that of mild steel. The data taken from Matweb [71] is reproduced in Table 3-3. The casing is meshed using a combination of quadratic hexahedral elements with reduced integration (C3D20R) and quadratic tetrahedral (C3D10M) elements to avoid phenomena such as shear and volumetric locking [72]. This combination of elements in the mesh is necessary due to the creation of

circular partitions on the bottom flange of the casing, equal to the bolt sizes, as shown in Figure 5-2. Moreover, to generate the hexahedral elements, the casing is partitioned into eight sectors as can be seen in Figure 5-2. These partitions are fixed to the fixture plate through a 'tie' constraint to simulate a bolted joint; the fixture is meshed using C3D20R elements.

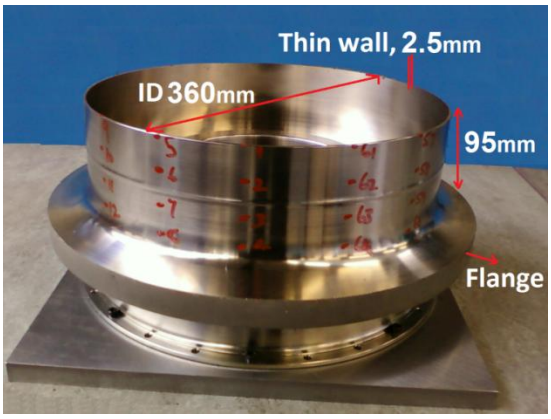

(a)

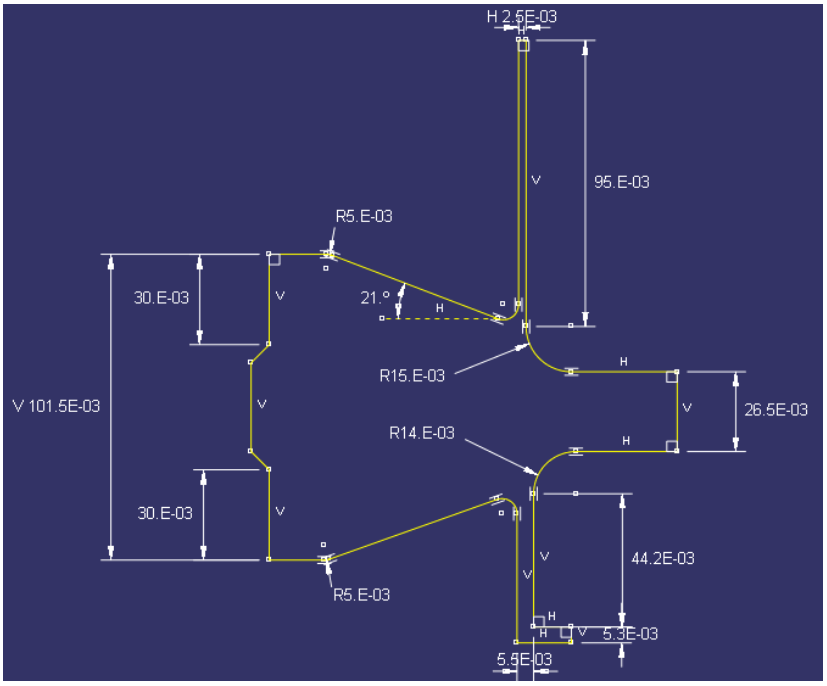

(b)

Figure 5-1. Test casing (a) section of revolution for FE modelling of casing

Table 5-1 Material properties used in Abaqus®

	Waspaloy™ (Casing)	**Mild steel (Fixture plate)**	**Units**
Density	8200	7860	Kg/m^3
Modulus of Elasticity	213	202	GPa
Poisson ratio	0.3	0.29	

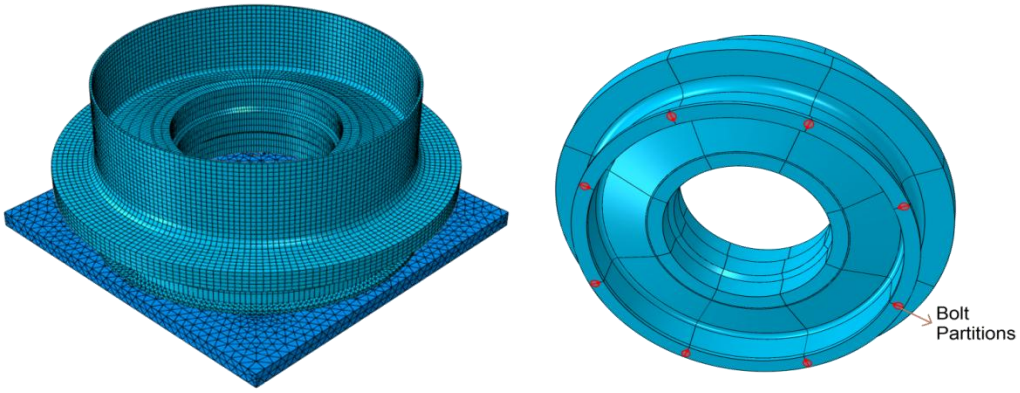

Figure 5-2. Finite element model of the casing with fixture plate (a) bottom view of casing showing partitions used as bolt surfaces which are tied to fixture plate

The mesh refinement was selected based on extensive convergence studies of natural frequencies. As most of the modes observed are circumferential modes of the thin shell of the casing, the number of elements on the casing thin wall periphery is chosen for mesh refinement, which provides a direct indication of the highest possible mode that can be captured. Four different mesh sizes were studied: 96, 160, 200 and 240 elements along the casing periphery and the mesh size that gives similar natural frequencies over successive mesh refinements was chosen. From

Table 5-2, it can be seen that a mesh refinement of 200 elements along the periphery is capable of representing all modes with sufficient accuracy.

Table 5-2 Variation of natural frequencies with mesh refinement

Mode no. [Hz]		Number of elements along casing periphery			
		96	**160**	**200**	**240**
	1	1287.5	1289.7	1290	1290.2
	2	1332.5	1334.3	1334.7	1334.7
	3	1384	1386.5	1387	1387

5.3 FE modal analysis

Modal analysis was carried out using the frequency extraction step in Abaqus®, as explained in section 3.5.1.1. Lanczos solver was used as it has the most general capabilities such as computation of modal damping factors and modal participation factors [72]. The boundary conditions used while evaluating the modal frequencies are similar to those in the machining set up (shown in Figure 5-3), which allows a true representation of the casing in the actual operation condition.

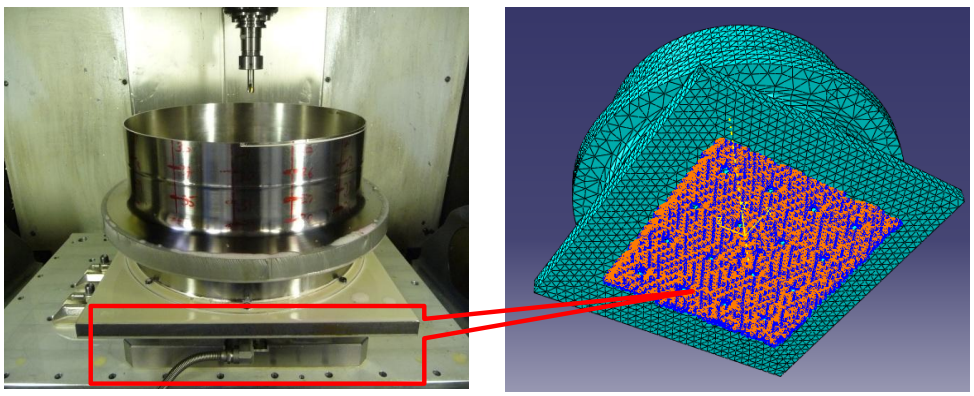

Figure 5-3. Machining set up for the casing and corresponding FE boundary condition where the area corresponding to the dynamometer is fixed

Some of the important observations from the modal analysis of casing are as follows:

1. The fundamental modes of the casing involve only its thin wall, Figure 5-4, as it has highest tendency to vibrate than the hub or the casing as a whole.
2. Being symmetrical in shape, the circular thin wall has repeated roots: the same frequency with different mode shapes which are orthogonally separate. For example, for the first fundamental frequency the mode shape has 6 circumferential waves (shown in Figure 5-4(a)). Its symmetric shape has 90/6 = 15 degree rotation of wave shapes.

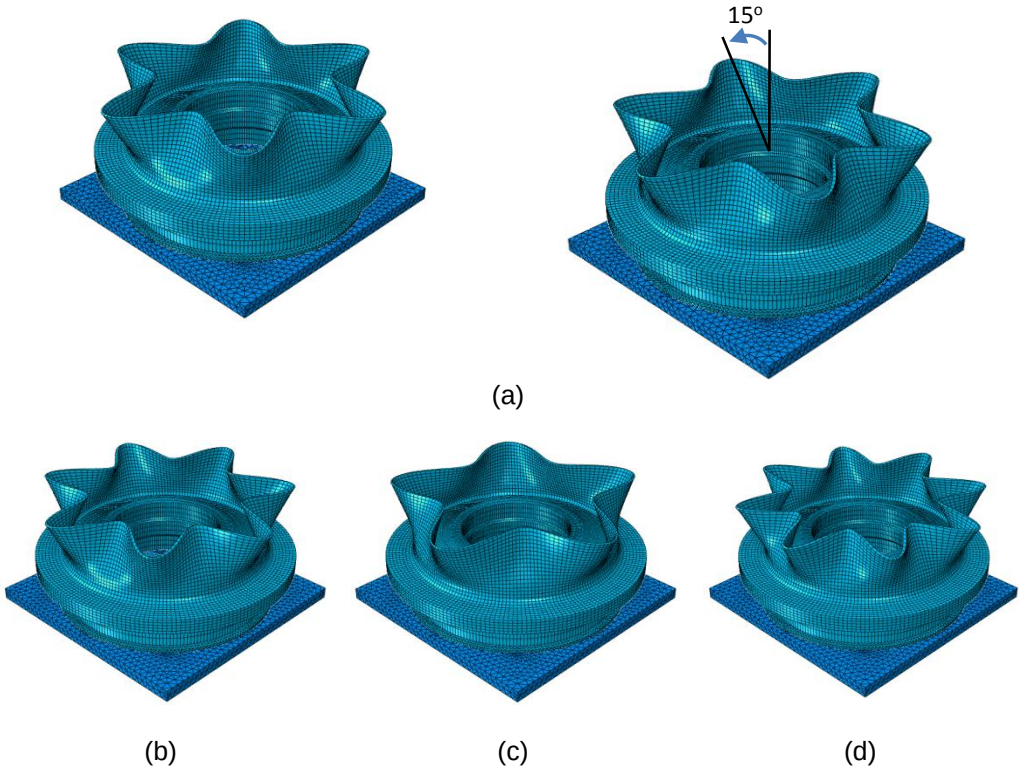

Figure 5-4. (a) First fundamental mode shape and its symmetric mode – 1290.2Hz; (b) Mode shape 2 – 1334.7Hz; (c) Mode shape 3 – 1387Hz; (d) Mode shape 4 – 1496.4Hz

The pattern in which the number of waves in mode shapes appears corresponds to typical shell characteristics. For example, as can be observed from Figure 5-4, mode shape 1 has six circumferential waves, mode shape 2 has seven, and mode shape 3 has five, and so on. Also at higher frequencies, the number of axial half waves increase and the same number of circumferential waves repeat again, as shown in Figure 5-5. When the number of circumferential waves is plotted against the frequencies at which they occur, a typical cup-shaped plot is obtained. This is shown in Figure 5-6, along with a similar plot obtained using an analytical shell (Flügge's) theory as given in [73]. The analytical curve is plotted for a different ordinate axis value, Ω – called the fundamental frequency parameter, which is given by Eq. 5-1.

$$\Omega = \omega R\sqrt{(1-\nu^2)/E} \qquad \text{Eq. 5-1}$$

where R is the radius of the casing, ν is Poisson ratio, and E is Young's modulus.

However, in this equation, as the parameters other than ω are constant for a given casing, it is pertinent to compare the plots. Also various curves are plotted for the (l/mR) parameter in which 'm' in the denominator indicates the number of axial half waves. Hence, a decreasing value of (l/mR) indicates an increasing value of the axial number of half waves, for a casing of a given length (l) and radius (R). The similarity in the profile of the curves in Figure 5-6 shows the accuracy of FE prediction of the frequencies for this shell type of casing. Further validation of the FE

prediction will be presented through experimental modal analysis, to be presented in section 5.5.

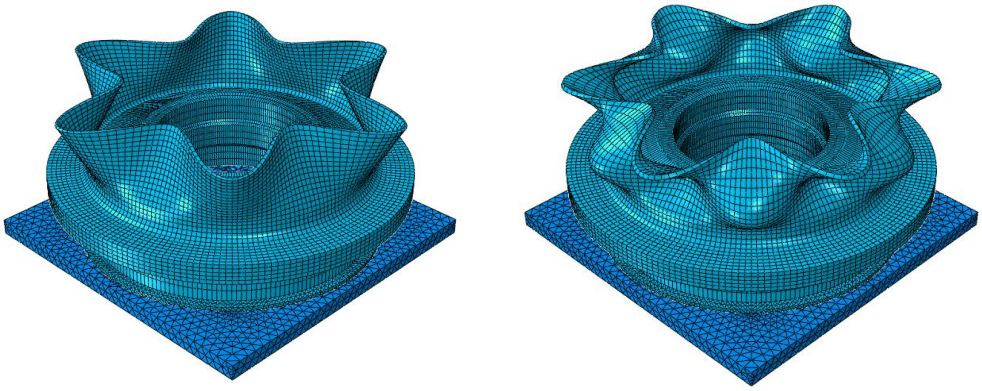

Figure 5-5. Mode shapes with the same number of circumferential waves but different axial half waves

5.4 Simplified modelling of thin wall

From the results of modal analysis, as the fixture plate modes are not seen as significantly dominant within the range of this study and since most of the modes correspond to only the thin wall of the casing, a simplified FE model with only a thin wall is generated. The simplified thin wall FE model is shown in Figure 5-7. To replicate the boundary conditions of a thin wall with a hub as accurately as possible, a ring of elements from the hub are retained. This ensures that the inertia of elements at the base of the thin wall is similar to that of the original full casing. All the remaining material properties are retained as that of full casing.

Modal analysis was carried out with the elements at the base of the simplified thin wall fixed. The first three mode shapes are shown in Figure 5-8 and a comparison of frequencies for the first 10 modes for the detailed and simplified models are shown in Table 5-3. These frequencies will be

compared against experimentally measured frequencies using impact hammer testing.

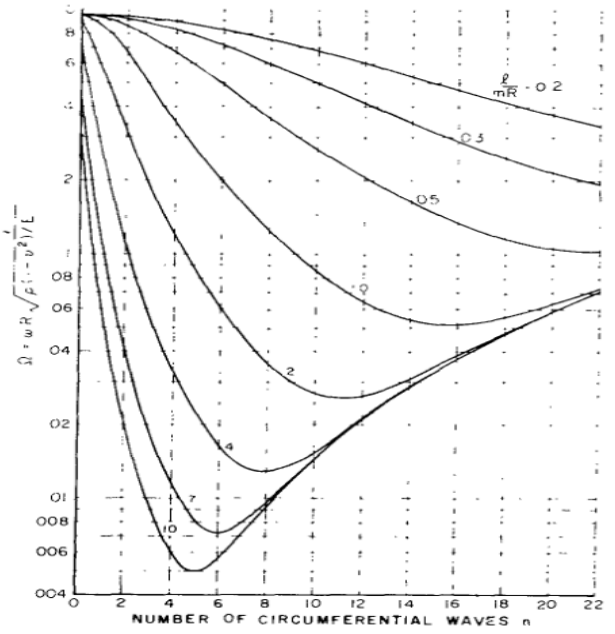

Variation of the fundamental frequency parameter Ω with n; Flügge theory, $\nu = 0.3$, $R/h = 2000$.

(a)

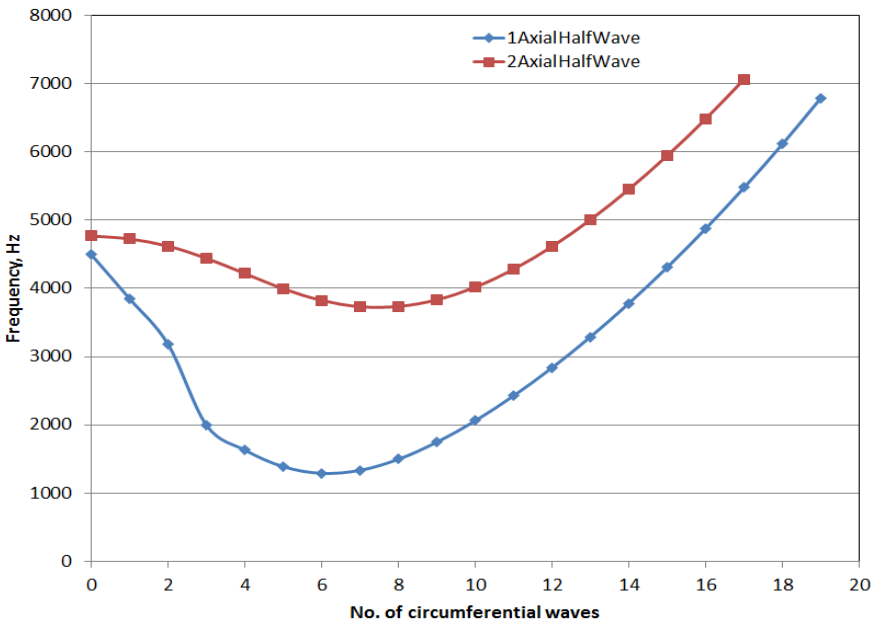

(b)

Figure 5-6. Plot of circumferential waves in mode shape against frequency: (a) Analytical plot given in reference [73] (b) FE plot for the casing used in this research (R/h = 72 and l/mR=0.26&0.52)

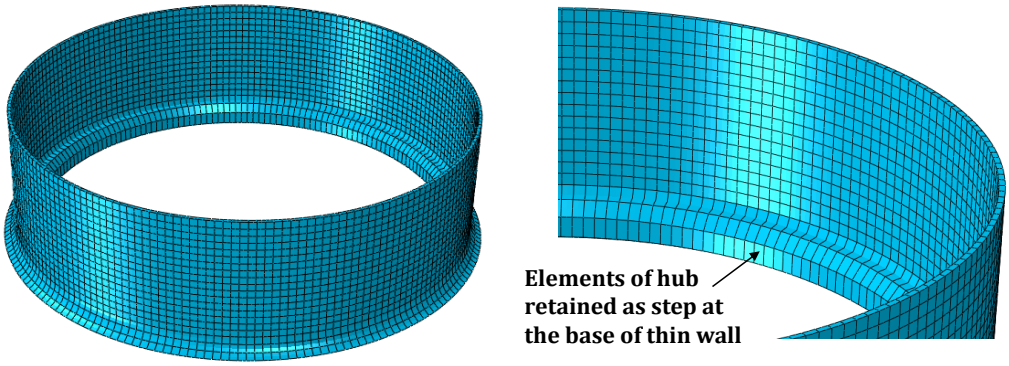

(a) (b)

Figure 5-7. Simplified FE model with only thin wall of casing (a) Geometry (b) Close up of the model showing elements of the hub retained as a step

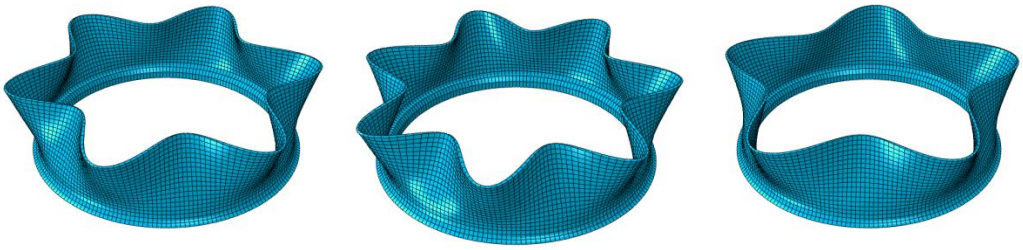

(a) (b) (c)

Figure 5-8. Mode shapes of simplified thin wall: (a)Mode1 – 1347Hz; (b) Mode2 – 1371Hz; (c) Mode3 – 1472Hz

Table 5-3 Comparison of frequencies for detailed casing model and simplified thin wall model

Mode	Full casing (Hz)	Simple thin wall (Hz)
1	1290.2	1347.4
2	1334.7	1371.7
3	1387.0	1472.8
4	1496.4	1520.6
5	1629.5	1683.2
6	1745.6	1763.0
7	1994.4	2058.1
8	2059.9	2074.7
9	2426.1	2441.1
10	2837.0	2854.5

5.5 Experimental modal analysis of undamped casing

5.5.1 Modal analysis procedure

The frequencies predicted through finite element analysis are validated through experimental modal analysis. In section 3.4, the methodology for measuring the dynamic response using an impact hammer was explained. Modal analysis is a process whereby a structure is described in terms of its natural characteristics which are frequency, damping, and mode shapes. Often, measuring the dynamic response at only one or two points may not reveal all the frequencies, as the points chosen for excitation and response measurement may fall at nodal points where the structural response is very low. Moreover, to obtain the mode shapes of the structure at different frequencies, responses have to be acquired at multiple points. These multiple response curves, known as Frequency Response Functions (FRFs), are then curve fitted using various algorithms either in time or frequency domains. This procedure of curve fitting of responses is called modal parameter estimation. The modal parameters which are estimated are: natural frequency, damping and residues. The equation of frequency response for a multi degree of freedom system with structural damping is given as shown in Eq. 5-2 [74].

$$\propto_{jk}(\omega) = \sum_{r=1}^{N} \frac{rA_{jk}}{\omega_r^2 - \omega^2 + i\eta_r\omega_r^2} \qquad \text{Eq. 5-2}$$

where α_{jk} = receptance form of frequency response

ω_r = natural frequency of r^{th} mode

η_r = structural damping factor

$_rA_{jk}$ = residue of r^{th} mode between j^{th} excitation and k^{th} response points

The information about the mode shapes is contained in the numerator i.e. in the modal residues. Modal residues are functions of the input force location, output response location and also the mode in question. So a modal residue for a particular mode r is defined as the product of mass normalised mode-shape vectors at a given input location 'j' and a given response location 'k'.

Thus, the modal residue $_rA_{jk}$ is given by Eq. 5-3.

$$rA_{jk} = \varphi_{jr}\varphi_{kr} \quad \text{Eq. 5-3}$$

where

φ_{jr} and φ_{kr} are mass normalised mode shape vectors at j^{th} and k^{th} locations.

Usually the modal parameter estimation software uses a partial fraction representation of the frequency response equation as shown in Eq. 5-4 [75].

$$h_{ij}(j\omega) = \sum_{k=1}^{N}\left(\frac{r_{ijk}}{(j\omega - \lambda_k)} + \frac{r^*_{ijk}}{(j\omega - \lambda^*_k)}\right) \quad \text{Eq. 5-4}$$

where

* denotes complex conjugate

λ_k = pole value for mode k and is given by Eq. 5-5.

$$\lambda_k = -\zeta_k\omega_{nk} + j\omega_{nk}\sqrt{1-\zeta_k^2} \quad \text{Eq. 5-5}$$

where

ω_{nk} = undamped natural frequency of mode k

ζ_k = damping ratio of mode

The residue is expressed as product of three terms as shown in Eq. 5-6.

$$r_{ijk} = a_k v_{ik} v_{jk} \quad \text{Eq. 5-6}$$

where

v_{ik} = mode shape coefficient at response DOF i of mode k

v_{jk} = mode shape coefficient at reference DOF j of mode k

a_k = a complex scaling constant, whose value is determined by the scaling of the mode shapes

The main process of parameter estimation consists of adjusting the parameters in the model, so that the data predicted by the model curve-fit the measured data as closely as possible.

While the measured frequency response functions are directly curve fitted in the frequency domain, for time domain methods they are converted to impulse response functions using inverse FFT algorithms. Usually, time domain methods are used for lightly damped structures and frequency domain methods for heavily damped structures. The reason being that time domain presents more data for lightly damped structures whereas frequency domain for heavily damped structures, as shown in Figure 5-9. Commercially available modal analysis software has algorithms employing both of these methods. For example, Least Square Complex Exponential (LSCE) is a time domain method and Least Square Frequency Domain (LSFD) and Frequency Domain Direct Parameter Identification (FDPI) are frequency domain methods. The description of the algorithms for each of these methods can be found in the software theory manuals.

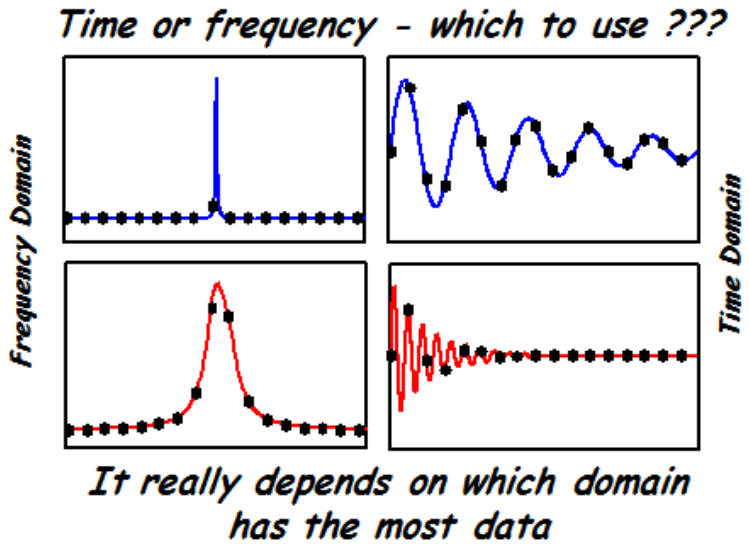

Figure 5-9. Application scope of time and frequency domain curve fitting for modal parameter estimation [76]

One useful tool which is employed to determine the optimum number of modes while curve fitting the frequency responses is the stabilisation diagram. The stabilisation diagram is a visual presentation of the frequency location of the estimated modal frequencies, as a function of increasing model order (number of modes), plotted on a background of an FRF [77]. Symbols are used to represent whether successive estimates of modal parameters, using the next higher model order are stable are not. The conditions on which stability is evaluated are presented in Table 5-4 and the symbols shown in Figure 5-10 [75]. The tolerance on each of these parameter values, to determine if they are stable are not, can be set. For example, 5%, 1%, and 2% variation in damping, frequency and vector values respectively. The vector parameter here refers to a mode shape such as an Eigen vector or a modal assurance criterion which measures the uniqueness of the mode shape compared to all other mode shapes.

Table 5-4 Description of symbols on the stabilisation diagram [75]

Symbol	Description
o	The pole is not stable
f	The frequency of the pole does not change within the tolerances
d	The damping and frequency of the pole does not change within the tolerances
v	The pole vector does not change within the tolerances
s	Both frequency, damping and vector are stable within the tolerances

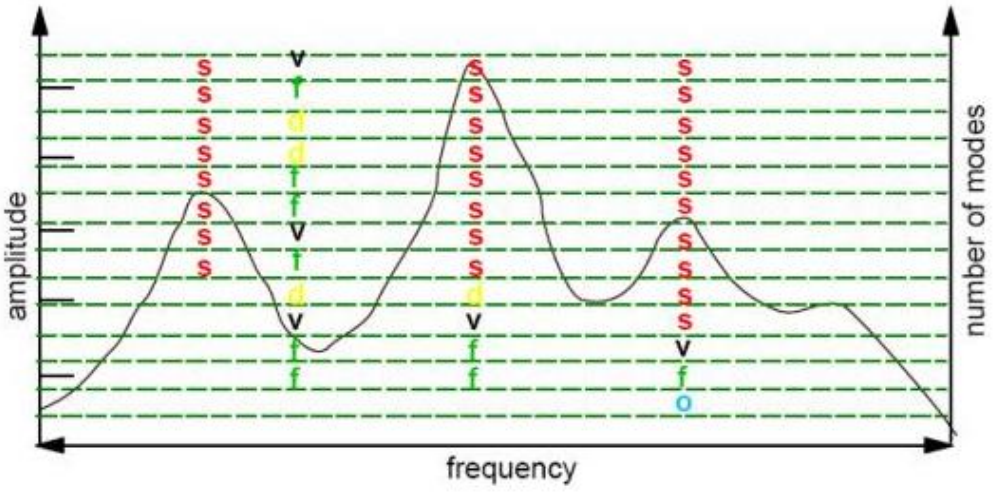

Figure 5-10. Stabilisation diagram [75]

While the stabilisation diagram helps in identifying the modes on the frequency response curves, they also indicate many computational (i.e. mathematical, non-true) modes. This clutters the stabilisation plot and makes it difficult to distinguish the modes, as shown in Figure 5-11 (a). Recently, however, the software has incorporated a new parameter

estimation technique that curve fits in Z-domain: a frequency domain model derived from a discrete time model as shown in Eq. 5-7. Complete algorithm details can be found at [78]. This algorithm is called POLYMAX by the LMS Test.Lab Modal Analysis software [79] and Z-polynomial method by the ME'scopeVES software [80]. An improved stabilisation diagram with the POLYMAX method is shown in Figure 5-11 (b).

$$z = e^{-j\omega\Delta t} \qquad \text{Eq. 5-7}$$

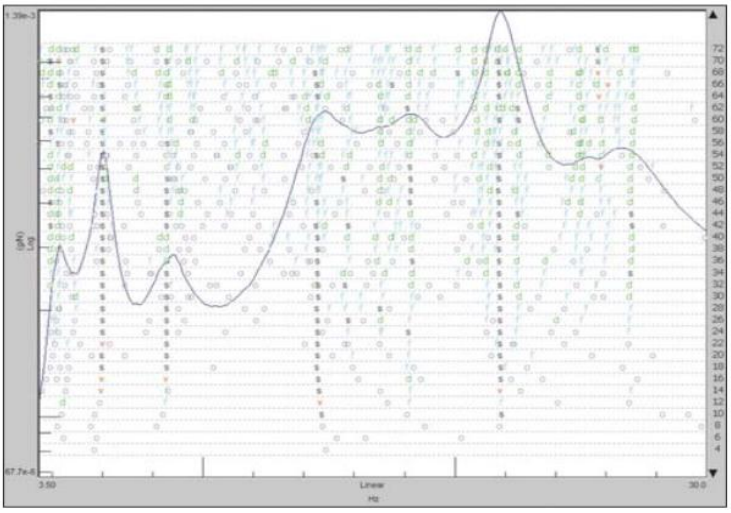

(a)

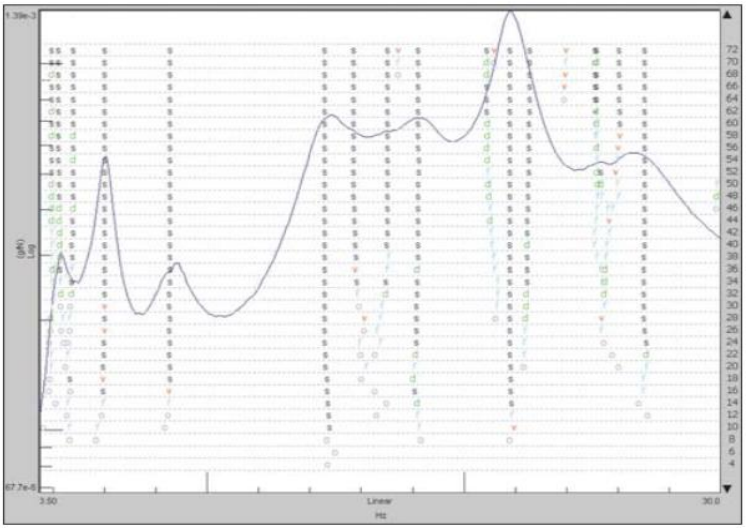

(b)

Figure 5-11. Stabilisation diagrams: (a) LSCE method (b) POLYMAX method [78]

The benefits of this Z-domain model are:

- It can deal with a large frequency range and very large model orders thereby speeding up the estimation process
- The computational or non-physical poles are estimated with a negative damping ratio so that they can be excluded before plotting them, thus providing a clean stabilisation diagram
- As this method depends on a frequency domain model derived from a discrete time model, the limitation that the frequency domain should be used only for heavy damping and that the time domain has to be used for lightly damped structures is no longer valid

Due to the above advantages, the Z-domain method is used in this research for estimating the model parameters.

Another useful tool which helps in identifying the modes from the frequency response curves is the Mode Indicator Function (MIF). MIFs are frequency domain functions that exhibit local minima at the natural frequencies of real normal modes. Basically the mathematical formulation of the MIF is that the real part of the FRF is divided by the magnitude of the FRF. As the real part rapidly passes through zero at resonance, the MIF generally tends to have a much more abrupt change across a mode. The real part of the FRF will be zero at resonance and therefore the MIF will drop to a minimum in the region of a mode [81]. The number of MIFs that can be computed for a given data set is equal to the number of input locations that are available. The so-called primary MIF will exhibit a local

minimum at each of the structure's natural frequencies. The secondary MIF will have local minima only in the case of repeated roots. Depending on the number of input (reference) locations for which data is available, higher order MIFs can be computed to determine the multiplicity of the repeated root. This feature is very useful for symmetric structures such as the casing where repeated roots exist – the same frequency but a different mode shape pattern, as shown in Figure 5-4(a). So a root with a multiplicity of four will cause a minimum in the first, second, third and fourth MIF, for example. There are several types of mode indicator functions such as multivariant, complex, imaginary, real MIFs, etc. A detailed explanation of their physical meaning and their application is given in the software theory manuals [75]. Figure 5-12 [81] shows the FRF with two mode indicator functions due to two references plotted on it. It can be seen that where there is a repeated root, there is a dip in both the MIFs.

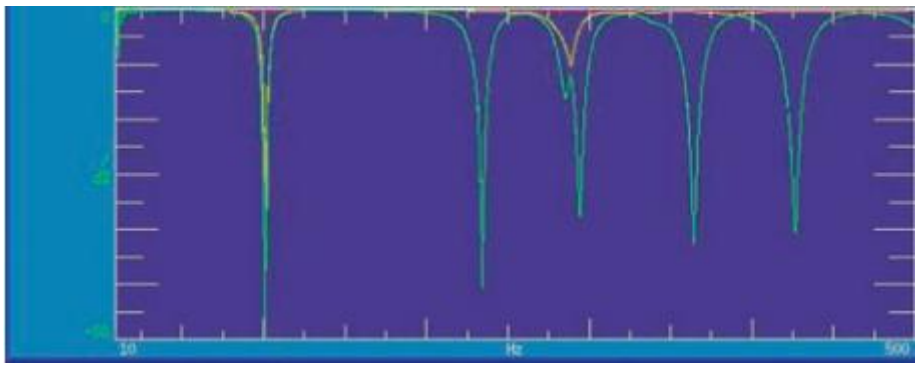

Figure 5-12. Multiple MIFs showing repeated roots [81]

5.5.2 Modal analysis of casing

Modal analysis was carried out on the casing used in this research to identify the natural frequencies and mode shapes and thereby validate the finite element model developed. The modal testing was carried out in the actual machining set up on the machine, as shown in Figure 5-13. Of the total casing, the thin wall portion is only modally active, i.e. actively participates in the vibration. This is clear from the FE prediction results where the mode shapes involving only thin wall casing are significant. This is also justified as the casing has a sturdy mass at its base (76kg) and this makes the vibration study relevant only to the thin wall (4.47kg). Hence, the modal testing was carried only on the thin wall, as shown in Figure 5-13, and the corresponding geometry modelled as a cylinder in the modal analysis software, as shown in Figure 5-14, in a cylindrical coordinate system.

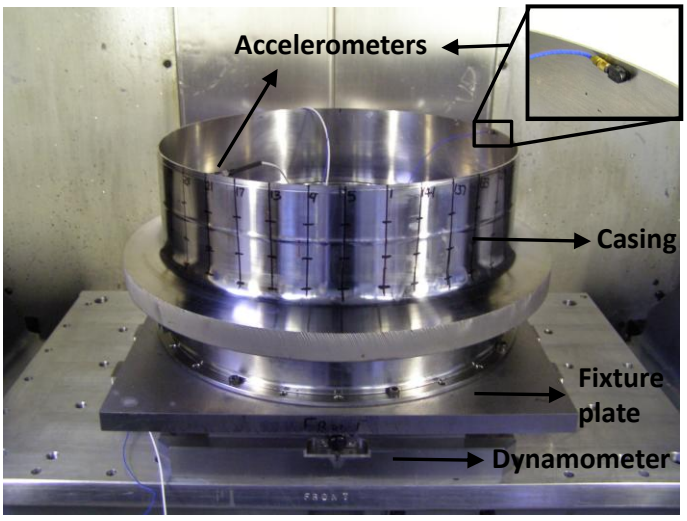

Figure 5-13. Test casing in the experimental modal test set up

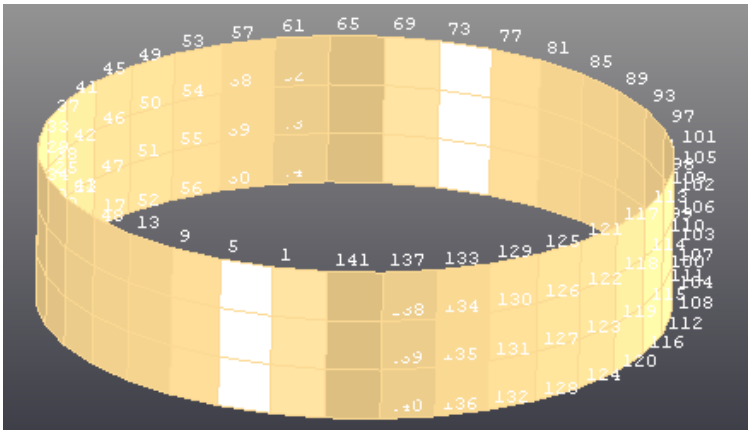

Figure 5-14. Casing thin wall geometry modelled in modal analysis software

The casing thin wall was discretised into 36 sections circumferentially and 4 sections longitudinally as can be seen in Figure 5-14. This grid size was decided after studying the mode shapes in the finite element analysis. As the height of the thin wall of the casing is small when compared to the diameter, the casing has a relatively easier tendency to vibrate at higher order circumferential modes as compared to the axial direction. This can be observed from the fact that up to 6000Hz, seventeen circumferential and second axial modal orders are noticed. To obtain minimum 4 points per circumferential wavelength and considering mode shapes up to 9 circumference waves, 36 points would be needed circumferentially. Similarly to capture a second order axial mode, four axial sections are needed. Therefore, a total of 36X4 = 144 points are used to acquire the responses. That is 144 locations are excited using an impact hammer. To average out the variations in excitation, five responses are acquired at each node.

Considering the symmetric nature of the thin wall, to capture the repeated roots (symmetric modes), two accelerometers are mounted (shown in Figure 5-13) to capture two responses for every excitation point. Responses are acquired using the Prosig DATS Acquisition software. Initial checks are made before acquiring responses such as checking the presence of anti-resonance peaks between every two resonance peaks, checking that all peaks in imaginary form of the frequency response have the same sign, reciprocity of responses, etc. Also, while acquiring each of the responses, it is ensured that coherence of the acquired signal is near to unity (>0.9) at all resonance peaks. Figure 5-15 shows one of the drive point FRF with coherence overlaid on it. It can be seen that the acquired signal coherence is close to unity over a wide range for all the resonance peaks. The drop in coherence after 10kHz is due to the poor (non-flat) force spectrum. Though the used steel tip of the impact hammer theoretical flat spectrum of force is up to 8kHz, it can be expected to give a good response up to 12kHz. However, in this case, the steel tip had to be covered with an insulation tape so as to avoid the ground loop problem which existed on all the machine tools in the workshop due to poor ground connection. Attaching an insulation tape ensured very good coherence but reduced the flat spectrum of the force signal. However, as the frequency range of interest is only up to 5-6kHz, this is not considered to be a problem.

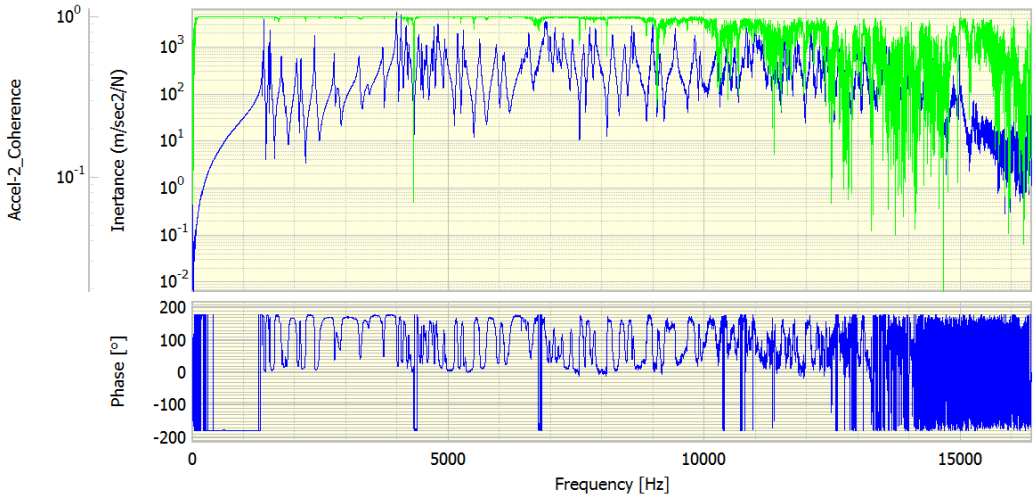

Figure 5-15. Drive point FRF with coherence overlaid on it

After acquisition of the responses, post-processing of results was done such as assigning the measured responses to each of the nodes on the casing geometry in the modal analysis software, defining reference node responses, etc. the LMS Test.Lab Modal Analysis software was used for modal parameter estimation. As explained in section 5.5.1, the Z-domain parameter estimation algorithm (POLYMAX) was used for estimating the parameters. A snapshot of the FRF (red colour) with the stabilisation diagram and the mode indicator functions (blue and green curves) is shown in Figure 5-16. It can be seen that wherever repeated roots appear, the second mode indicator function (blue colour) also dips indicating the presence of a mode. Curve fitting is basically a two-step process with the first step involving estimation of the frequency and damping parameters and the second step involving calculating the residues. While calculating residues the effect of the upper and lower residuals is considered – that is the effect of modes that are not considered on the upper and lower sides of the curve fitted band will be accounted for. The upper residuals account

for lower effects of the upper modes only. That is, the upper residual accounts stiffness line (below the frequency effect for a SDOF FRF) of the upper modes. Similarly, the lower residuals account for the mass line (above the frequency effect for SDOF FRF) of lower modes. Detailed explanations of this can be found in the software theory manuals [75].

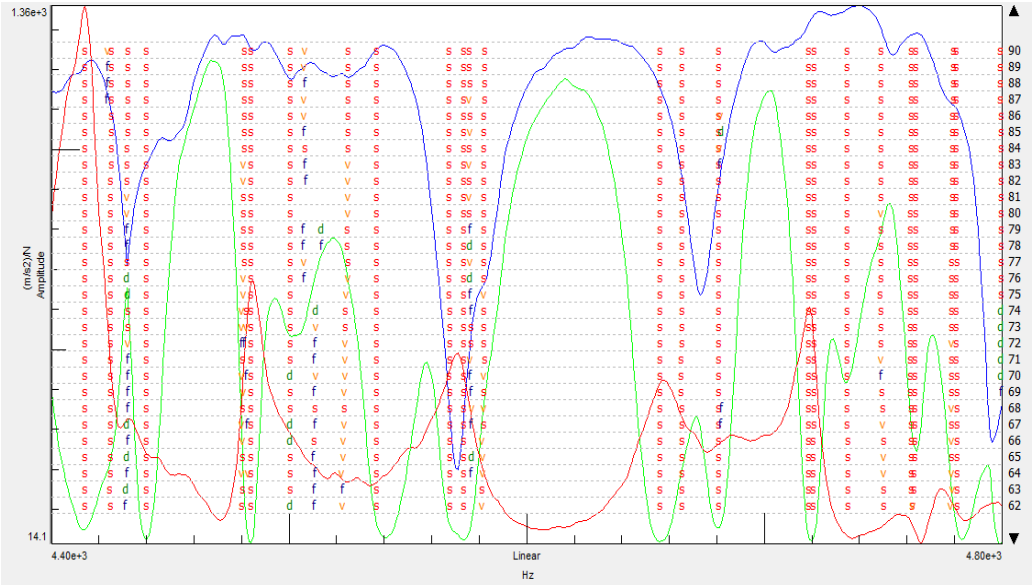

Figure 5-16. Curve fitting the FRF for modal parameter estimation

After extraction of the modal parameters, the FRF synthesised from the extracted parameters is matched as shown in Figure 5-17 and a very good correlation of 91% was found between the measured and the synthesised drive point FRFs.

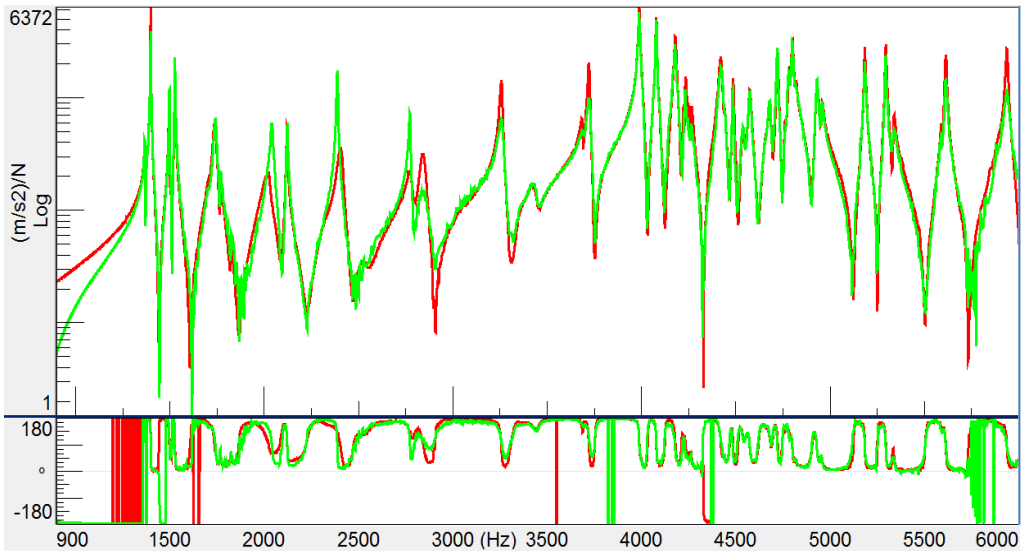

Figure 5-17. Correlation of measured and synthesised FRFs

A comparison of a few experimental and finite element predicted mode shapes is shown in Figure 5-18. The difference in the predicted frequencies with respect to the experimentally measured ones is given in Table 5-5. It can be noticed that overall error is less for the FE model of only the thin wall in comparison to the full FE casing model. This could be due to the fact that the material properties used for the casing material, which were taken from the Matweb portal [71], might be slightly variant with respect to the actual material properties. This translates into relative difference in stiffness of the boundary conditions between the thin wall only and the full casing FE models. Considering the computational advantage with a greatly reduced number of elements and the better accuracy prediction of frequencies, the FE model of only the thin wall is considered for further damping studies. However, in all the cases, the simulations were carried out also on the full scale model to verify any discrepancies.

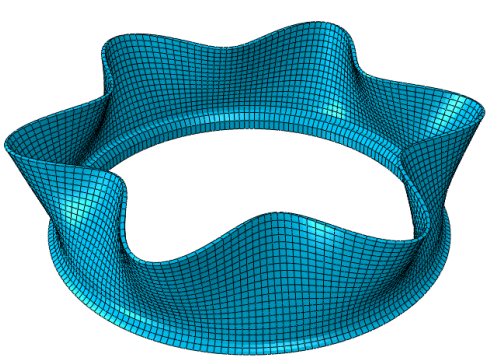

FE Mode: 1347Hz

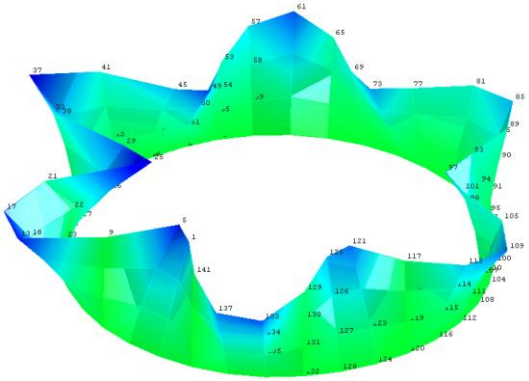

EMA Mode: 1372Hz

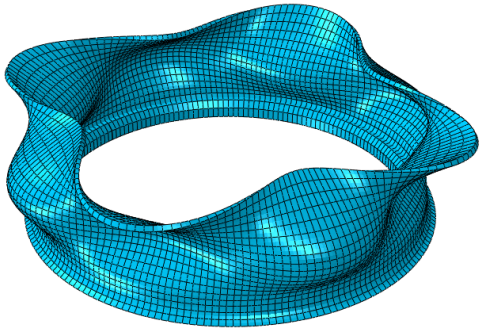

FE Mode: 4232Hz

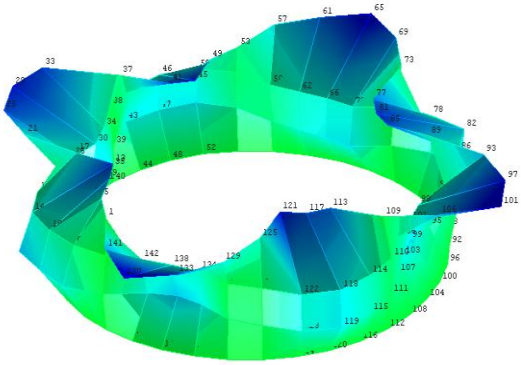

EMA Mode: 4427Hz

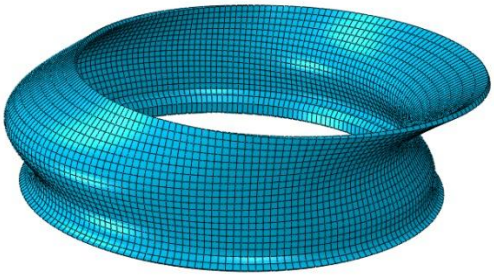

FE Mode: 4722Hz

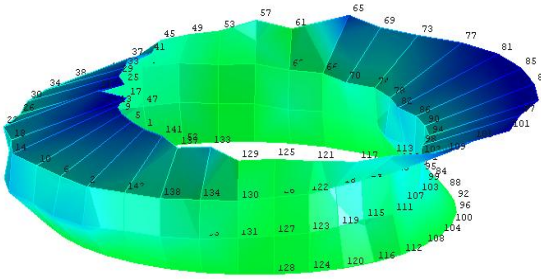

EMA Mode: 4833Hz

Figure 5-18. Comparison of FE and experimental mode shapes

Table 5-5 Comparison of experimental and FE predicted frequencies

Experiment	**Full casing (Hz)**	**Error (%)**	**Only thin wall (Hz)**	**Error (%)**
1372.85	1290.20	6.02	1347.40	1.85
1396.20	1334.70	4.41	1371.70	1.76
1481.88	1387.00	6.40	1472.80	0.61
1527.81	1496.40	2.06	1520.60	0.47
1657.29	1629.50	1.68	1683.20	-1.56
1758.47	1745.60	0.73	1763.00	-0.26
2019.42	1994.40	1.24	2058.10	-1.92
2057.64	2059.90	-0.11	2074.70	-0.83
2406.05	2426.10	-0.83	2441.10	-1.46
2808.25	2837.00	-1.02	2854.50	-1.65

5.6 Frequency response analysis

5.6.1 FE prediction through harmonic analysis

The frequency response of the structure for a given excitation load is usually evaluated through harmonic analysis, as explained in section 3.5.1.2. While evaluating the dynamic response, two methods are possible: mode-based and direct integration methods. In the mode-based methods, the eigenmodes of the system are used as a basis for calculating the response. In such cases the necessary modes and frequencies are calculated first in a frequency extraction step. The mode-based procedures are generally simple to use and a dynamic response analysis is

usually not expensive computationally, although the eigenmode extraction can become computationally intensive if many modes are required for a large model. In the direct integration method, the global equations of motion of the system must be integrated through time. This makes these methods significantly more expensive than the mode-based methods. However, in situations where non-linearity is present, mode-based methods are not effective as the changing stiffness of the system necessitates reformulation of stiffness matrix. Hence direct integration methods must be used when a nonlinear dynamic response is being studied [72].

In the present case, although evaluating the harmonic response of an undamped casing represents a linear problem, the direct integration method is used as for all remaining cases (such as with tuned dampers and surface dampers). The same method is used to account for material non-linearity (viscoelasticity). Hence in Abaqus®, a Steady State Dynamics, Direct Integration step was used to evaluate the harmonic response at all the extracted natural frequencies in which the thin wall of the casing participates.

Damping is an important parameter in defining the structural response. Most common sources of damping are [82]: energy dissipated within the materials of construction, energy dissipated at structural discontinuities, energy dissipated into the surrounding media (aerodynamic, acoustic, etc.). The first two sources are together referred as ‘structural damping’. These damping sources are generally represented by various types of

damping models: viscous damping, hysteretic or structural damping, and coulomb damping.

Viscous damping provides a force which is proportional to velocity and acts in the opposite direction to velocity. The energy loss increases with the square of the amplitude and is directly proportional to the frequency and damping constant, as shown in Eq. 5-8.

$$\Delta U = \pi\, c\, \omega\, r_o^2 \qquad \text{Eq. 5-8}$$

Hysteretic damping is defined as a damping which has the property of being independent of frequency but in phase with the velocity and proportional to the displacement. The energy loss increases with the square of the amplitude, is independent of frequency and is directly proportional to the damping constant, shown in Eq. 5-9.

$$\Delta U = \pi\, h\, r_o^2 \qquad \text{Eq. 5-9}$$

Coulomb damping provides a force that is constant and opposes the motion of the body. The energy dissipation per cycle by this damping method is proportional to the amplitude and independent of frequency.

Although the viscous damping mechanism provides a convenient form of the equation of motion, experimental results seldom correspond closely with a viscous type of energy-loss behaviour. Test evidence showed that the energy loss is only very weakly dependent on the excitation frequency. Hence hysteretic damping is generally used to model the damping due to the material. For the present casing, a material structural damping factor

of 0.1% was included in the analysis. This value was selected from the damping estimates of the experimental modal testing of the casing.

While conducting the harmonic response analysis, a unit excitation load was applied on a node and its response measured at the same point. Such a response, called the drive point response, is useful to compare with the experimental predicted response. The predicted harmonic response is shown in Figure 5-19 as the log of amplitude in receptance form. As is typical for a drive point response, anti-resonance can be observed between every two resonant peaks. The sharpness of the peaks shows the low damping in the system.

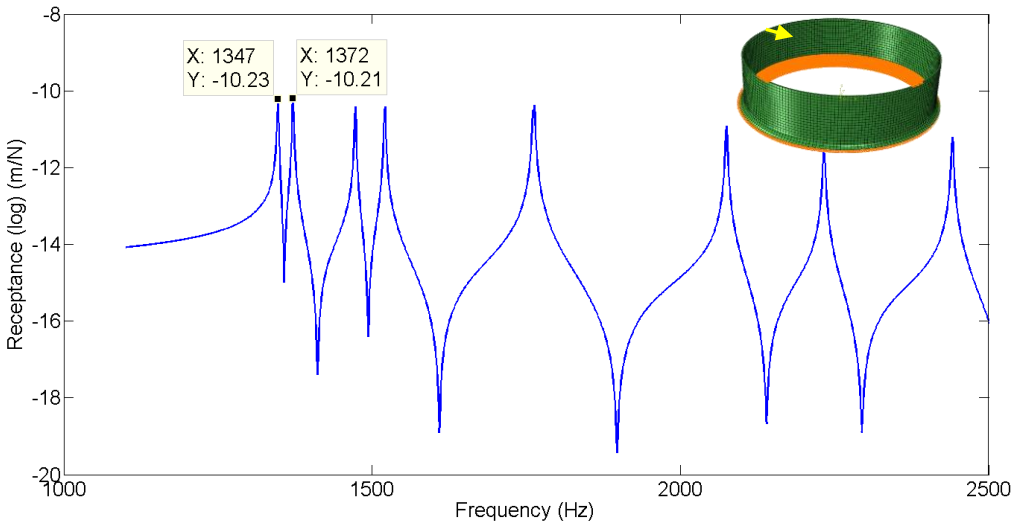

Figure 5-19. FE predicted harmonic response of undamped casing [inset: drive point location where response is measured]

5.6.2 Comparison between experimental and FE predicted responses

From the impact hammer testing experiments carried out on casing, and as described in section 5.5, the frequency responses are measured. A comparison of experimental and FE predicted frequency response curves

is shown in Figure 5-20. It can be seen that the curves match reasonably well and that the mismatch between the curves is due to slight variations in the material properties, and modelling damping which can be addressed through model updating. Also, the amplitude variation error can be explained due to the fact that a uniform structural damping factor was used in the FE analysis whereas the actual damping varies for each mode. However, the similarity in the sharpness of peaks indicates the reasonableness of the assumed structural damping factor value.

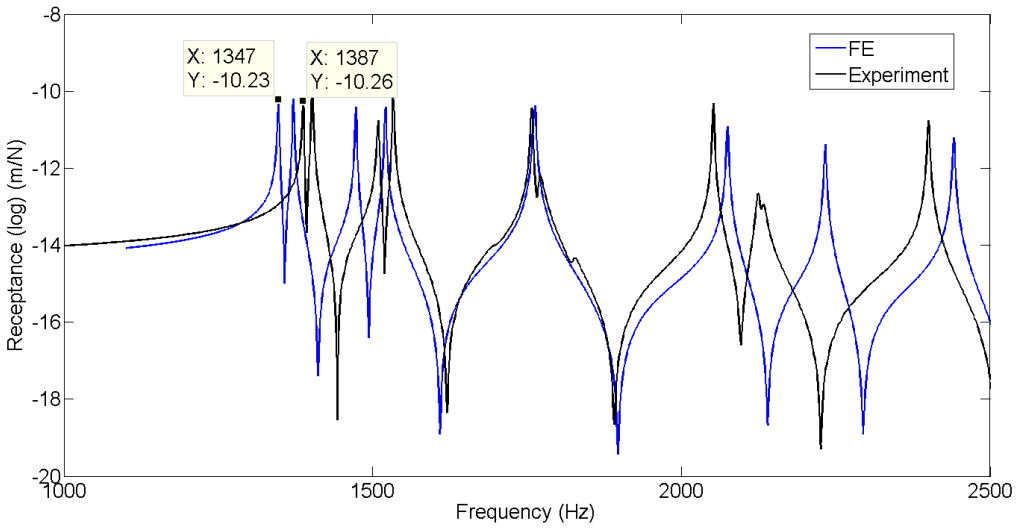

Figure 5-20. Comparison of FE and experimental frequency responses

5.7 Conclusion

In this chapter, the FE modelling of the thin wall casing and its experimental validation are detailed. Modelling methodology, full casing vs only thin wall and mesh convergence studies, are presented. Natural frequencies of the casing FE model are predicted through modal analysis. Experimental modal analysis of the casing is also presented in detail with the results of mode shapes and the accuracy of synthesised FRFs

calculated from the estimated modal parameters. The experimentally measured frequencies are then compared against those of the FE models and it is observed that the simplified thin wall model predicted accurate frequencies, though by only a small margin. This could be attributed to the variation in the material properties which were taken from an online site for material properties, Matweb. In the case of the simplified thin wall, its base is rigidly fixed through the boundary conditions, whereas in the case of the full casing the stiffness offered by bottom hub material is responsible for the base stiffness. Finally, the frequency response curves are predicted through FE harmonic analysis and compared with the experimentally measured FRFs. This validates the accuracy of the assumed damping factor for the FE model. Thus a complete FE model of the casing is experimentally validated and used for further studies with damping solutions.

6 Vibration suppression with tuned mass dampers and its FE modelling

6.1 Introduction

In Chapter 4, the coupled response interaction studies between the tool and the thin wall workpiece showed that the cutting tooth harmonics are modulated by the tool and the workpiece natural frequencies. At higher depths of cut it is the tool torsional mode that is dominantly modulating and at lower depths of cut the workpiece first fundamental mode modulates. It is to make use of this feature of dominance of a single mode that the tuned mass dampers were attempted. As explained in Figure 2-15, a tuned vibration absorber (TVA) is essentially a simple mass tuned for the targeted frequency and mounted through a bolt or some mechanical means, whereas a tuned mass damper (TMD) is a TVA with added damping in the form of a viscoelastic damping material. While most of the elastomers are viscoelastic in nature, specific viscoelastic damping materials are commercially developed which are effective over a desired frequency and temperature ranges.

While the design of tuned mass dampers for manufacturing applications has been researched earlier, such as for machine tools [58], [59] and on solid workpieces [62], thin walled and closed geometry structures such as casings were not investigated. In the following sections, the design and manufacturing of tuned dampers, their application on the casing and the observed benefits are presented. Finally FE modelling of tuned dampers

and the predicted dynamic response with and without dampers and their experimental validation are presented.

6.2 Viscoelastic material modelling

Selection of a viscoelastic material to be incorporated in a tuned mass damper is important. Below a very brief background on different modelling methodologies along with the relevant terminology is given.

6.2.1 Constitutive modelling

Viscoelastic materials are sometimes called materials with "infinite memory", in the sense that their actual mechanical response is modulated by past history. Therefore, the viscoelastic constitutive behaviour relies on the assumption that the current value of the stress tensor depends upon the complete past history of the strain tensor components. The constitutive equation for viscoelastic behaviour in the time domain is represented as follows[83].

$$\sigma(t) = G_{rel}(t)\varepsilon(0) + \int_0^t G_{rel}(t-\tau)\frac{\partial\varepsilon(\tau)}{\partial\tau}d\tau \qquad \text{Eq. 6-1}$$

where σ(t) and ε(t) are time dependent stress and arbitrary strain component histories, respectively, and $G_{rel}(t)$ is called the *constitutive time varying shear characteristic relaxation function* of the material. ε(0) is the limiting value of ε(t) when t ⟶0.

Such a time domain representation is useful for the transient response analysis of viscoelastic materials. However, if the viscoelastic material is subjected to steady-state oscillatory forcing conditions then a frequency domain representation, shown in Eq. 6-2, would be useful.

$$G^*(j\omega) = G'(\omega) + jG''(\omega) \quad \text{Eq. 6-2}$$

where ω is the frequency

G*(jω) is complex shear modulus

G'(ω) is shear storage modulus which accounts for the recoverable energy

G''(ω) is the shear loss modulus which represents energy dissipation effects

The loss factor of viscoelastic materials is defined as shown in Eq. 6-3.

$$\eta(\omega) = \frac{G''(\omega)}{G'(\omega)} \quad \text{Eq. 6-3}$$

This allows the complex shear modulus to be represented as shown in Eq. 6-4.

$$G^*(j\omega) = G'(\omega)[1 + j\eta(\omega)] \quad \text{Eq. 6-4}$$

For a linear, homogeneous and isotropic viscoelastic material, equivalent representations of the previous equations hold for the complex elastic modulus E(jω) and its relationship with the complex shear modulus G(jω) is given by

$$G^*(j\omega) = \frac{E^*(j\omega)}{2[1 + \nu(j\omega)]} \quad \text{Eq. 6-5}$$

where ν(jω) is Poisson's ratio. However, for simplicity, a real frequency independent Poisson's ratio ν(jω) = ν is usually assumed, leading to identical loss factors of the shear and elastic complex moduli, i.e., $\eta_E(\omega) = \eta_G(\omega) = \eta(\omega)$.

Figure 6-1 shows the variation of the complex shear modulus with time and frequency. It can be seen that the loss factor is highest in the

transition region. In finite element analysis, one has to provide the viscoelastic property data in a tabular form consisting of frequency, storage and loss moduli of the material. Also, the equilibrium or relaxed modulus, G_e has to be provided.

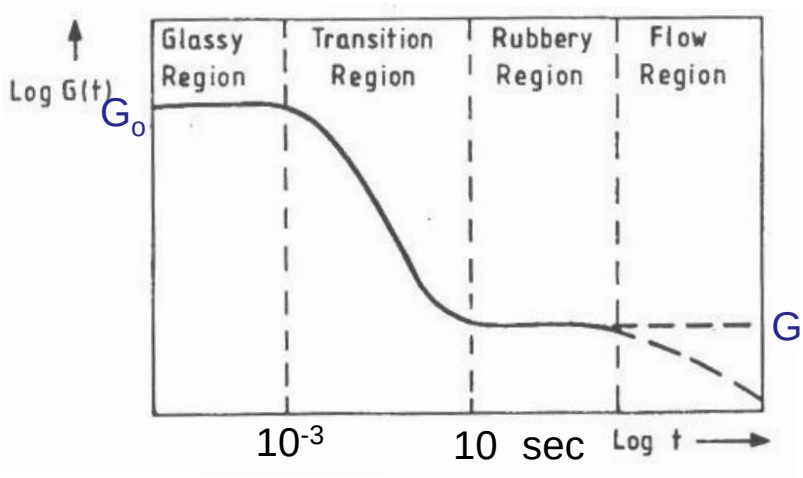

(a)

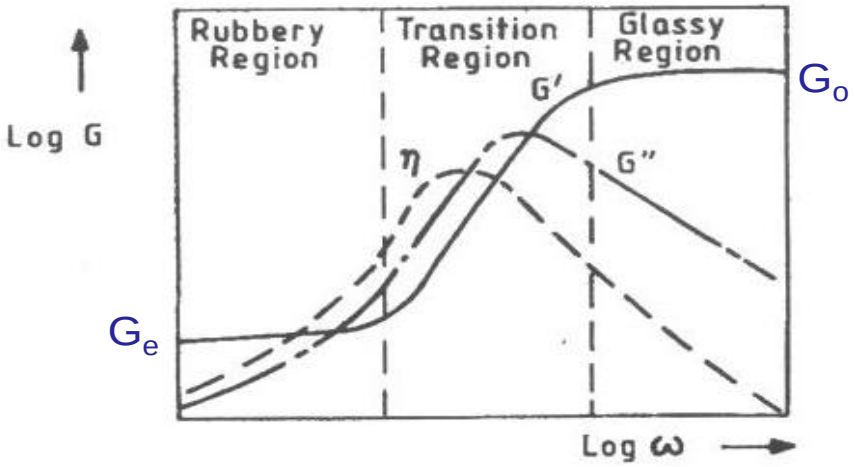

(b)

Figure 6-1 Variation of complex modulus in time and frequency domains [84] G_o – Instantaneous or glassy modulus; G_e – Equilibrium or relaxed

6.2.2 Finite element implementation

Similar to the constitutive models, equivalent modelling approaches exist in the finite element method for time and frequency domains. It may be pertinent to note that in formulating the finite element problem, the

general equation of motion for an elastic system with viscous damping is given by Eq. 6-6.

$$M\ddot{x} + C\dot{x} + Kx = f \qquad \text{Eq. 6-6}$$

where M, C, and K are mass, damping and stiffness matrices and *f* is the load vector.

For a viscoelastic material, in a time domain method, which is used for evaluating transient response, the equation of motion is formulated as follows.

$$M\ddot{u}(t) + D\dot{u}(t) + K^E u(t) + G_{rel}(t)K^V u(0) + \int_0^t G_{rel}(t-\tau)K^V \frac{\partial u(\tau)}{\partial \tau} d\tau = f(t) \qquad \text{Eq. 6-7}$$

where M and D are the global mass and viscous damping matrices, respectively, K^E is the elastic stiffness matrix and K^V is the viscoelastic stiffness term after factoring out the shear modulus. There are different time domain based approaches such as Golla-Hughes-Mc Tavish (GHM) model, Anelastic Displacement Fields (ADF) model, etc. [83].

For the frequency domain approach, the equation of motion is represented as

$$M\ddot{u}(t) + D\dot{u}(t) + [K^E + K^V(j\omega)]u(t) = f(t) \qquad \text{Eq. 6-8}$$

where K^E and $K^V(j\omega)$ are the elastic and complex frequency dependent viscoelastic stiffness matrices, respectively, and u(t) and f(t) are the displacement degrees of freedom and applied loads vectors, respectively. This method is referred to as the Direct Frequency Response (DFR)

analysis approach. Other approaches such as the Modal Strain Energy (MSE), Iterative Modal Strain Energy (IMSE), and Iterative Complex Eigensolution (ICE) exist. A detailed review of modelling and FE implementation of viscoelastic damping including mathematical descriptions of models and FE modelling approaches is given in [83], [85]. In this research, as the interest is in obtaining the frequency response of a structure with viscoelastic damping, the frequency domain approach (DFR) is employed using Abaqus® software.

6.3 Validation of viscoelastic material properties

As explained in [86], three design factors have to be considered while choosing a viscoelastic tape: maximum loss factor, maximum shear modulus, and the variation of these parameters with both frequency and temperature. Important among all these is the variation of the shear modulus with temperature. Since the temperature in the material can increase during its use due to energy dissipation, the shear stiffness of the viscoelastic spring of the tuned damper can change significantly. Therefore, ideally the temperature dependent change in the shear modulus should be as low as possible in the range of application. The 3M® Company manufactures a range of viscoelastic tapes for commercial applications. Different materials from 3M® product range were considered and compared for the desired properties. These included 3M® ISD-110, 112, 130 and 3M® VHB tapes. After analysis of the data [87], [88], ISD-112 was found to be suitable for the present application with a target frequency of 1387Hz and a temperature range of 10-35^{o}C. It has the

highest loss factor and a comparatively moderate value of the modulus and its variation in the design range of temperature and frequency. Another important consideration in choosing ISD-112 is its ease of application. While most other tapes need temperature for bonding, ISD-112 needs only hand pressure. The data given in the manufacturer's manual is shown in Figure 6-2 and the tabular data extracted from the same graph is given in [89] and reproduced here in Table 6-1. A relaxed shear modulus of 69042 Pa is used [89]. This data is used in the present FE model for tuned mass dampers.

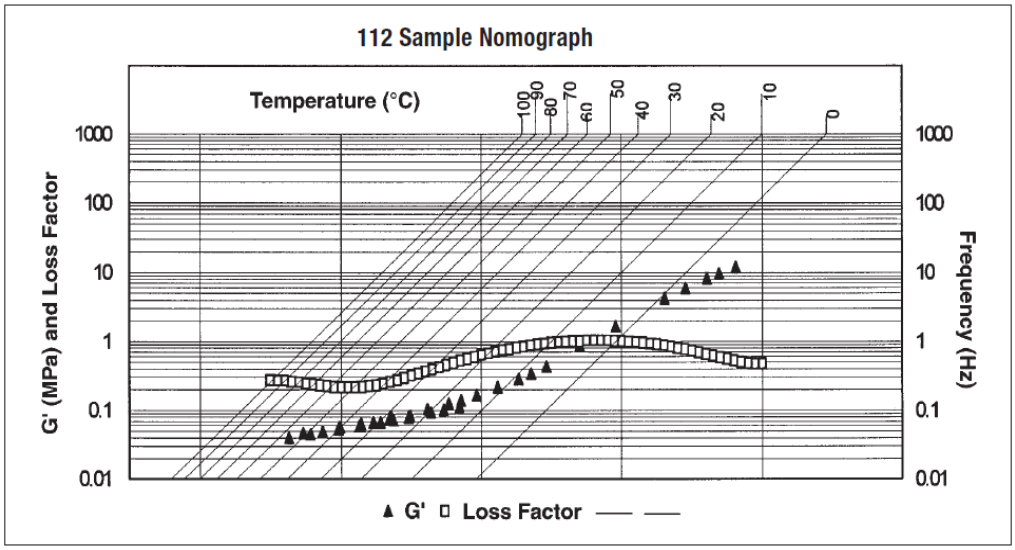

Figure 6-2 Nomograph of 3M® ISD-112 viscoelastic damping tape [88]

Table 6-1 Frequency domain data for viscoelastic material 3M ISD-112 [89]

Frequency (Hz)	**Storage Modulus (Pa), G'**	**Loss Factor, η**
0.1	7.00E+04	0.4
0.5	1.00E+05	0.6
1	1.40E+05	0.7
2	1.70E+05	0.8
3	2.00E+05	0.85
4	2.10E+05	0.9
5	2.40E+05	0.9
10	3.40E+05	1
20	5.00E+05	1
50	7.50E+05	1
70	9.00E+05	1
100	1.00E+06	1
200	1.60E+06	1
500	2.50E+06	0.9
700	3.00E+06	0.9
1000	3.50E+06	0.85
5000	7.00E+06	0.6
10000	9.00E+06	0.5

A point worth noting here is that the loss factor of the viscoelastic tape is maximum between 10 – 200Hz and gradually reduces to 0.5 by 10kHz. It is for this reason that most of the commercially available viscoelastic tapes cannot be used for the damping tool torsional mode which is around 15kHz.

To validate this data and also the FE modelling and meshing methodology, literature was surveyed. One example is found in [90] where the viscoelastic material 3M® ISD-112 was simulated as a part of constrained layer damping treatment, as shown in Figure 6-3. This paper provides results at temperatures 11.5^{o}C and 17.5^{o}C; however the datasheet shown

in Figure 6-2 and Table 6-1 is for 20^{o}C. The paper presents three variants of modelling the constrained layer damping treatment:

Model 1: The constraining and base layers, shown in Figure 6-3, are modelled as plate elements and connected to the viscoelastic layer through rigid links. The viscoelastic layer was modelled in all three cases with solid brick elements.

Model 2: The constraining and base layers are modelled using plate elements and their nodes are localised by offset of half of the plate thickness to the plane in contact with the solid element, instead of remaining in the standard mid-plane.

Model 3: All the three layers are modelled using solid elements.

However the paper presents harmonic response results only for model 2. In a curved shell this does not represent correctly the outside layer [90]. This is due to change in diameter of circular shell due to offsetting of nodes towards viscoelastic brick elements. Hence the FE model used to validate the results is modelled as Model 3 in Figure 6-3.

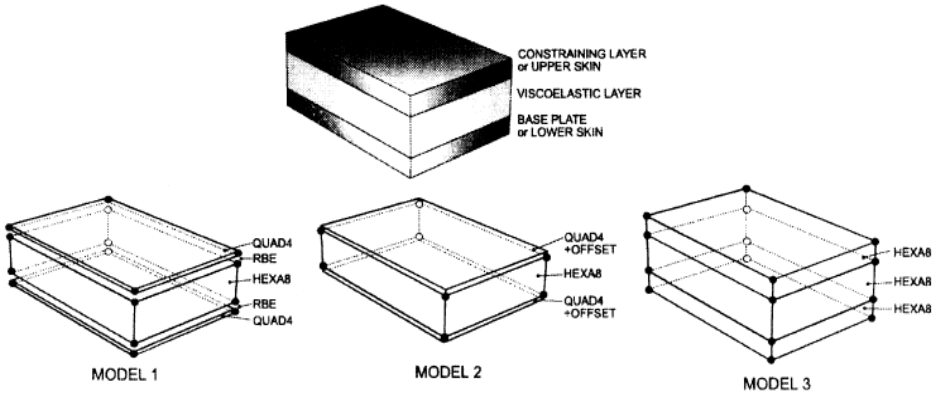

Figure 6-3 Modelling strategies for constrained layer damping [90]

Figure 6-4(a) shows the grid pattern on the plate sandwich on which the responses were acquired and Figure 6-4(b) shows the drive point harmonic response at node 17, reproduced from reference [90]. Figure 6-4(b) shows both the FE predicted and experimentally measured responses.

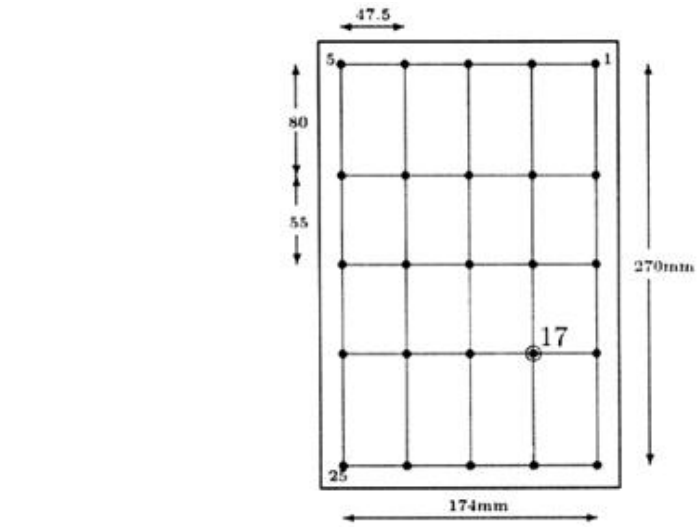

(a)

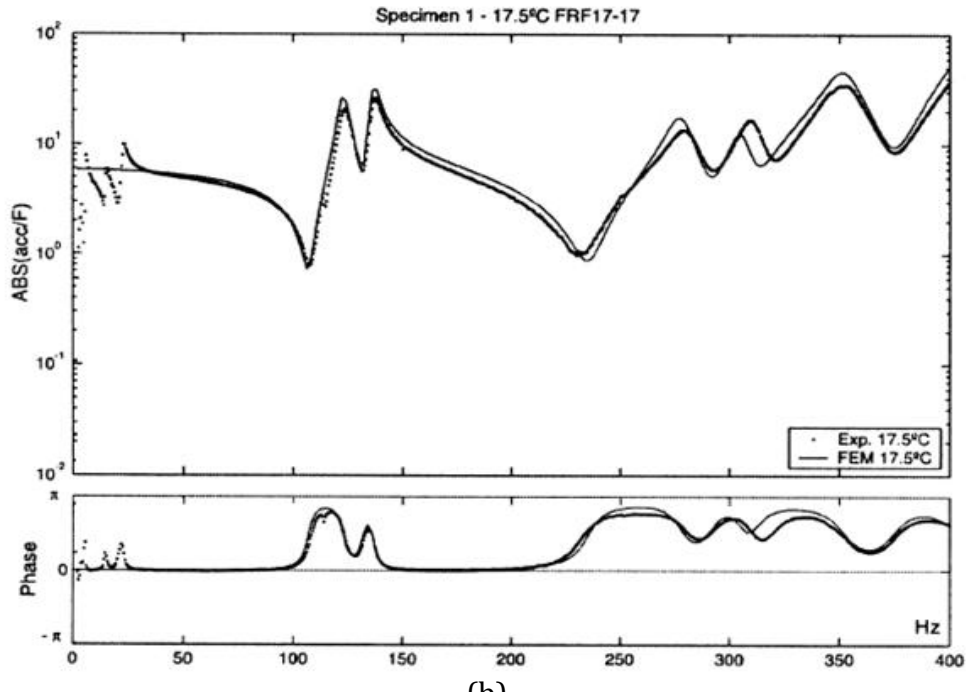

(b)

Figure 6-4 FE Mesh and drive point harmonic response for constrained layer plate [90]

Figure 6-5(a) shows the model of the constrained layer damping treatment used to simulate harmonic response in the FE software Abaqus®. The dimensions are modelled identical to those given in the paper. The predicted harmonic response at the location corresponding to node 17 as given in paper is shown in Figure 6-5(b). It can be seen from Figure 6-4 and Figure 6-5 that the predicted FE result matches very well with that shown in the paper.

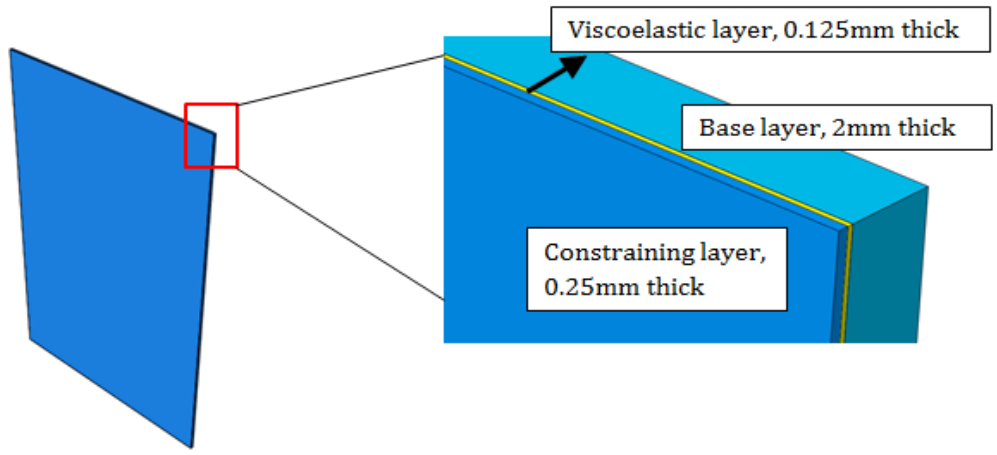

(a)

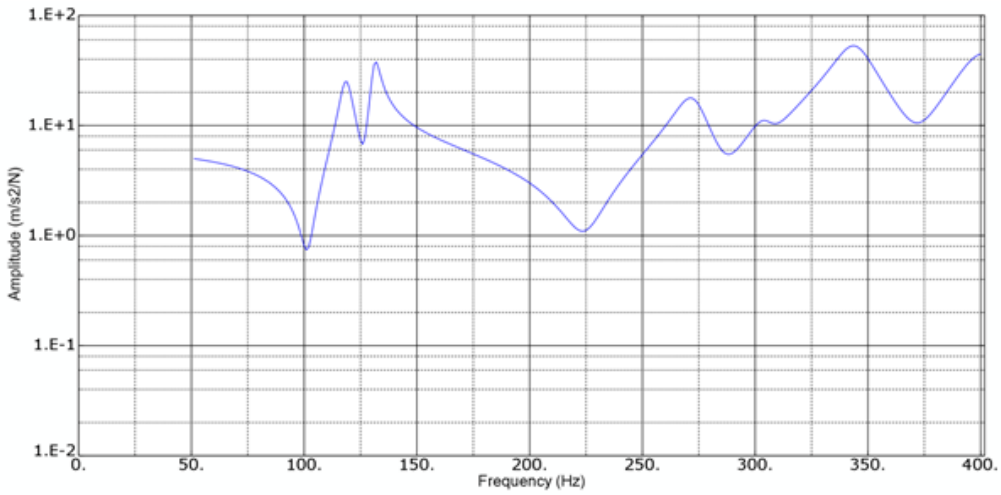

(b)

Figure 6-5 FE model generated and drive point harmonic response at equivalent point on plate

Table 6-2 Comparison of frequencies and amplitudes of frequency response as given in reference [90] and predicted through FE modelling

Frequencies in paper, Hz	Frequencies simulated, Hz	Amplitude of modes in paper, m/s^2	Amplitude of modes, simulated, m/s^2
125	119	25	25
137.5	132	30	38
250	250	3	5
278	272	17	17
310	305	13	11
350	344	50	53

Quantitative comparison of the frequency responses from the paper and the FE prediction is carried out. The results from the paper are measured approximately matching with the X and Y-axis scales on the graph. Table 6-2 shows the comparison of frequencies and amplitudes of the responses. It can be seen that the error is very small and can be attributed to following factors:

- Variation in modelling strategy: While the frequency response shown in the paper is for Model 2 (offset-node plate elements for constraining and base layers), the predicted frequency response is for all solid brick elements. As explained earlier, this is done as the offsetting of nodes in a circular casing will not produce a proper outer layer.
- Possible variation in material properties due to the temperature difference: The frequency response given in the paper is for

material properties evaluated at 17.5°C while the FE simulated results are from a datasheet which gives properties at 20°C.

- Density of material: The paper reports the density of the material used (3M ISD-112) as 1100 kg/m^3. However the latest datasheet of 3M ISD-112 reports the density as 1000 kg/m^3, which is used in FE simulation.

Hence this simulation study validates the chosen material properties of the viscoelastic material and also the modelling methodology including the type of element chosen and boundary conditions employed to connect the viscoelastic layer with the surface layers.

6.4 Design of tuned mass dampers

Tuned mass dampers are popular and are relatively old technologies being used in civil (bridges, buildings, etc.) and mechanical (compressor mountings, machine tools, electrical razor, etc.) structures. Hence, their design principles are widely covered [56], [91]. The design considerations for tuned dampers which use viscoelastic material as the damping material are covered in [92] and are briefly described here.

For tuning the damper for the casing used in the present research, there are two modes: the tool torsional mode which is dominant at higher depths of cut and the workpiece first fundamental mode at lower depths of cut. Of the two, the latter was chosen for suppression mainly for two reasons: (a) the consequences of the forced vibration are prominent (such as a poor surface finish) during the finish machining operations and the depths of cut during such finishing operations are generally low and hence

suppressing the workpiece mode becomes important, (b) tool torsional mode frequency is usually very high. For example, as shown in Figure 4-9, the tool torsional mode for a 58mm tool overhang is 14044Hz. However, as explained earlier, most of the commercially available passive damping treatments such as viscoelastic tapes are designed to have a high loss factor at a much lower frequency (10-1000Hz). Hence in this research tuned mass dampers are designed for the workpiece first fundamental mode. Considering that the first fundamental mode of the casing is 1387Hz, the experimentally designed viscoelastic dampers are tuned for this frequency. In this work, the FE model is not updated, as explained in section 5.6.2, to match the frequencies with that of the experiment as the difference is very small. Hence, for FE analysis 1347Hz frequency was chosen as the target frequency for the tuned damper.

For a given target frequency, the design parameters are the mass of the damper block and the thickness of the viscoelastic tape. It is usual to take the damper block mass as 1-5% of the vibrating mass [59], and calculate the corresponding thickness of the viscoelastic tape. The lower the mass of the tuned damper, the tuning has to be more accurate and the system is less robust to variations in the dynamic parameters of the system, an important factor in thin wall machining. For a casing with a locally vibrating structure such as a thin wall, such a local feature has to be considered as a vibrating mass (in this case 4.47kg). For a mild steel damper block with a mass equal to 5% of the vibrating mass, this works out as (0.05X4.47) = 0.224kg. With a 7800 kg/m^3 density, and a surface

area of 40x40mm, the damper block thickness works out as 18mm. Hence, the damper blocks are made with dimensions 40X40X18mm with a radius to match that of the internal radius of 177.5mm.

For a target frequency of 1387Hz and a damper block mass of 0.224kg, the required stiffness is calculated using the following equation:

$$k = m\omega_n^2 = 0.224 \times (2 \times \pi \times 1387)^2 = 17013370\ N/m \qquad \text{Eq. 6-9}$$

For the surface area of 40X40mm, the thickness of the viscoelastic tape was calculated as follows:

For a target frequency of 1387Hz, the shear modulus has to be found through linear interpolation from the tabular data given in Table 6-1. The data points of (1000Hz, 3.5MPa) and (5000Hz, 7.0MPa) are used.

$$G'_{1387} = 3.5 + (1387 - 1000) \times \frac{(7 - 3.5)}{(5000 - 1000)} = 3.83MPa \qquad \text{Eq. 6-10}$$

The elastic modulus can be calculated from the shear modulus using Eq. 6-11

$$E = 2G(1 + \nu) = 2 \times 3.83(1 + 0.49) = 11.42MPa \qquad \text{Eq. 6-11}$$

For a damper block area of 40X40mm, the thickness of viscoelastic tape can be obtained using

$$L = \frac{AE}{K} = \frac{40 \times 10^{-3} \times 40 \times 10^{-3} \times 11.42 \times 10^{6}}{17013370} \qquad \text{Eq. 6-12}$$

$$= 0.001074m = 1mm$$

Therefore, a viscoelastic tape of 1mm was applied onto the damper blocks.

6.5 FE modelling and dynamic response prediction with tuned mass dampers

A FE model, as shown in Figure 6-6, was created with the above parameters for the tuned masses and the viscoelastic layer. Major considerations while modelling viscoelastic materials using FE analaysis are [84]:

- Similar element thicknesses to be maintained at the elastic-viscoelastic interface to account for the sharp discontinuity in material properties
- Quadratic continuum elements to be used to account for the high deformation and strains in the viscoelastic components
- Hybrid elements to be used to represent viscoelastic materials. These elements have an additional hydrostatic pressure degree of freedom to account for incompressible materials (Poisson ratio-0.5)

Following the above guidelines, the damper block was meshed using C3D20R elements, similar to the casing, and the viscoelastic layer was meshed using hybrid continuum elements C3D20RH. The damper block, the viscoelastic tape and casing are 'tied' together in the FE model. This means that before the start of the solution, the FE software will match the nearby nodes on these layers. Hence, to avoid any excessive mesh distortion the damper block and the viscoelastic tape are meshed in with same element size as that of casing.

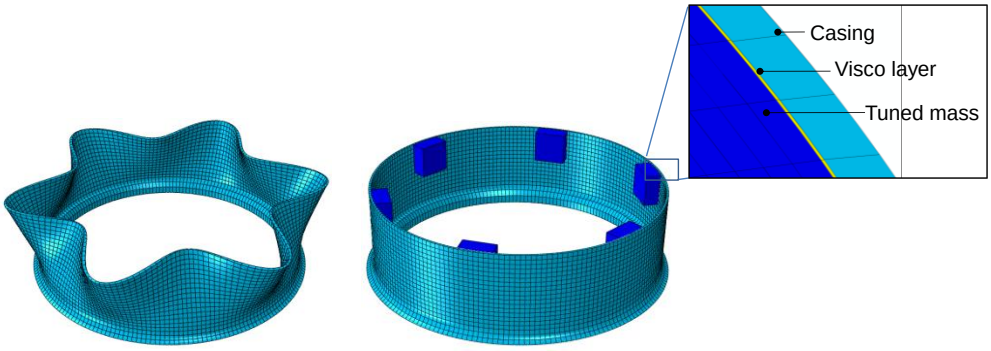

(a) (b)

Figure 6-6 (a) First mode shape (1347Hz) of the casing (b) Corresponding arrangement of the tuned dampers

The mode shape of the 1387Hz frequency to be damped, Figure 6-6 (a), has six circumferential waves. Preliminary FE analysis of mounting only one tuned damper revealed that while the targeted frequency was reasonably damped, other dominant modes of the workpiece modes are existent which could be excited during machining. Hence a total of 6 tuned dampers are used corresponding to 6 anti-nodes of the first fundamental mode, as shown in Figure 6-6 (b), with the intention of providing a higher mass ratio of dampers. The reason for choosing such a high mass ratio is two-fold. Firstly, to dampen frequencies of the casing over a wider bandwidth as thin wall casings have a significantly higher number of modes with a similar magnitude across a wide frequency range. For example, about 250 modes corresponding to the thin shell of the casing exist up to 15kHz. Secondly, in machining thin wall casings, unlike a rigid machine or tool structure, where tuned masses were applied earlier, the forced vibration due to the tool is significant. In such a situation it is highly

desirable to improve the mass of the vibrating structure so that the increased inertia forces tend to minimise the vibration amplitude.

Harmonic analysis was carried out on the FE model. As the maximum response is expected to be in between two damper blocks, the drive point where the casing has to be excited and the response measured was chosen there. Steady State Dynamics with a direct integration step was used to account for the viscoelastic property of varying modulus with frequency.

Experimental verification of the dynamic response is carried out using impact hammer testing. As shown in Figure 6-7, six tuned mass dampers were mounted on the casing and an accelerometer mounted in between the two masses. The dynamic response was acquired at the location of the accelerometer. Figure 6-8 shows the harmonic response of the casing with six tuned mass dampers along with the experimentally obtained FRF. It can be seen that the amplitude of the response has decreased significantly. Also, in addition to the targeted mode of 1387Hz, all the neighbouring modes are significantly damped. This is the perceived advantage of mounting six damper blocks, i.e. to damp the modes on a wider bandwidth by having a higher mass ratio of dampers, which is important from the perspective of thin wall casings which have a significant modal density in any given bandwidth.

The reasonably close matching of the FE and experimental FRFs indicates the accuracy in modelling the damping. The maximum error in predicted and measured frequencies is 8%, as shown in Figure 6-8. The mismatch in the frequencies and damping is mainly due to the non-updated finite

element model. Updating a FE model involving viscoelastic damping needs consideration of non-proportional damping. All the existing commercial FE software for model updating assumes that the damping matrix [C] is proportional to the mass [M] and the stiffness [K] matrices. This approach works well in general for homogeneous structures. However, for structures on which tuned dampers or local damping treatments are mounted, the assumption of proportionality will not be accurate. Such a feature is not available in existing commercial software and is a topic of research interest in the structural dynamics community [93], [94]. However, considering that the error in the frequencies is 7-8%, the present level of prediction is considered to be acceptable. This level of accuracy shows that the developed finite element model is capable of predicting the effectiveness of the mounted tuned dampers, particularly in instances where the workpiece modes are dominant such as in finishing operations.

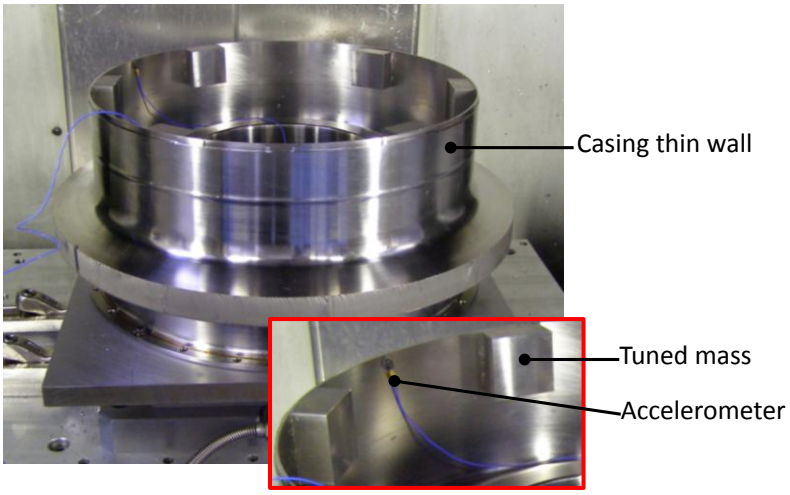

Figure 6-7 Experimental set up for dynamic response testing on casing with tuned mass dampers

As explained in section 5.1, this finite element model can be further enhanced to include the coupled interaction of the tool's frequency, thereby enabling the simulation of roughing operations where the tool's frequency is dominant throughout the spectrum. That is, the tuned dampers will then have to be designed for tool's torsional frequency and the effect of the dampers on minimising such modes can be studied. This is the scope for future research. In the next section, the quantified improvement in vibration reduction due to the mounting of tuned dampers is presented along with the analysis of the coupled interaction of the tool and the workpiece.

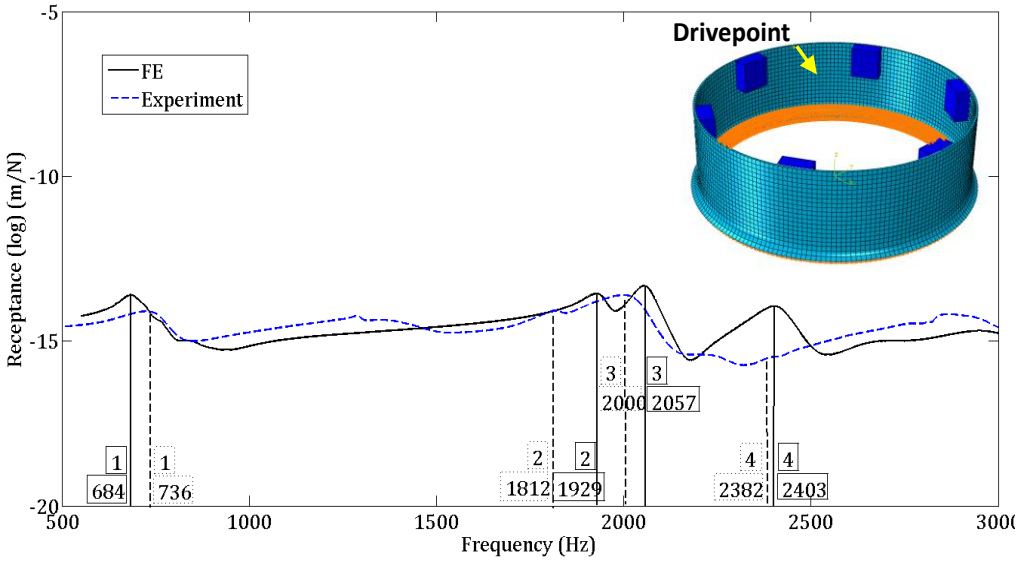

Figure 6-8 Harmonic response of casing with six tuned mass dampers

6.6 Dynamic response analysis in milling of casing with tuned dampers

6.6.1 Improvements in vibration reduction

The casing with six tuned dampers is machined in a similar setup to that of the undamped casing. As shown in Figure 6-9, one quadrant of the casing

was machined in four sectors to obtain data at various sections of the casing with and without a damper. Also, the data being acquired at a higher sampling rate of one million samples per second, machining in four sectors makes data handling easier than machining whole quadrant in a single pass. The tool overhang was maintained as constant at 46mm for all the experiments and the bending and torsion modes of tool for this overhang are 4800Hz and 16200Hz respectively as predicted from the FE analysis. Considering that the casing is prone to a higher vibration in between two damper blocks, the accelerometer is mounted between them, as shown in the inset in Figure 6-9, and the correspondingly the data acquired in sector II will be presented and discussed here. With the dampers mounted in place, the casing exhibited an overall improvement in rigidity which can be observed by the absence of high frequency sounds (such as whistling) and machining characteristics akin to that of a rigid solid component.

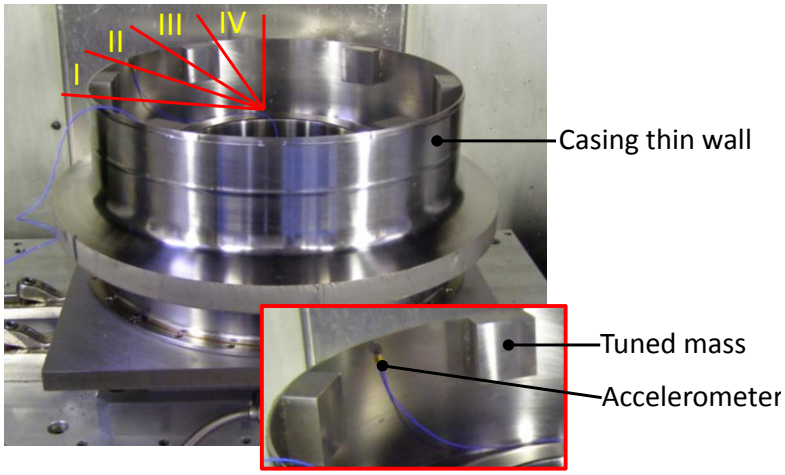

Figure 6-9 Experimental set up of casing with six tuned dampers showing the machined sectors

The efficacy of the damper blocks in reducing machining vibration can be evaluated through different statistical features. In this work the 'effective value' as represented by Root Mean Square (RMS) value of the acceleration signal acquired during machining, is chosen, which is defined as follows:

$$x_{rms} = \sqrt{\frac{x_1^2 + x_2^2 + \cdots + x_n^2}{n}} \qquad \text{Eq. 6-13}$$

where x_1, x_2, …, x_n are data points and n is the total number of points.

As suggested in Teti et al. [95], the initial and final parts of the sensor signal are related to transient machining conditions and should be eliminated to get rid of misleading information. Hence while calculating RMS the initial transient portion of data where the signal is slowly increasing in magnitude was discarded and only steady state data was used. Figure 6-10 shows the machining vibration signal acquired in sector II for a_p = 2mm and a_e = 1mm. It can be noticed that the vibration reduction was significant in terms of the RMS value, 2.29 times. This is significant due to the fact that the entire signal was acquired in between two damper blocks. The reduction in vibration at the damper is still higher (about 5 times), but the evaluation in between the dampers represents the worst case scenario. Machining tests were conducted at other depths of cut as well to evaluate the efficiency of the dampers. Figure 6-11 shows vibration reduction for a_p=0.5mm and a_e = 0.5mm, where it can be seen that the improvement is little more significant, about 4 times. This phenomenon could be due to the lower excitation of the tool's forced

vibration and also the excitation of the workpiece (casing) modes at a lower depth of cut which are now adequately damped through the mounted masses. However, this will be determined through studying the frequency content presented in the following sections. Apart from proving the effectiveness of the proposed solution, these results show that damping in thin wall machining is also dependent on the depth of cut (i.e. contact pressure between the cutting edge and the workpiece).

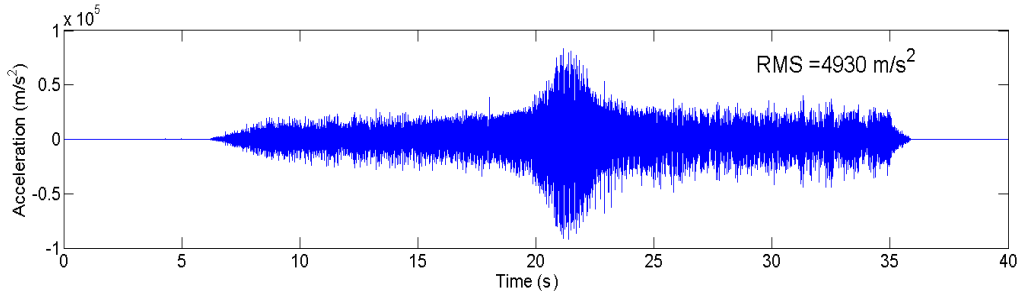

(a)

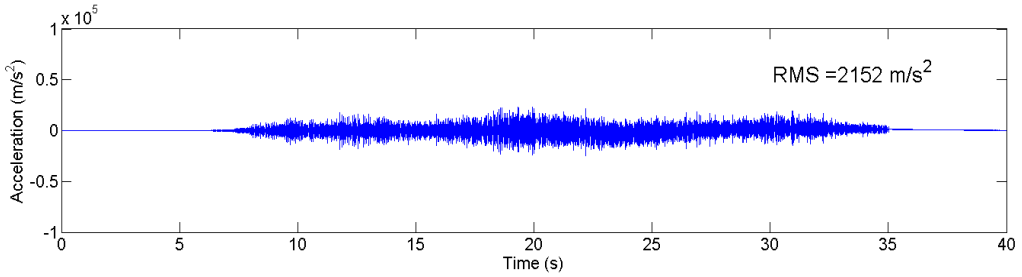

(b)

Figure 6-10 Vibration reduction when milling thin wall casing at a_p=2mm, a_e=1mm; (a) undamped, (b) with tuned dampers

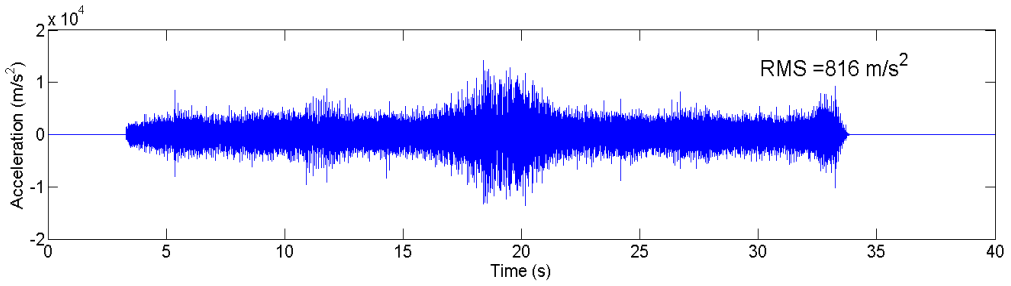

(a)

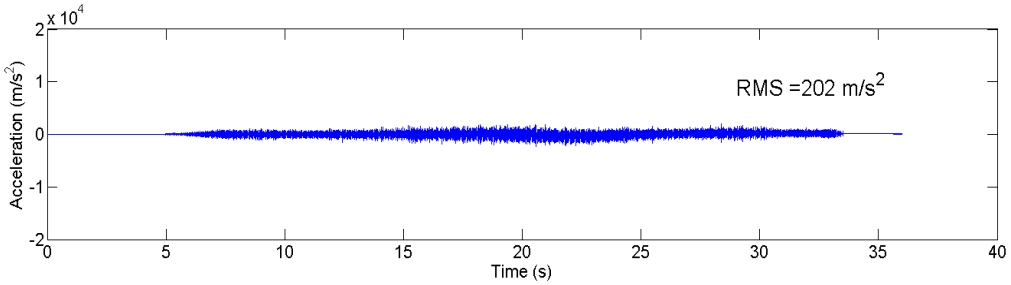

(b)

Figure 6-11 Vibration reduction when milling of thin wall casing at a_p=0.5mm, a_e=0.5mm; (a) undamped, (b) with tuned dampers

6.6.2 Analysis of coupled interaction between tool and workpiece with tuned dampers

To study the frequency content and thereby understand the coupled interaction between the tool and the workpiece in the presence of tuned dampers, a time-frequency analysis was carried out on the acquired acceleration signals. For all the analyses, the signal closest to the accelerometer is considered as it would give the direct vibration near the tool tip and hence an indication of effect of damping in the machining zone. Fast Fourier Transformation (FFT) was carried out on the acceleration signal for one revolution of the tool at various sections of 0.005 seconds each; the acceleration signals shown in Figure 6-10 and Figure 6-11 are used for this purpose. The detailed methodology of the coupled interaction analysis procedure is provided in section 3.4. Figure 6-12

shows the 3D time-frequency plot for acceleration signals of a_p=2mm, and a_e=1mm.

It can be observed that in undamped casing frequency spectra (Figure 6-12(a)), the harmonics of tooth cutting frequency near the tool torsion mode are significantly dominant. However for the sake of clarity in explaining the results, these harmonics are henceforth referred to as the frequency near to the component (e.g. tool or workpiece) frequency they are excited. For example, the harmonics that are distinctly excited near the tool torsion mode are referred to as the tool torsion mode frequency only. These frequencies need not be same as the original resonant frequencies near which they are excited as they are harmonics of the tooth cutting frequency.

From Figure 6-12(a) it can also be observed that the tool bending mode and the fundamental workpiece frequency are excited but dwarfed by the excitation of the torsional mode. The continuity in the excitation of the torsional mode even after the disengagement of the cutting tooth indicates the strong forced vibration of the tool imparted onto the workpiece. This shows a strong coupling of the tool's torsional mode with that of the workpiece.

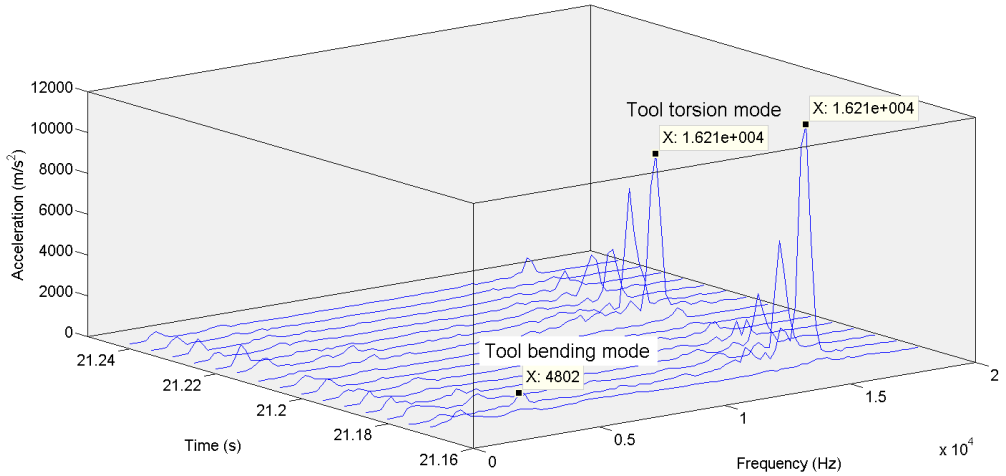

(a)

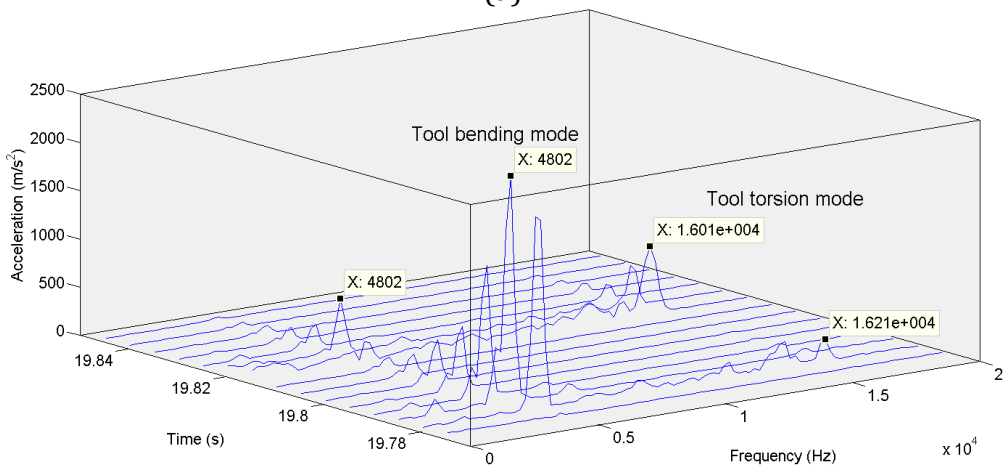

(b)

Figure 6-12 Time-frequency analysis of acceleration signal when milling casing at large depth of cut (a_p=2mm, a_e=1mm): (a) undamped (b) with tuned dampers

With the damper blocks in place, Figure 6-12(b), the important feature that can be noticed is that the tool bending mode, which was not dominant in the undamped casing, is distinctly dominant and that the torsional mode is no longer significantly dominant. The acceleration signal corresponding to other tool revolutions near to the accelerometer showed a similar pattern with varying amplitudes of the tool torsional mode, but always comparable or less than that of the bending mode excitation. This

is an interesting observation as it shows a change in the coupling interaction of the workpiece to the tool's frequencies. This could be explained as follows; in the undamped condition, due to the inherent stiffness of the casing in the tangential direction, the tool's torsional mode significantly couples with the workpiece. With the mounting of damper blocks intermittently, the section of the casing in between two blocks acts more like a cantilever fixed at both ends and thereby offering a dynamic characteristic similar to that of a straight thin wall. This characteristic is then responsible for the coupling of the tool's bending mode with the workpiece. This also matches with the observation that while milling straight thin walls, the tool's bending mode couples with the workpiece, as mentioned in section 4.2.1.

From Figure 6-12(b), it can be noticed that most of the workpiece modes, including the fundamental modes, are significantly damped indicating a damping effectiveness over a wide bandwidth due to the higher mass ratio of dampers. However, the continuity of the tool's forced vibration (of bending and torsional modes) even after disengagement of the cutting tooth indicates a strong coupling of the tool and the workpiece due to the forced vibration. Similar analysis was carried out on acceleration signals with a_p=0.5mm and a_e=0.5mm and the results are presented in Figure 6-13. The lower depth of cut excites the tool's forced vibration to a lesser extent and hence the dominant appearance of the workpiece modes. In addition to the fundamental mode, the workpiece modes near the tool torsional mode are also excited. Mounting the dampers leads to a similar

observation – dominant participation of the tool's bending mode as compared to torsional mode, Figure 6-13(b), similar to that of a higher depth of cut (a_p=2mm and a_e=1mm). Although a few workpiece modes do not seem to be sufficiently damped, it may be noticed that the targeted mode of 1387Hz was totally damped and that the magnitude scale is so small that other workpiece modes look significant. As can be seen, these modes are excited only during the instance of cutting tooth engagement and quickly get damped after the tool disengagement. Thus, both the cases of depths of cut showed that a change in the coupled interaction of the workpiece and the tool's dynamic response is involved with the mounting of tuned dampers.

To study the effect of such a variation in coupling from torsional to bending mode, the thickness of the machined thin wall of the casing was measured. Machining trials were conducted in the third and fourth sectors of the casing, shown in Figure 6-9, thereby covering an area with and without a tuned mass. Axial and radial depths of cut of 2mm and 1mm were used to achieve a wall thickness of 1.5mm. The thickness variation measured on the casing thin wall, as shown in Figure 6-14, clearly shows that in between the damper blocks the thickness is different by 70 microns as compared to the area where the damper block is situated. This can be explained from the observation made by Bravo et al [17], that in down milling of a thin wall, the cutting force tends to push away the thin wall relative to the tool, as shown in Figure 6-15. In the present case of the thin wall casing with intermittent damper blocks, the casing is locally

acting as a cantilevered thin wall with rigid damper blocks at either end. Hence, the casing thin wall is pushed away from tool resulting in a higher thickness as compared to the location where the damper mass is situated.

(a)

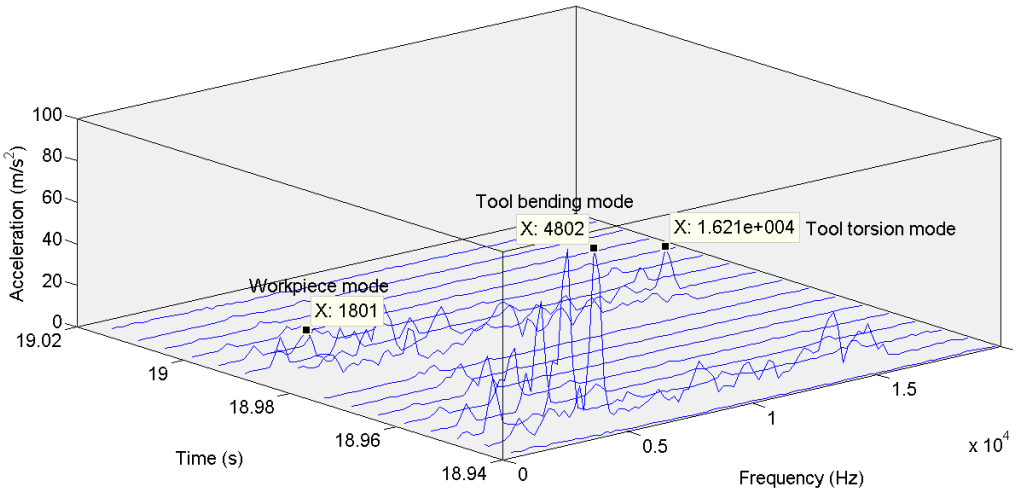

(b)

Figure 6-13 Time-frequency analysis of acceleration signal when milling casing at small depth of cut (a_p=0.5mm, a_e=0.5mm): (a) undamped (b) with tuned dampers

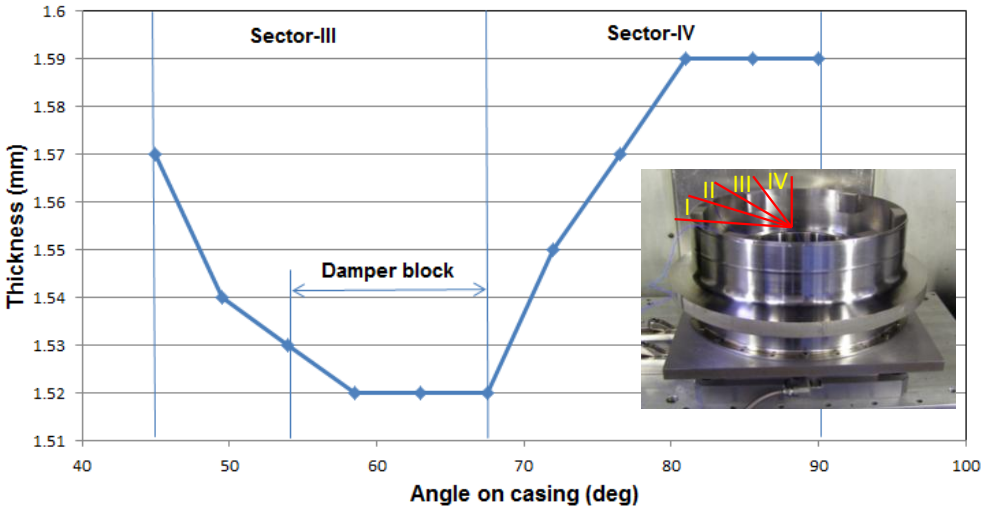

Figure 6-14 Thickness variation of thin wall casing in sectors 3 and 4

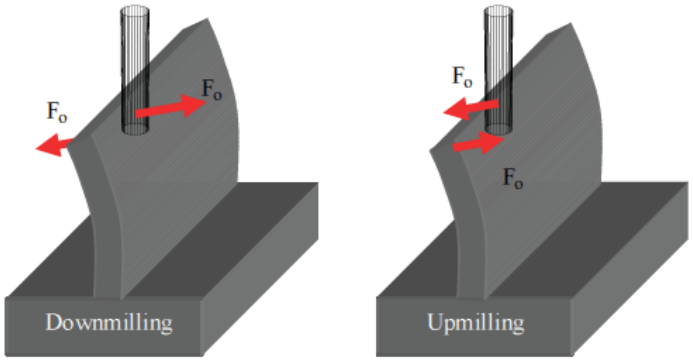

Figure 6-15 Schematic of cutting force direction in down & up milling [17]

6.7 Conclusions

In this chapter, tuned mass dampers were designed and validated for damping machining vibrations. After briefly covering the modelling procedures for viscoelastic materials, the test case for validating the viscoelastic material properties taken from the datasheet is presented. The predicted frequency response for a plate with a constrained layer damping treatment is compared against the results given in a research paper. The natural frequencies and amplitude of the frequency response matched very closely, thereby validating the viscoelastic material properties and the FE modelling methodology. The design considerations and calculations for tuned mass dampers for the workpiece first

fundamental mode of casing are presented. Although the dampers are theoretically tuned for the first fundamental mode, due to the higher mass ratio of dampers (with 6 dampers), the damping is expected and observed to be over a wider bandwidth.

For thin wall casings with large surface area, investigating such high mass ratio tuned dampers is useful. Tuned mass dampers on the casing are modelled using FE analysis. Considering that during the finishing operations it is the workpiece first fundamental mode that is dominant, the developed FE model can be used for estimating the damping effectiveness for finishing operations. The FE predicted harmonic response is experimentally validated through an impact hammer testing. The response curves matched well with the error in the natural frequency prediction at 8%. Considering that the FE model is not updated, this error is considered to be reasonable and useful for predicting damping effectiveness.

The effectiveness of tuned dampers in actual machining conditions is evaluated by measuring the reduction in the vibration RMS value. The vibration value reduced by 2.3 times and 4 times for 2mm and 0.5mm depths of cut respectively, showing a moderate dependence on the depth of cut. This could be possibly due to the fact that at higher depths of cut the forced vibration due to the tool at the tool's torsional frequency is high and hence the damper effectiveness is less. The dynamic coupling between the tool and the workpiece shows a variation from a tool torsional mode behind the damper block to a tool bending mode between two damper

blocks. This resulted in a variation of the machined wall thickness to the order of 70 microns for the machining parameters used.

Application of tuned dampers for thin wall casings has not been researched earlier and hence the findings reported here in terms of vibration reduction, coupled interaction and FE modelling are novel and will help in appropriate use of this damping solution.

7 Vibration suppression with surface dampers and its FE modelling

7.1 Introduction

In the previous chapter, tuned mass dampers were employed to damp the machining vibrations in the thin wall casing. While they are good at damping the vibration, due to the intermittent nature of spatial damping that they offer, the vibration reduction is not uniform over the entire casing. This has two major implications; variation in the machined wall thickness and variation in the vibration levels across the damper block. While the former can lead to dimensional variations, the latter can result in surface finish variations. To address these issues, a total surface damping solution was envisaged. The premise of such a damping solution is to cover the entire surface area of the casing thin wall while providing the necessary stiffness, mass, and damping to minimise the vibration.

Surface damping solutions are popular in minimising thin panel vibrations such as automotive, aerospace structures, machine tools, ships, turbines, etc. These are typically in the configuration of either free layer damping treatment or constrained layer damping treatment. Figure 7-1 [96] shows these variations and also the mode in which a viscoelastic material is deformed for these configurations. In a free layer damping (FLD) treatment, one side of the viscoelastic layer is free and hence its longitudinal deformation (extension and compression) takes place during vibration. The damping is dependent on the composition of the damping material and increases with damping layer thickness.

In constrained layer damping (CLD), being fixed between constraining and base layers, the viscoelastic layer undergoes shear deformation. CLD systems are used to increase damping in stiff structures. When the system flexes during vibration, shear strains develop in the damping layer and energy is lost through shear deformation of the material. CLD treatments are more efficient than FLD treatments on the basis of damping versus added weight, though this is achieved with some difficulty of application [92]. Commercial viscoelastic tapes with paper backing and with constrained layer aluminium foil backing are available from 3M® company. The former can be used for FLD treatments and the later for CLD treatments.

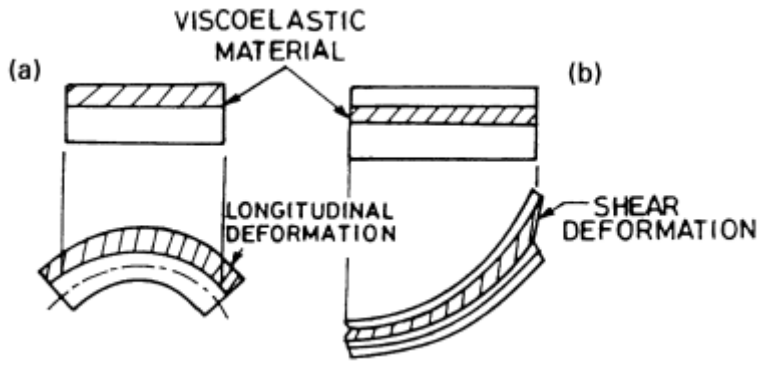

Figure 7-1 Configurations of viscoelastic surface damping: (a) Free layer damping treatment, (b) Constrained layer damping treatment [96]

Although such surface damping treatments can be attempted for covering thin wall casing surface areas, machining applications have the following considerations which need to be taken into account while designing damping solutions.

1. The frequencies to be damped while machining a thin wall casing need not be always one of its resonant modes, as is common in typical

vibration minimisation applications. As presented in Chapter 4 about coupled dynamic response interaction, the dominant frequencies on a thin-walled parts during milling depend on the depth of cut: (i) for smaller depth of cut values, the tool torsional mode dominate during the contact of the cutting tooth while the workpiece fundamental modes dominate during the non-contact period; (ii) for higher depth of cut values, the tool torsional mode is always dominant. Therefore, in milling thin-walled parts, not only the workpiece resonant vibrations but also the imposed tool's forced vibration need to be minimised. Damping is effective in vibration amplitude minimisation only at resonance of the part that is vibrating, as shown in Figure 7-2. Hence, in a forced vibration situation such as in this case, the proposed solution should offer not only damping but also improve the mass and the stiffness of the structure.

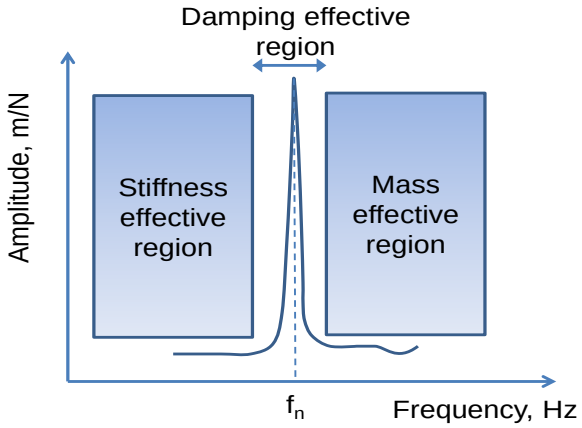

Figure 7-2 Pictorial representation showing the areas of mass, stiffness and damping significance for a single-DOF system

2. The frequency range to be damped in machining can be typically up to 10 kHz and depends on the stiffness of the connection dynamics [97] and hence the proposed damping system should be effective over a

wider bandwidth. Commercial surface damping tapes are designed for a limited bandwidth, as most of the non-manufacturing applications are focussed on resonant vibrations of structural panels (e.g. automotive car body panel, aircraft fuselage panel, etc.)

3. For the automotive applications, due to light-weight requirements, the treatments are designed for maximum energy dissipation only through shear deformation of the viscoelastic layer, for fixturing applications in machining. Mass addition is not as critical and hence, in addition to damping, mass and stiffness improvement can be considered.

7.2 Proposed surface damping solution

Considering the above factors, a novel surface damping solution is proposed, modelled and validated on the thin wall casing. The proposed damping solution consists of a flexible viscoelastic substrate layer (e.g. neoprene), onto which discrete masses are attached at particular locations determined by analysis of the results from both impact testing and FE modelling. The substrate layer, whose role is to conform to any part geometry and offer damping, can be mounted on thin-walled casing with a viscoelastic or suitable adhesive tape. The attached masses not only help in adding mass to the workpiece (hence increasing inertial forces) but also in anchoring the substrate at intermediate points allowing it to stretch, as shown in Figure 7-3, during vibration and hence imparting stiffness to the workpiece.

Thus, this solution improves upon all three characteristics - mass, stiffness, and damping of fixturing system. Being very compact, the proposed damping solution can be used in components such as Front Bearing Housing (see Figure 1-3 in Chapter 1) where space constraints exist due to subsequent machining operations and criticality of internal components such as vanes for fixture to be loaded.

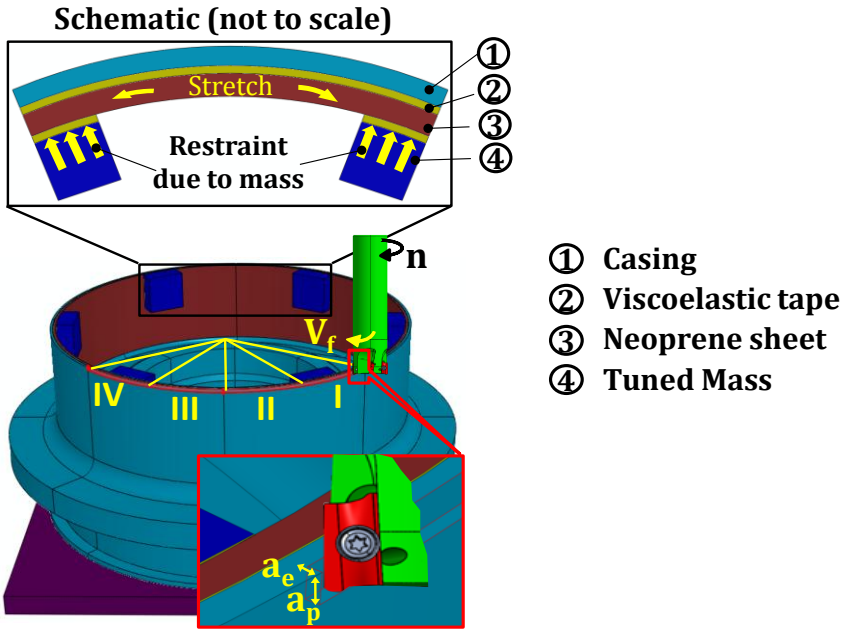

Figure 7-3 Concept of surface damping solution

Damping is offered by both the viscoelastic tape used and the flexible sheet. In this research, the viscoelastic tape used is same as that used for tuned mass dampers i.e. 3M® ISD-112, and neoprene is used as the flexible sheet. Neoprene is chosen as it has good flex and tear strength while also performing well in contact with oils and many chemicals since it will be exposed to cutting fluids during machining [98], [99]. Moreover, neoprene is widely available and cheaper than most other elastomers. In this research, commercially available Neoprene rubber 264C from RS

Components [100] is used and its physical properties are given in Table 7-1.

Table 7-1 Physical properties of Neoprene 264C rubber [100]

Property	**Limits**
Hardness, IRHD	55-70
Density, g/cc	1.4±0.2
Tensile strength, MPa min	5
Elongation at break, %min	200
Compression set, %max	30

The available thicknesses for this neoprene sheet are 1.5mm, 3mm, 5mm, etc. It can be seen that the lower the thickness, the more elastic is the sheet and vice versa. For the present application, we need a moderate stiffness to be exerted on the casing due to stretching of the sheet while also offering a constraining layer effect on the underlying viscoelastic tape. Hence, for this research a 3mm sheet is chosen for all experimental studies. The masses shown in Figure 7-3 were tuned for the first fundamental mode of the workpiece after mounting neoprene sheet, determined through FE analysis. However, before performing FE analysis, the viscoelastic properties of the neoprene have to be evaluated, i.e. the storage and loss modulus and their variation with frequency have to be determined.

7.3 Evaluation of viscoelastic properties of neoprene

There are different techniques for the experimental determination of complex moduli functions of a viscoelastic solid material. The methods operate either in time or frequency domains and cover different frequency (or time) scales as shown in Figure 7-4, reproduced from [84] in which a brief explanation and experimental procedure of the methods are given. The various methods can be classified as follows:

1. Creep and stress relaxation methods
2. Torsion pendulum method
3. Forced vibration non-resonance methods
4. Resonance methods
5. Wave propagation methods

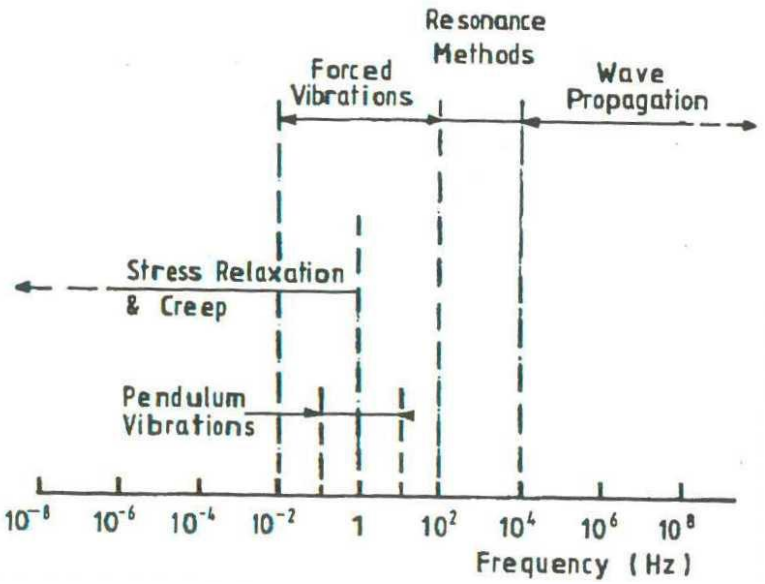

Figure 7-4 Approximate frequency ranges for various experimental methods [84]

In the present study, the forced vibration non-resonance method is used and hence will be briefly explained here.

The forced vibration non-resonance method is a direct technique for the measurement of the complex moduli of a viscoelastic solid in the frequency range from about 0.1 to 200Hz. One end of a rod or bar sample of the material is fixed rigidly while the other end is connected to a vibrator as shown in Figure7-5. The free end of the sample is subjected to an axial sinusoidal displacement $x_o(t)$ with the output force $f_o(t)$ from the sample being simultaneously monitored. The ratio of the output force $f_o(t) = F_o^* e^{j\omega t}$ to the input displacement $x_o(t) = X_o e^{j\omega t}$ directly gives the complex stiffness of the polymer sample as,

$$k^* = k' + jk'' = \frac{F_o^*}{X_o} = \frac{F_o e^{j\emptyset}}{X_o} = \frac{F_o}{X_o}(cos\emptyset + jsin\emptyset) \qquad \text{Eq. 7-1}$$

which gives

$$k' = \frac{F_o}{X_o}cos\emptyset \quad ; \quad k'' = \frac{F_o}{X_o}sin\emptyset \qquad \text{Eq. 7-2}$$

and the magnitude of the complex stiffness and loss factor as,

$$k = (k'^2 + k''^2)^{1/2} = F_o/X_o \qquad \text{Eq. 7-3}$$

$$\eta = \frac{k''}{k'} = tan\emptyset \qquad \text{Eq. 7-4}$$

where X_o is the peak amplitude of the input displacement, F_o is the peak amplitude of the output force, and Ø is the phase angle between $x_i(t)$ and $f_o(t)$.

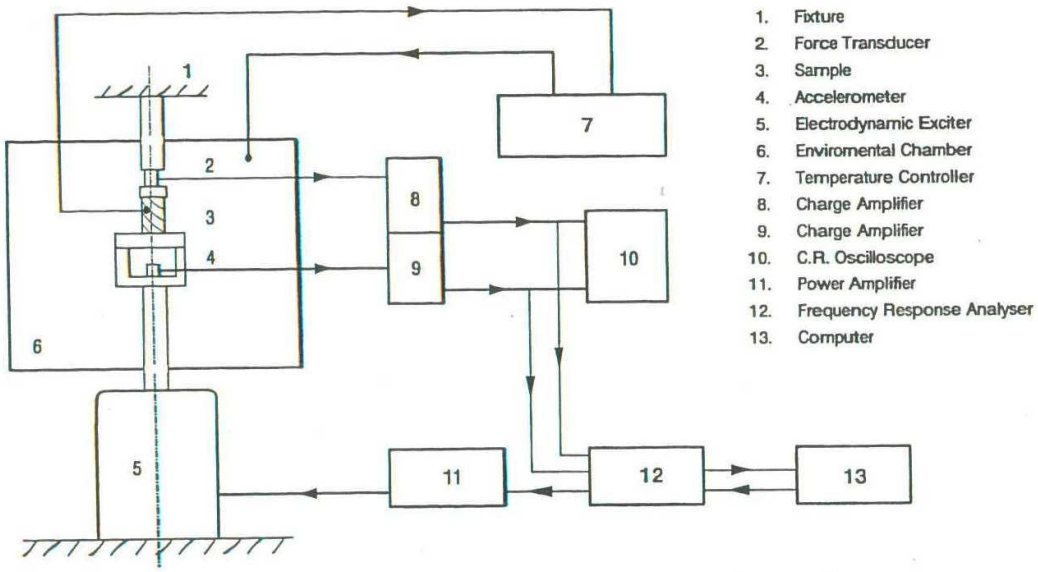

Figure7-5 Direct measurement of complex stiffness using Forced Vibration Non-Resonance method [84]

From the measured complex stiffness and the geometrical dimensions, the appropriate complex modulus can be derived. However, there are shape effects which introduce shape factors. Thus, the true complex shear modulus G* is related to the measured or apparent complex modulus G_a^* by Eq. 7-5.

$$G^* = G_a^*\left(1+\frac{t^2}{36r^2}\right) \quad where \quad G_a^* = \frac{k^* t}{2A} \qquad \text{Eq. 7-5}$$

wher t, A, and r are the thickness, cross-sectional area and radius of gyration of the cross-section about the neutral axis of bending, respectively. For a sample with a cross-section of length L and breadth b, for example,

$$G^* = G_a^*\left(1+\frac{t^2}{3L^2}\right) \qquad \text{Eq. 7-6}$$

Thus, if t<L/4, then $G^* = G_a^*$.

The forced vibration non-resonance method has some advantages over other methods. In particular, it enables the investigation of the effects of

frequency, static prestrain and dynamic strain amplitude on the dynamic properties of polymers over continuous and wide ranges.

This forced vibration non-resonance method is commercially available as Dynamic Mechanical Analysis (DMA). TA instruments DMA Q800, shown in Figure 7-6, is used to evaluate the viscoelastic properties of neoprene. The testing can be done in various modes; tension mode is chosen as it simulates the application requirement of stretching of neoprene sheet. Testing was carried out in an isothermal multi-frequency sweep mode where the sample is initially raised to the set temperature and then oscillated at constant amplitude sweeping across the set frequency range. Experiments were carried out from -40°C to +60°C in steps of 20°C. The sample was equilibrated at the desired temperature for 5 minutes before applying the frequency sweep. The frequency range swept was 0.1 – 200Hz with an amplitude of ±15μm. The dimensions of the sample tested are: 20 X 8.5 X 3mm, as suggested by the equipment supplier.

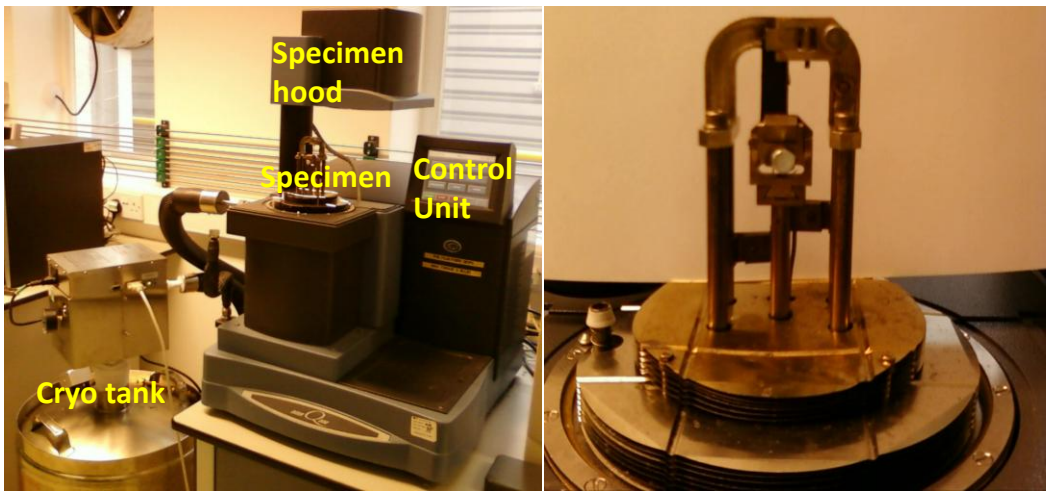

Figure 7-6 Dynamic Mechanical Analysis equipment (a) and close up view of specimen held between chucks

Using the procedure as explained before, the storage and loss modulus for each of the isothermal test are evaluated for the whole frequency sweep. These plots are shown in Figure 7-7. As predicted, the shear (and hence elastic) modulus of the neoprene is high at lower temperatures. The frequency range is limited to 200Hz due to the resonance of the structural parts of the testing machine itself. However, to extend the frequency range, a principle called Time-Temperature Superposition (TTS) is used [84]. This principle is also called Time-frequency or Reduced Variables technique. According to this technique, the modulus and loss factor data obtained at different temperatures and over a narrow frequency band are reduced to a single master curve of modulus and loss factor which cover many decades of frequency at a chosen reference temperature. The detailed procedure is given in [84] and schematically shown in Figure 7-8. While shifting the data, different shift models can be used to find the shift factor. For many viscoelastic materials, the magnitude of the frequency shift required is found to follow the William-Landel-Ferry (WLF) model [84].

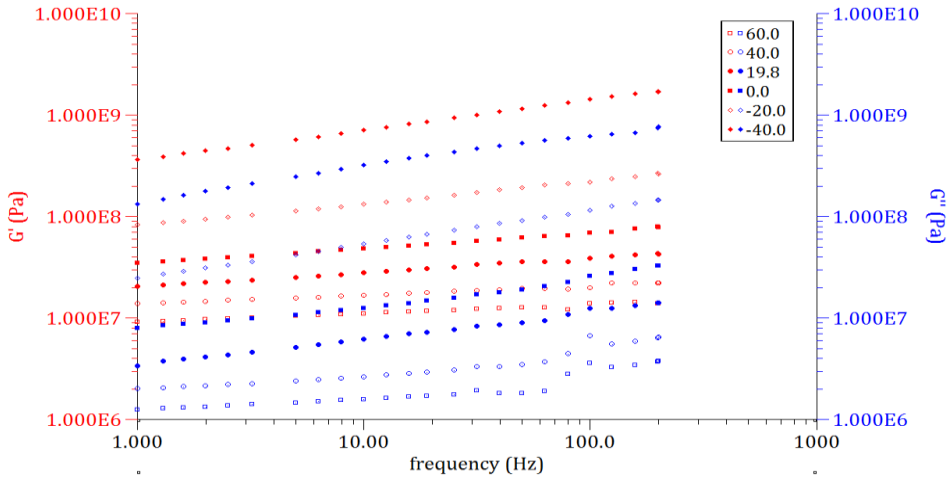

Figure 7-7 Plot of storage and loss modulus for neoprene at various temperatures as extracted from DMA tests

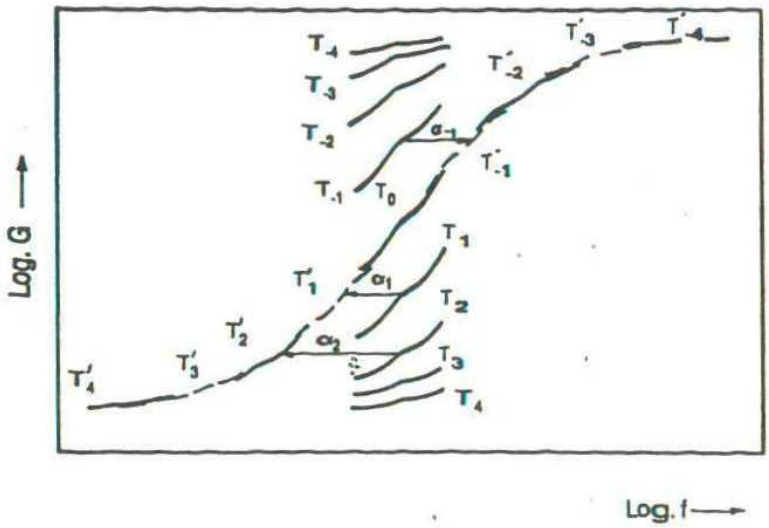

Figure 7-8 Concept of reduced variables technique [84]

For the present data, the WLF model is used with a reference temperature of 20^{o}C and the shifted data is shown in Figure 7-9. It can be noticed that the data now spreads over many decades of frequency. However as the range of interest for this research is only up to 10 kHz maximum, corresponding data is only used for FE analysis. One important observation that can be made from the data is that the loss and storage moduli are increasing with frequency and tend to reach a maximum around 1E9Hz. Therefore, with such a material, one can expect that higher frequencies will be more readily damped than those of lower frequencies. To evaluate the loss factor, η, of the neoprene, the ratio of loss modulus to storage modulus is calculated. It varies from 0.22 to 0.32 in the range of 10Hz to 10,000Hz. Therefore, as compared to the viscoelastic tape 3M® ISD 112 (loss factor varies from 1 to 0.5 in the same range) with which the neoprene sheet is attached to the casing, the damping offered by neoprene is not significant. However, the modulus values are at least two orders higher which provide necessary stiffness to support the masses while also

providing the conformability making it an appropriate choice for the proposed solution.

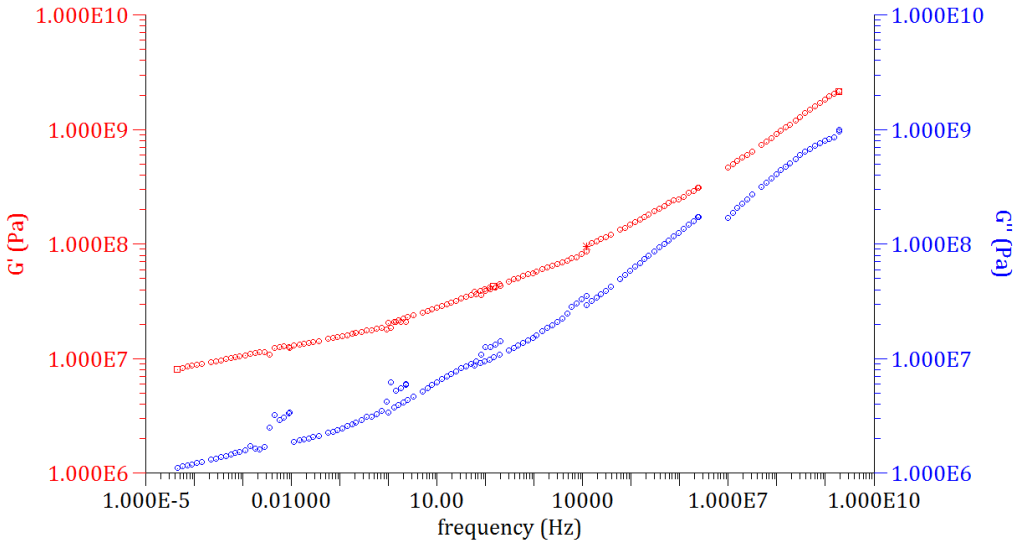

Figure 7-9 TTS shifted data plot of storage (G') and loss modulus (G") for neoprene

7.4 FE analysis of the proposed surface damping solution

A Finite element model of the thin wall casing with a neoprene sheet is created as shown in Figure 7-10. As can be noticed, to avoid any element distortion due to tying of the nodes of neoprene to the visco tape and the visco tape to the casing, all three parts are discretized with the same number of elements. The viscoelastic material properties of neoprene as evaluated through dynamic mechanical analysis are input into the FE software. For the viscoelastic tape, 3M® ISD-112, the properties as given in Chapter 6 were used. Modal analysis was carried out to find the frequencies and mode shapes. It must be noted that while solving the eigenvalue problem in modal analysis, the stiffness matrix has to be constant. For this, the FE software provides an option of specifying the frequency at which the modulus value has to be considered for building

the stiffness matrix. Hence, all the natural frequencies calculated through FE modal analysis will not be accurate, except for the ones near the specified frequency. In the present case, the first fundamental mode of the casing was specified as frequency at which the modulus has to be considered. It is noticed that the order of the modes of casing with a neoprene sheet is the same as that of an undamped casing, though the frequency varies (due to mass and stiffness addition of neoprene).

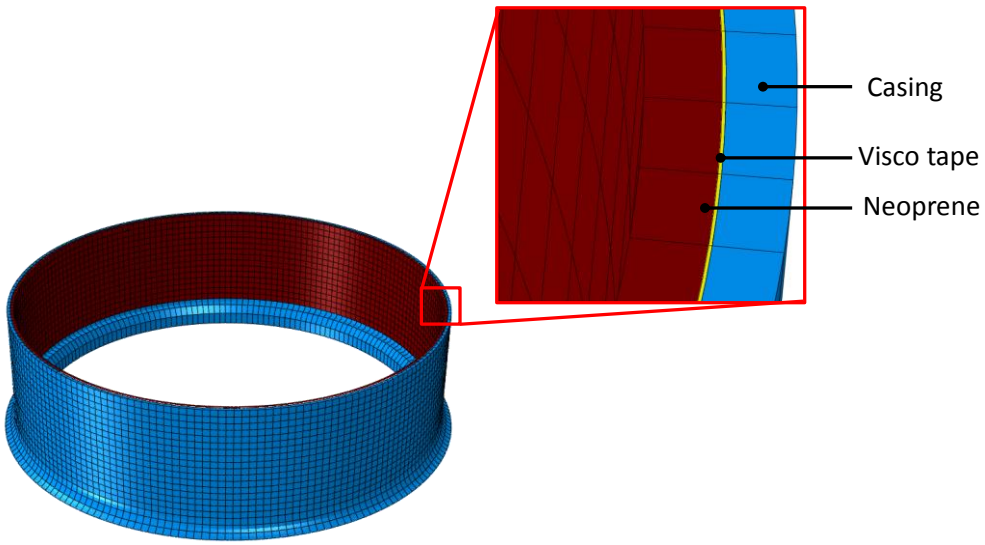

Figure 7-10 FE model of casing with neoprene

Preliminary machining tests are conducted on a casing with a neoprene sheet attached. The acquired vibration signal was converted to the frequency domain using FFT and the result is shown in Figure 7-11. It can be seen that the first fundamental mode, 1261Hz, of the workpiece is dominant in FFT. The first fundamental mode of FE model corresponds to 1207Hz due to non-updating of the model. Also, owing to the increasing loss factor with frequency for neoprene, higher workpiece modes are more damped than the lower modes. Also, the clear participation of the tool bending mode, 4802Hz, can be noticed. It should be noted that the

frequency scale on the X-axis is limited to 10,000 Hz to show the workpiece's first fundamental mode dominance clearly. The tool torsional mode is also present in the spectrum at 16200Hz.

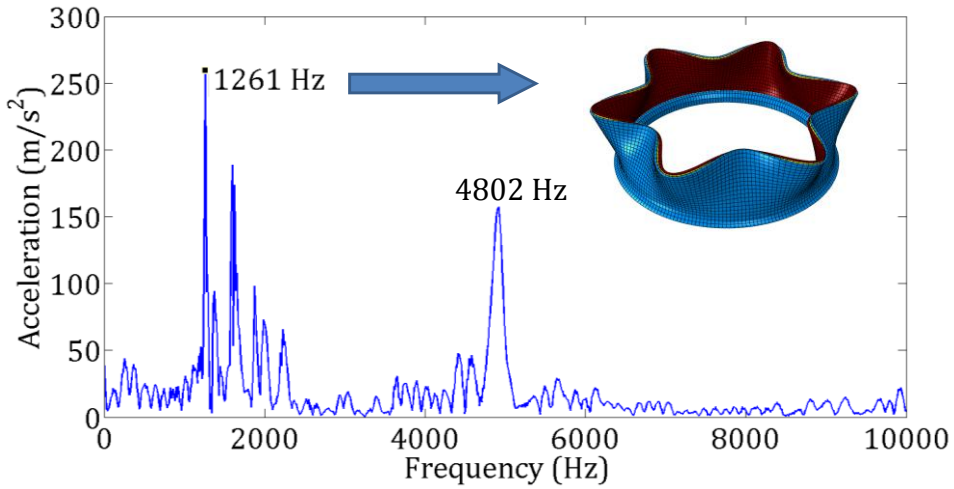

Figure 7-11 FFT of machining signal of casing with neoprene

From the observed results, the damper blocks were tuned for 1261Hz and six blocks were mounted as shown in Figure 7-12 (a). The same damper blocks as those used for the tuned damper analysis were used. However, the thickness of the viscoelastic tape was calculated to tune for the 1261Hz frequency, using the procedure given in section 6.4. The thickness of the viscoelastic tape worked out as 1.25mm.

These tuned damper blocks were modelled in FE software on the top of the neoprene sheet, as shown in Figure 7-12 (b). Modal analysis was carried out and the elastic strain energy in the neoprene sheet is studied for the first few fundamental mode shapes. As shown in Figure 7-13, the strain energy in the neoprene sheet with masses has increased, indicating the elastic stretching phenomenon assumed in the proposed design

solution. This stretching offers stiffness to the casing, thereby minimising the vibration amplitude.

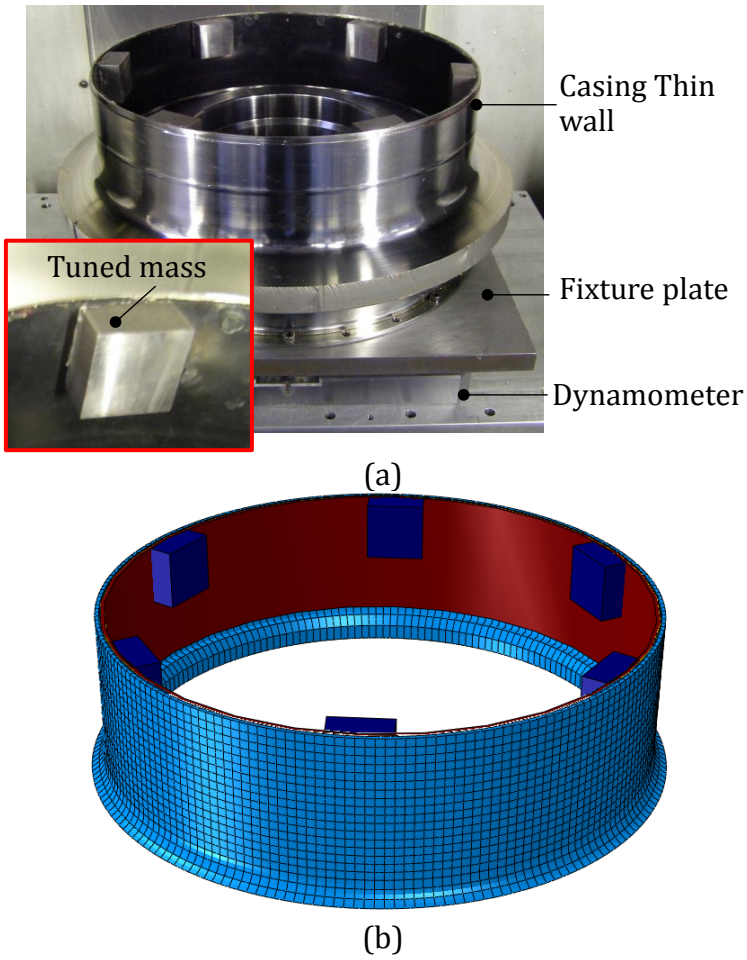

Figure 7-12 Casing with neoprene and tuned masses: (a) Experimental (b) FE model

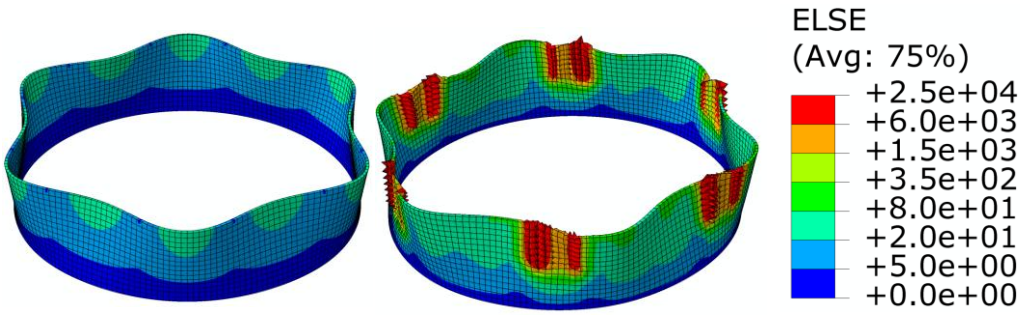

Figure 7-13 Strain energy in neoprene sheet for first fundamental mode without and with tuned masses

In addition to modal analysis, frequency responses were predicted using FE harmonic analysis and are validated through FRFs acquired during

impact hammer testing. Harmonic analysis was carried out on the FE model using direct integration to take into account the frequency dependent variation of the viscoelastic properties. The FRFs acquired and predicted are shown in Figure 7-14. For the sake of comparison of the damping achieved, the undamped frequency response is also shown.

The dynamic response of the casing with neoprene sheet and masses shows damping of all neighbouring modes in addition to the targeted mode due to the high mass ratio of the dampers. However, the relative reduction in amplitude of the response is not significant as compared to the neoprene sheet alone – reduced only by an order of magnitude. This can be explained as the vibration generated by a single impact damps out quickly due to the structural damping of the casing and the neoprene; hence, the effect of stiffness due to stretching of the neoprene is not significant for a single impact excitation. It can be noticed that the FE prediction of the order of magnitude is very reasonable. The maximum error in frequencies observed was respectively 4%, 7% & 8.5% for undamped, with neoprene, and neoprene with masses. This could be minimised through updating the boundary conditions and material properties in the FE model. However, as explained in section 6.5, model updating with non-proportional damping is not available in commercial software and is a topic of research interest. Thus, for the generated model for the present study, this level of error was considered acceptable and shows the effectiveness of the surface damping solution in damping the workpiece frequencies typical in milling of casings.

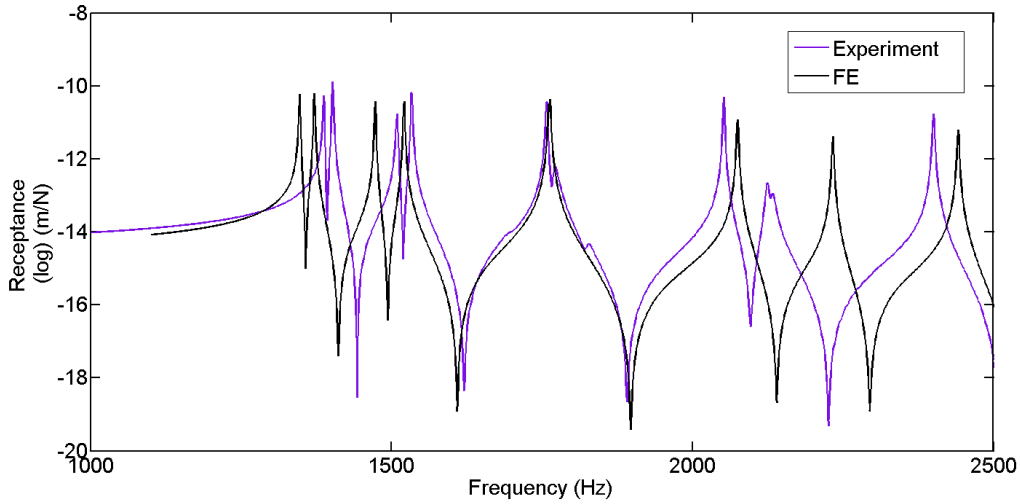

(a)

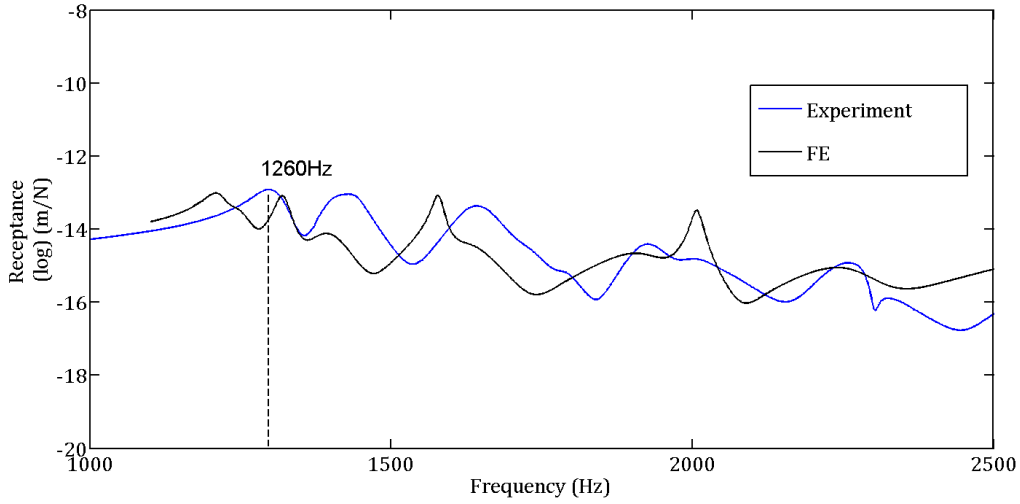

(b)

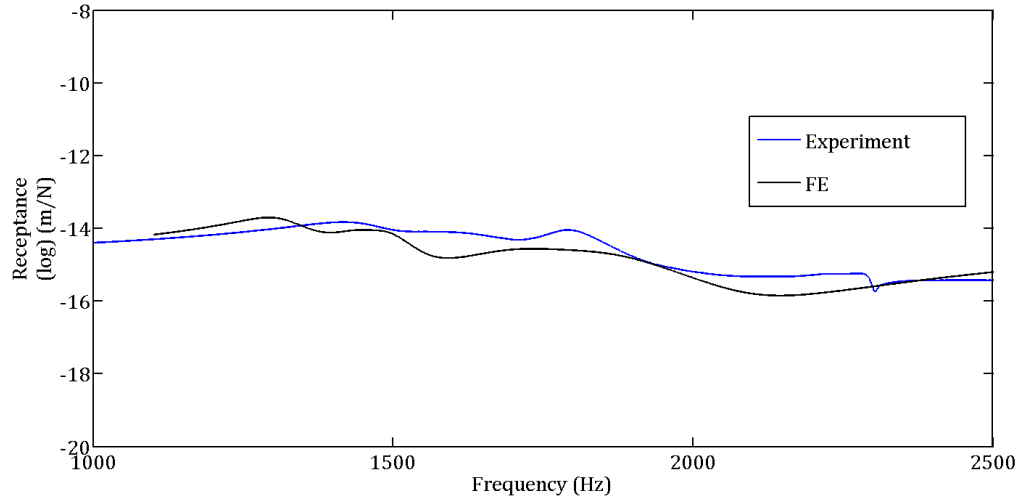

(c)

Figure 7-14 Frequency response comparisons – FE Vs Experimental: (a) Undamped (b) Casing with only neoprene (c) Casing with neoprene and 6 TMDs

Hence, it can be utilised for first order damping effectiveness prediction of a thin wall casing for evaluating newly proposed damping solutions. Again, as mentioned in the case of tuned dampers, this FE model can be extended to include coupled dynamic interaction, thus enabling the prediction of actual machining dynamics. This forms the future scope of this work.

7.5 Dynamic response analysis in milling of casing with proposed surface damper

7.5.1 Improvements in vibration reduction

The validation of the proposed damping solution was conducted by peripheral milling of the thin walled casing. In addition, the frequency content of the acceleration signals acquired during milling were analysed by Fourier transformation to identify the dominant modes contributing to the vibration. To analyse the frequency content of the signal for one tool revolution, acceleration and cutting force during machining were synchronously measured in one quadrant of the casing in four sectors. This break-up into four sectors was needed as data was collected at a higher sampling rate of million samples per second to obtain a better frequency resolution of spectrum. The same tool overhang of 46mm was maintained. Milling parameters were chosen to reflect industrial conditions over a range of values (a_p=0.5 to 2mm; a_e=0.5 to 2mm) with a constant cutting speed (v_c=40m/min) and feed per tooth (f_z=0.1mm/tooth).

The reduction in machining acceleration is quantified in terms of the root mean square (RMS) value of the signal acquired, the methodology of

which is given in section 6.6.1. Machining results for sector II of the casing, with machining parameters a_p=2mm, a_e=1mm, are presented in Figure 7-15. As can be seen, the reduction in vibration on the casing with the neoprene surface damping alone is not significant enough (1.47 times compared to the undamped structure) as compared to the casing with the neoprene with masses (3.76 times compared to the undamped structure). This trend is in variation with that observed from the FE results, simulated for a single impact excitation, where the casing with neoprene showed significant relative reduction in the vibration amplitude (Figure 7-14(b)) as compared to that of the casing with the neoprene and masses (Figure 7-14(c)). This variation can be explained as follows. Unlike in a single impact excitation, as simulated in the FE analysis (section 7.4); in machining it is a multiple excitation where the cutting energy is continuously fed into the casing through forced vibration during the cutting action of the tool. Hence, the simple damping effect of neoprene sheet is not sufficient and the stiffness offered by stretching of neoprene sheet between the masses is useful in minimising the vibration. Moreover, the additional damping offered by compression of the neoprene under the tuned masses also helps in vibration minimisation.

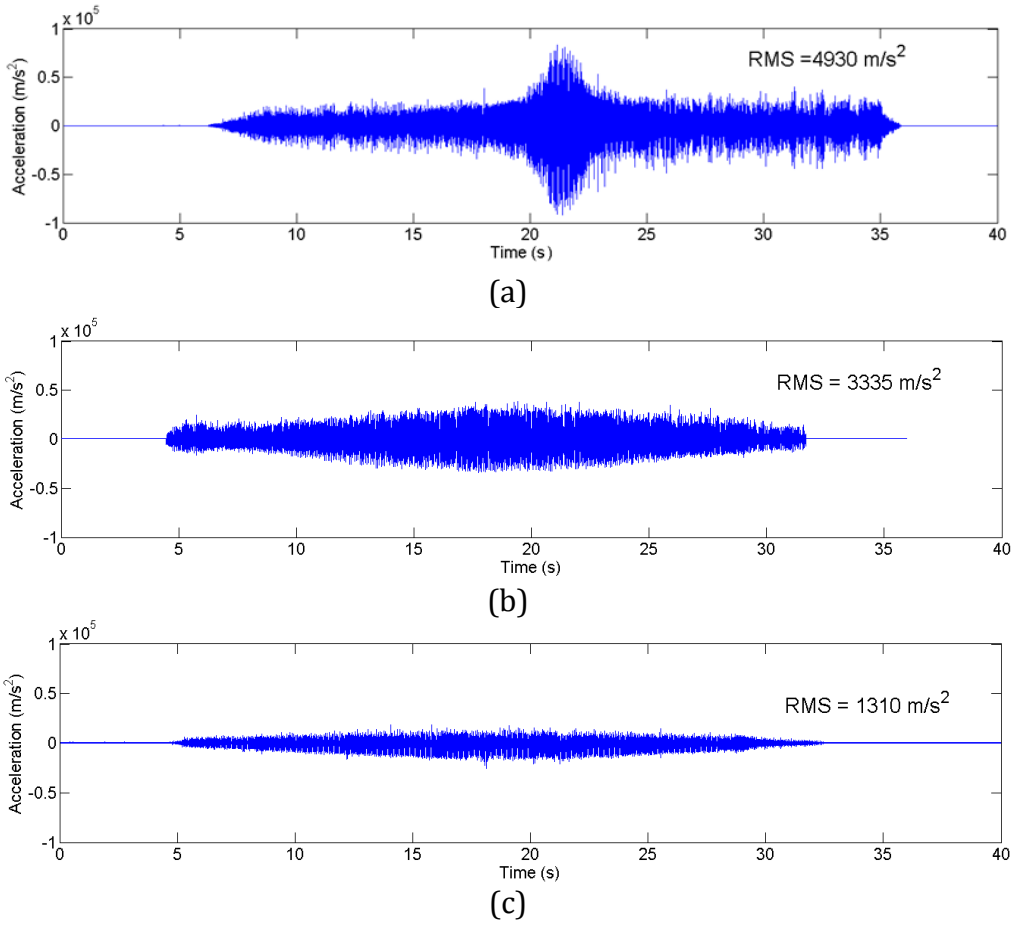

Figure 7-15 Machining acceleration signals of the casing: (a) undamped (b) with neoprene sheet (c) with neoprene and tuned masses

7.5.2 Analysis of coupled interaction between tool and workpiece with surface damper

The coupled interaction between the tool and the workpiece was evaluated by studying the frequency content in the machining vibration signal. This was performed using time-frequency analysis of the vibration signal across equi-spaced sections for one revolution of the tool. The detailed methodology of the coupled interaction analysis procedure is provided in section 3.4.

The time-frequency plot for the acceleration signals acquired on the casing with neoprene and neoprene and masses, for a_p=2mm and a_e=1mm,

is shown in Figure 7-16. As can be seen from Figure 7-16 (b), there is a decrease in the amplitude of the modes in the spectrum. However, the torsional mode of the tool is still dominant with a slight appearance of tool bending mode. This can be explained as the casing remained a closely-stiff structure whereby the tool is excited tangentially during cutting leading to the appearance of the torsional mode. The slight appearance of the tool bending mode could be due to improvement of the stiffness of the casing by the mounting of neoprene. If the casing is stiff enough in the radial direction, the tool bending mode tends to participate which can be captured by the accelerometer. Also, the 'ringing' of the tool mode, after the tool has left the workpiece, is absent with the mounting of neoprene, indicating its suppression of the free vibration of the casing.

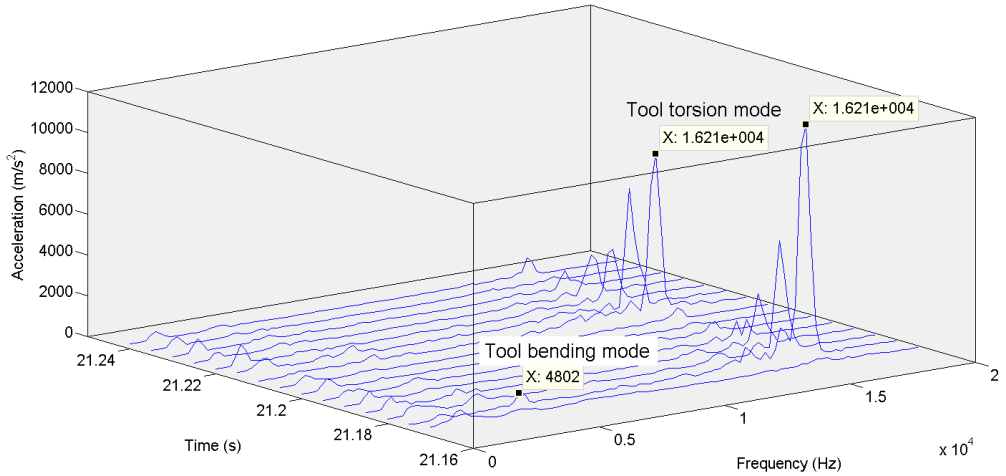

(a)

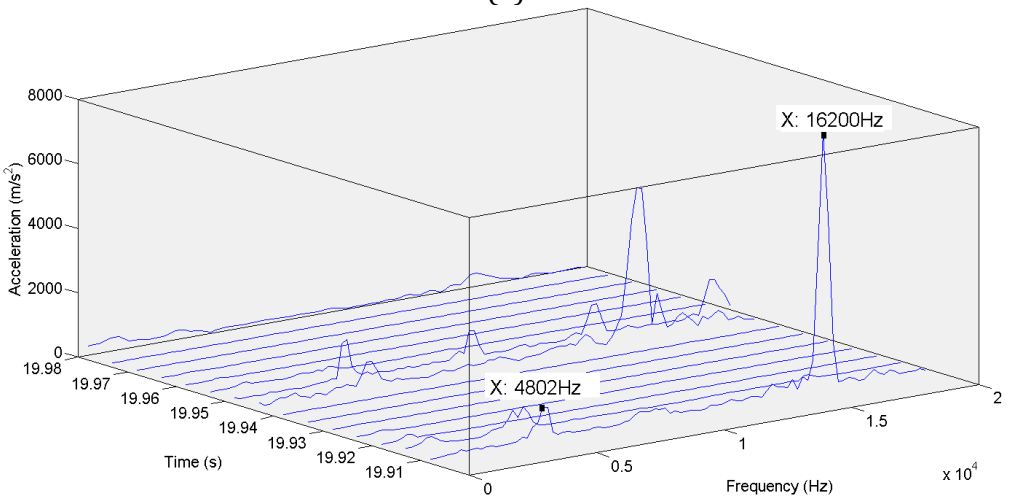

(b)

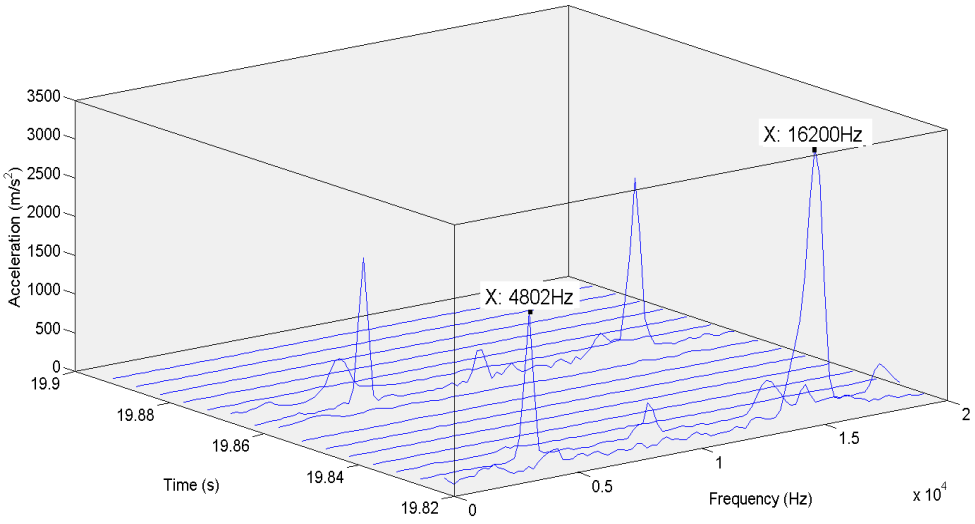

(c)

Figure 7-16 Time-frequency analysis of acceleration signal when milling casing at a_p=2mm, a_e=1mm: (a) undamped (b) with neoprene (c) with neoprene and tuned masses

As explained earlier, for the casing with tuned masses mounted on it, the signal is analysed exactly between two masses due to its likelihood of more vibration. Figure 7-16 (c) shows the time-frequency plot of such signals. It can be seen that after the masses are mounted, the amplitude of vibration reduced significantly. The tool bending mode also participates along with the tool torsion mode. This could be explained due to the fact that the casing between the masses acts as a cantilever beam fixed at two ends allowing the casing to bend and hence capturing the tool bending mode. This behaviour is similar to that of the casing mounted with simple tuned masses as explained in section 6.6.2. However, the participation of the tool bending mode is not as significant, as shown in Figure 6-12. This is due to the fact that the stretching of neoprene between the masses offers some stiffness and hence minimises the deflection of the casing between the masses. This results in a reduction of thickness variation of the machined thin wall of the casing.

7.6 Conclusions

In this chapter, a viscoelastic surface damper is proposed for thin wall casings. The key principle on which the proposed design stands is to enhance both the stiffness and the mass of the casing instead of the traditional method of improving damping alone. This principle is important considering that the machining vibrations are forced in nature rather than resonant. The proposed solution is a viscoelastic tape mounted neoprene sheet with intermittent masses tuned for the dominant workpiece mode. While the viscoelastic tape along with neoprene

provides damping, the masses provide for the inertia force. The stretching of the neoprene sheet between the masses when the casing vibrates offers some stiffness to it. To validate this stiffness offered by neoprene, FE analysis of the proposed solution was carried out and the elastic strain energy for different mode shapes was studied and was found to increase with the mounting of the masses. The viscoelastic properties of neoprene for FE simulation were evaluated using Dynamic Mechanical Analysis testing. The FE predicted dynamic response is validated against experimental FRFs acquired through impact hammer testing, and a maximum variation of 9% was observed. Considering that further improvement needs model updating taking into account non-proportional damping, which is a topic of current research interest, this error is considered to be acceptable. Hence, the developed FE model is useful in predicting the dynamic response with the proposed surface damper solution. The experimental validation consisting of the RMS evaluation of the vibration signal showed that the proposed solution is effective by nearly 4 times. The coupled dynamic response analysis showed that the proposed solution completely damped all the workpiece modes. The tool bending and torsional modes are also significantly damped. However, one noticeable feature is that with the mounting of the masses, the tool bending mode appears distinctly, though not completely as dominant as that mounted with tuned mass dampers alone (explained in Chapter 6). Finally, the proposed solution is shown to provide significant damping of forced vibrations, which are dominant in machining conditions of thin wall casings.

8 Vibration suppression with torsion spring fixture based surface damper

8.1 Introduction

In chapter 7, viscoelastic based surface damper was proposed using neoprene sheet and tuned masses. The attachment of the neoprene sheet to the casing and the tuned masses to the neoprene sheet was through commercially available viscoelastic tape, 3M® ISD 112. This tape not only adheres well to the casing withstanding heavy forced vibrations during machining, but also provides some damping. One of the side effects of using this tape is the residue left out on casing after removal of the neoprene sheet as can be seen as shown in Figure 1-3. The residue removal on the casing takes 10-15 minutes, depending on area of the surface to be damped. Secondly, the installation time for the viscoelastic tape based surface damper includes laying up the viscoelastic tape on neoprene for every component. This adds additional time to the setting of the damper on the component and hence may not be attractive on components needing only less amount of machining time.

Hence to be industrially more useful with a short set up time, a fixturing concept which does not make use of viscoelastic tape and also is quick for installation is required. Such a fixturing solution is proposed in this chapter which makes use of torsion springs. This fixture also meets the requirements of a structure such as Front Bearing Housing viz. access to the centre of component for multiple machining operations, self-standing

in its location so that it does not rest on the ring of vanes at the bottom thereby causing possible damage due to weight of fixture.

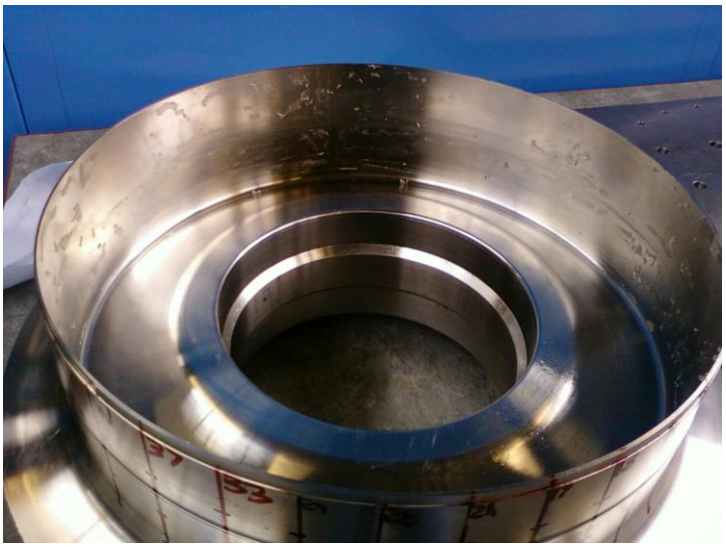

Figure 8-1 Residue of viscoelastic tape on casing

8.2 Torsion spring fixture – design and configuration

8.2.1 Design

The configuration of the fixture is made in such a way so as to improve the mass, stiffness, and damping properties of the thin wall casing. While the principle of obtaining stiffness and damping is same as that of viscoelastic surface based damper, the way inertia forces are exerted is different. In the place of masses, torsion springs are used to exert force on neoprene sheet thereby butting it against the casing, as shown in Figure 8-2. This removes the necessity of attaching neoprene sheet using viscoelastic tape.

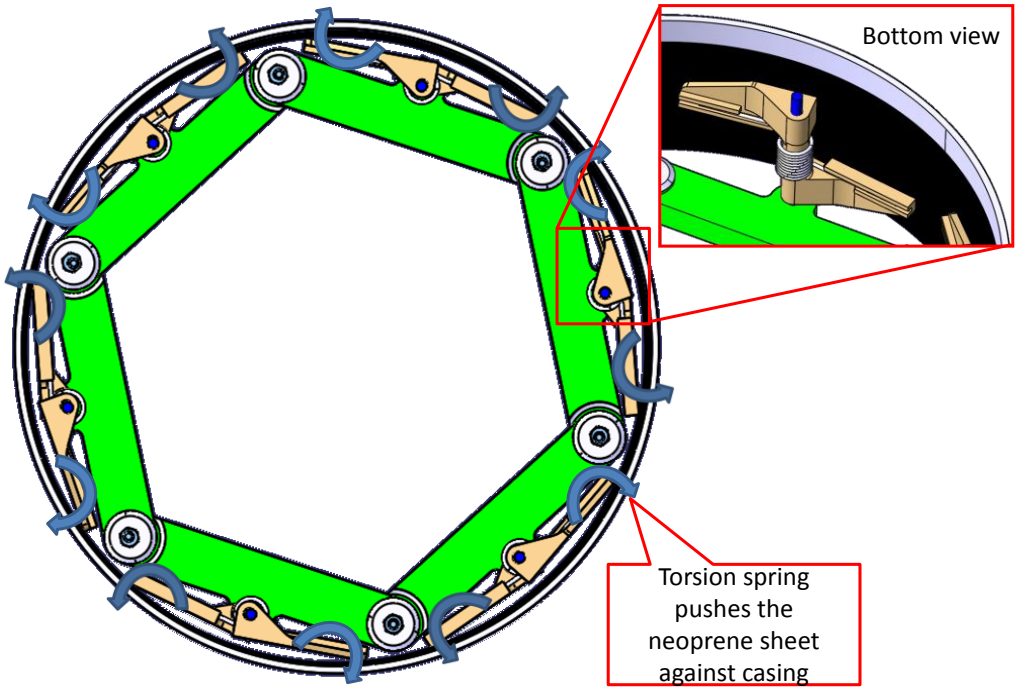

Figure 8-2 Principle of torsion spring fixture

The inertia force is offered by torsional flexing of the spring. Torsion springs come in different leg included angles as shown in Figure 8-3. For the present application of exerting force inside of a circular casing, a 270^{o} leg angle spring was chosen. The stiffness is offered by stretching of neoprene sheet in between springs during vibration of casing. The damping is offered by viscoelastic nature of neoprene sheet. The model of the fixture is shown in Figure 8-4(a), which shows that the springs are held in place using connecting links. The spring legs are inserted in the grooves of spring hinges for exerting a more uniform force.

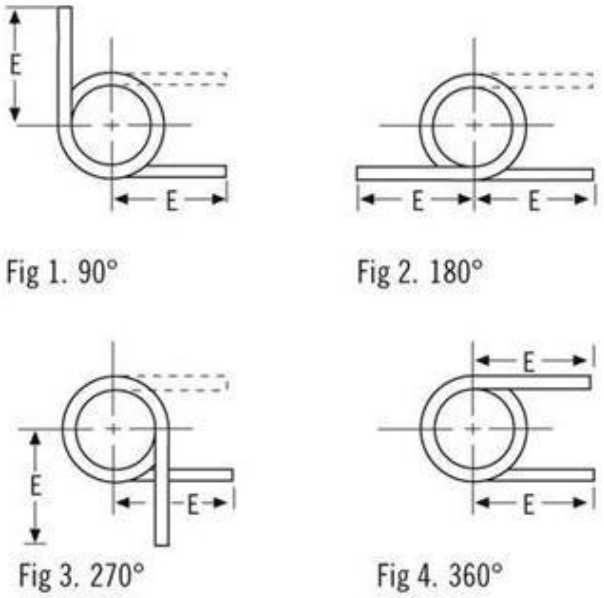

Figure 8-3 Different configurations of torsion spring leg angles [101]

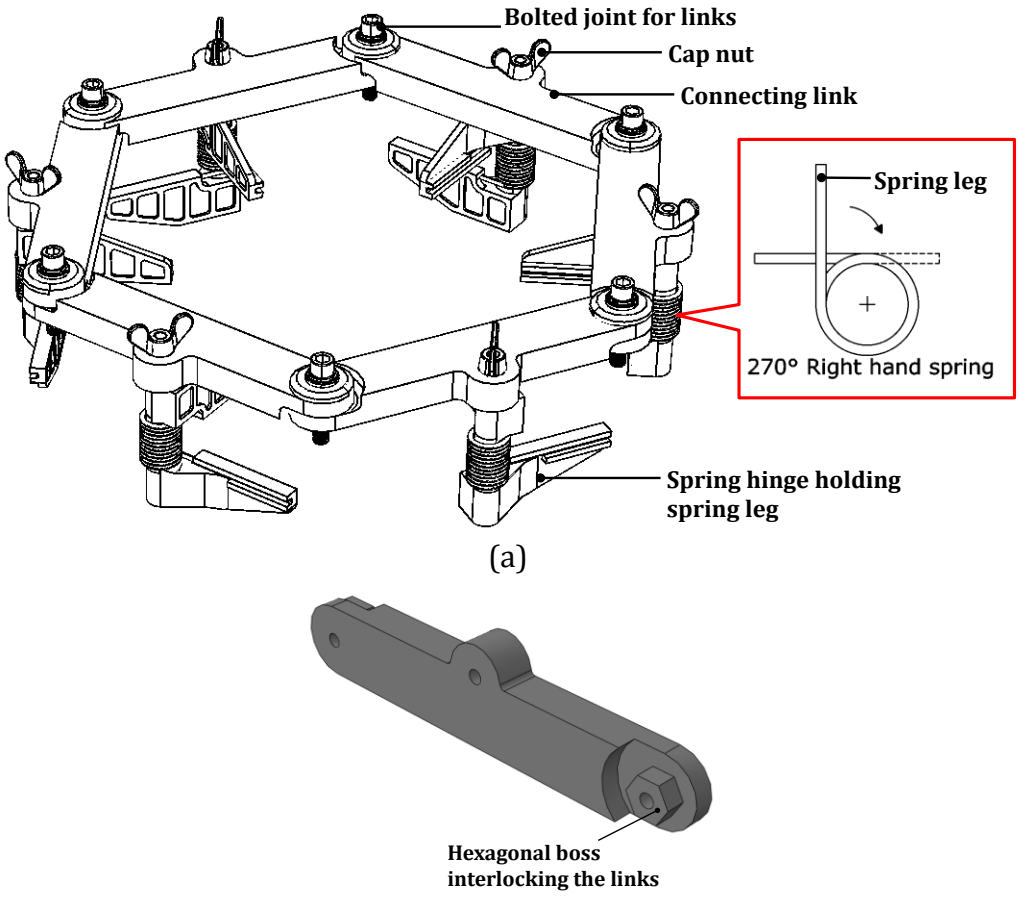

Figure 8-4 (a) Torsion spring fixture model (b) connecting link with internal hexagonal locking mechanism

The spring hinges, on which torsion springs are mounted, are locked in place through cap nuts. The spring hinges have a guiding mandrel for the spring to restrict its out of plane motion (i.e. bending of spring). The legs of spring hinges help in distributing the spring force over wider area. Each of the connecting links is locked with the adjacent link through a hexagonal socket and spigot joint as shown in Figure 8-4(b). Instead of hexagon shape, a splined boss arrangement also could be made which enables adjacent links to be connected at any angle. The reaction force exerted by casing on springs is taken by a structure made up of connecting links. The links are kept in place through bolted joints. The bolts help in restricting axial separation of links; it is the internal hexagonal boss connection that restricts rotational motion. The torsion spring can be designed for the required rotational leg travel and the force it can exert by varying the diameter of coil, number of coils, wire diameter and the material of the spring. Depending on the requirement of force, more than one spring can also be planned between two links. Alternatively the number of links, and hence the number of springs, can be varied to increase the magnitude and uniformity of the force exerted on the casing.

The simplicity of this fixture is that it is self-actuated and hence doesn't require any external mechanism such as driving motor, etc. The presence of spring in between two links implies that it is conformable to the geometry of casing and can take any angular variations in the part features. Also as the fixture is compact it can be used in applications where the access is very less and/or where multiple machining operations

need to be carried out in same setup at different locations of the part. The re-configurability of the fixture comes from the fact that the number of connecting links can be increased or decreased to meet the requirement of various diameter casings. Thus the fixture is totally modular and reconfigurable. And depending on the shape of the plates the fixture can be used to damp either circular or conical or other complex profiles. The spring hinges can be designed as clamping fingers with flexibility so that it can conform to any profile of the casing. For ease of installation the spring hinges can be designed with hooks so that the torsion springs can be initially (before inserting inside casing) primed by rotating spring leg with required pre travel and a pin inserted through hooks. Once inside the casing the pins can be removed for quick release of springs.

8.2.2 Configuration

The above concept of torsion spring fixture is configured for the casing used in this study. For the casing inner diameter of 360mm, the length of each connecting link (i.e. the side of each hexagon) was found to be 156mm leaving a gap of 15mm for the movement of torsion spring.

Configuring a torsion spring for a given application is dependent on many parameters such as number of coils, diameter of spring coil, diameter of spring wire, travel of spring leg, etc. The relation between these parameters and the spring force is as expressed: smaller coil diameter, lesser number of coils, thicker wire of spring, more travel of spring leg result in higher spring force. Designing a custom spring for the required force by varying these parameters is iterative and time consuming.

Moreover, the work that is carried out on this fixture is only as a proof-of-concept of utilising torsions springs for exerting force against casing. Hence choosing one spring from available manufacturer's catalogue is the best method. The practical constraints are the number of coils and spring wire diameters. Though the spring force can be varied by varying the number of coils, manufacturers usually give springs with fixed number of coils and hence cannot be altered. And a thicker spring wire diameter though exerts high force is difficult to install in casing where the spring leg has to be rotated to fit inside the casing. However with modified design of fixture where the legs of torsion spring are locked in preloaded condition and unlocked after inserting the fixture inside the casing, this constraint on spring wire diameter will not exist. In the present design of fixture without feature to lock the spring legs, a spring wire diameter of 2mm was chosen. And for this diameter the manufacturers' catalogue [101] for torsion springs result in 20mm coil diameter.

The initial leg angle configuration is chosen so that sufficient force can be exerted when the spring is mounted inside the casing. For the casing used in the research, the inner diameter is 360mm which gives an approximate included angle for spring legs as 175^0. So, as can be seen from Figure 8-3, it is only the 270^o initial configuration that will give more force for this situation. A 180^o spring would exert very less force. Once the initial spring leg angle and the diameter of casing are fixed, then the travel of spring leg also is fixed. With the above considerations, a right hand torsion spring,

made of Stainless Steel 302, and dimensions as shown in Figure 8-5, is used in this fixture.

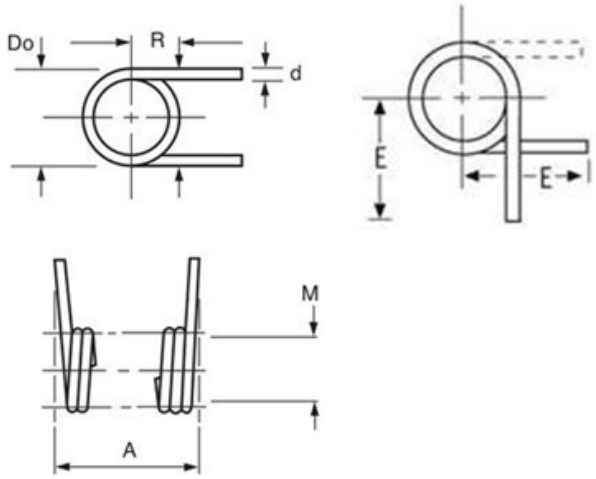

Parameter	Value (mm)
A	29.15
d	2.16
D_o	20.07
M	12.7
E	63.5

Figure 8-5 Parameters of the torsion spring chosen for the fixture

The selection of spring also took into consideration the amount of force it can exert. The selected spring has torque rate of 4.38N-mm/deg at undeformed leg angle of 270^o, as calculated from PlanetSpring Torsion Spring calculator [102]. For the casing with included angle of 175^o, the torque exerted is (270-175)*4.38 = 416N-mm. For a spring leg length of 63.5mm, this exerts a force of 6.55N. This equals to 667gms of force – exactly 3 times the force delivered by the 220gms tuned masses in surface damper solution, as explained in section 6.4. So this allows the opportunity to study effect of inertia forces on minimisation of vibrations.

8.3 Dynamic response testing on casing with torsion spring fixture

The effect of the proposed torsion spring fixture in minimising the vibrations is initially quantified through static impact hammer tests where the dynamic stiffness and damping can be evaluated. For the sake of

comparison with the viscoelastic based surface damper proposed in Chapter 7, impact hammer tests were also carried on casing mounted with that solution as well. The dynamic response for both the cases – torsion spring fixture and viscoelastic based surface damper, along with that of undamped casing is shown in Figure 8-6. As can be seen, the amplitude of vibration for dominant mode for both the solutions is one order less than that of undamped casing. All the high frequency modes are damped significantly in both the solutions owing to the higher loss factor of neoprene sheet with frequency. Moreover the dominant mode with the torsion spring fixture is around 1209Hz as compared to surface damper which has around 1926Hz. This is due to the inertia effect of the spring force which is 3 times to that of masses.

The damping for the dominant mode in the dynamic responses is calculated using half-power method [82] and shown on the graphs. While the undamped casing has 0.07% damping, viscoelastic based surface damper and torsion spring fixture have 3.5% and 4.6% damping respectively. This shows that, more than the damping contribution of viscoelastic tape in surface based damper, the material damping offered due to neoprene sheet under higher compressive forces of springs is more effective. In addition the compliant nature of springs not only offers

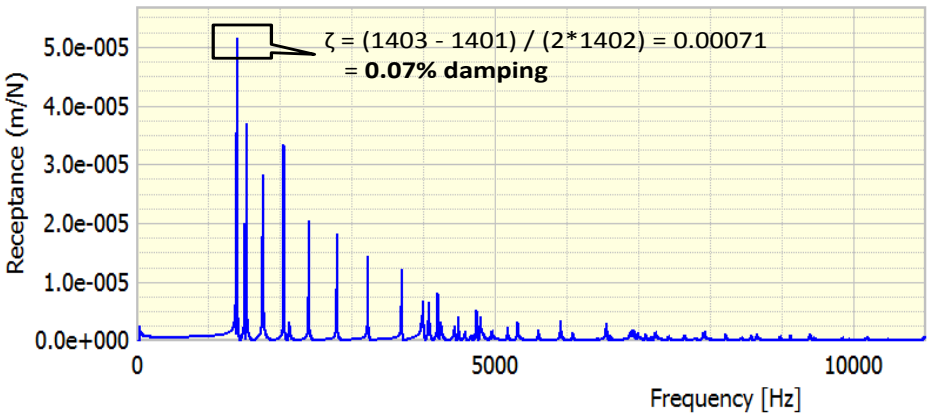

(a)

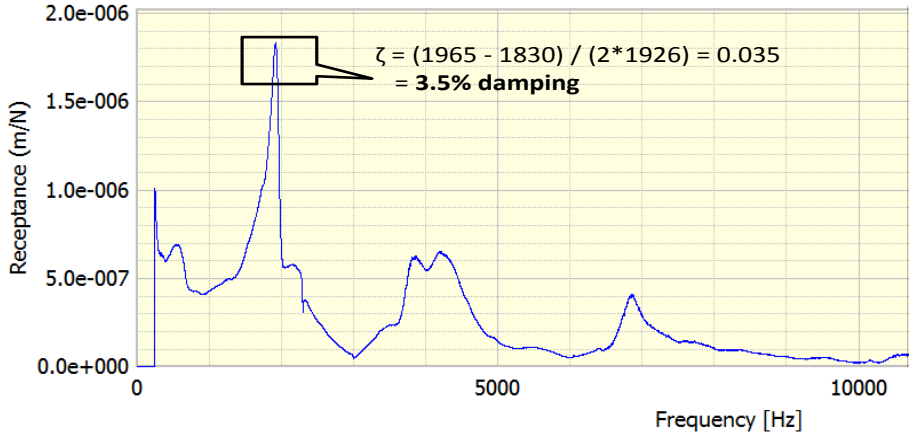

(b)

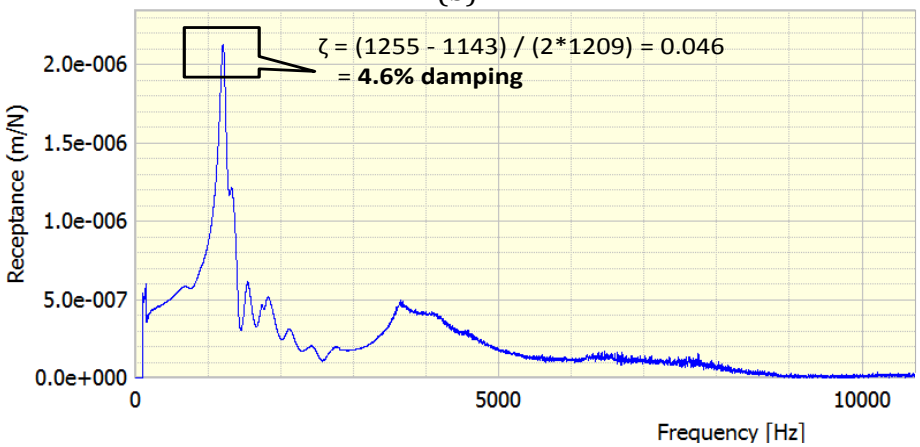

(c)

Figure 8-6 Dynamic responses acquired with impact hammer testing: (a) Undamped, (b) Viscoelastic surface damper (c) Torsion spring fixture

damping to the vibration by rotating about their torsional axis, but also induces shear forces in rubber causing viscoelastic damping to increase, schematically shown in Figure 8-7. The increase in damping can also be contributed to the fact that the force due to spring is distributed over wide

area (unlike tuned masses in surface damper) thereby resulting in more area of neoprene to undergo shear deformation.

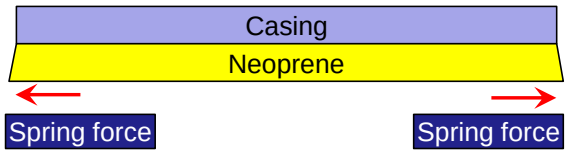

Figure 8-7 Concept of constrained layer damping

8.4 Dynamic response analysis in milling of casing with torsion spring fixture

8.4.1 Improvement in vibration reduction

Experiments were conducted on casing with the torsion spring fixture mounted in it, as shown in Figure 8-8. The experiments were carried out in sectors and data acquired using the data acquisition system, as explained in section 3.3.2.

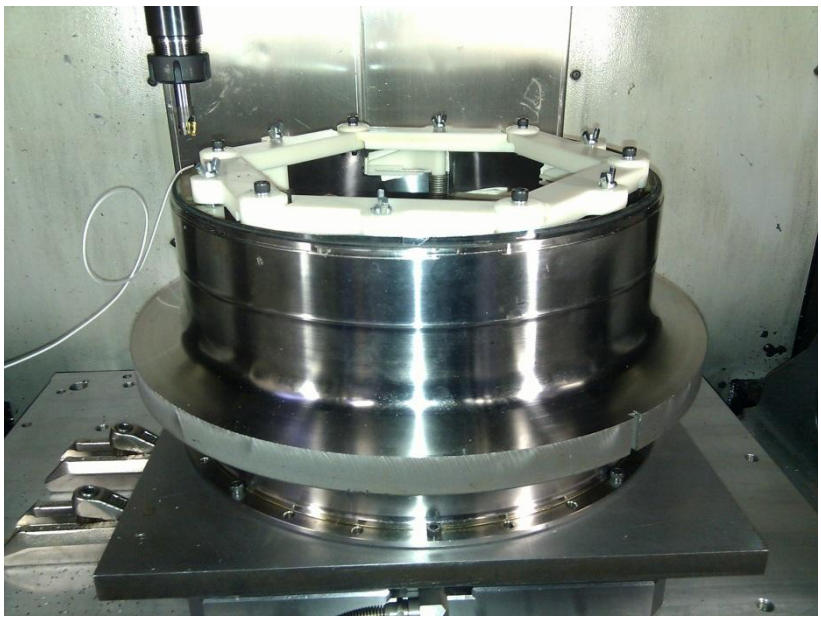

Figure 8-8 Experimental setup for casing with torsion spring fixture

Similar to that of tuned dampers and viscoelastic based surface damper, the proposed torsion spring fixture's effectiveness in vibration reduction is evaluated using root mean square value of the machining vibration signal. For the sake of comparison, experiments are conducted only at limited depth of cut parameters and the result for a_p=2mm, a_e=1mm is presented in Figure 8-9. As can be seen the reduction in vibration is nearly 8 times. When compared to that of viscoelastic surface damper result for same parameters, shown in Figure 7-15, this improvement is more than twice. This level of improvement cannot be singly attributed to 1% improvement in damping, as mentioned in previous section. The relative increase in inertia force exerted by springs over the tuned masses by 3 times is the main contributor. Also the stiffness contribution in torsion spring fixture increases due to higher anchoring force at springs thereby allowing the neoprene to stretch firmly in between springs. Thus, this fixture concept highlights the importance of improving the mass and stiffness of the fixture designs meant for reducing machining vibration in thin wall casings. In such situation forced vibrations are dominant where improvement of damping alone is of less significance.

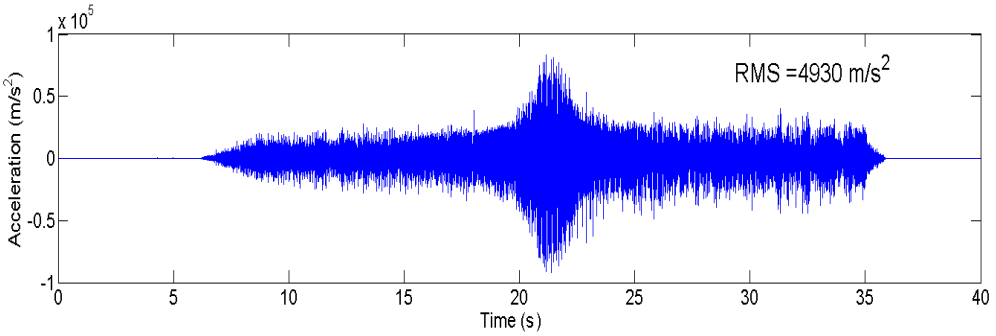

(a)

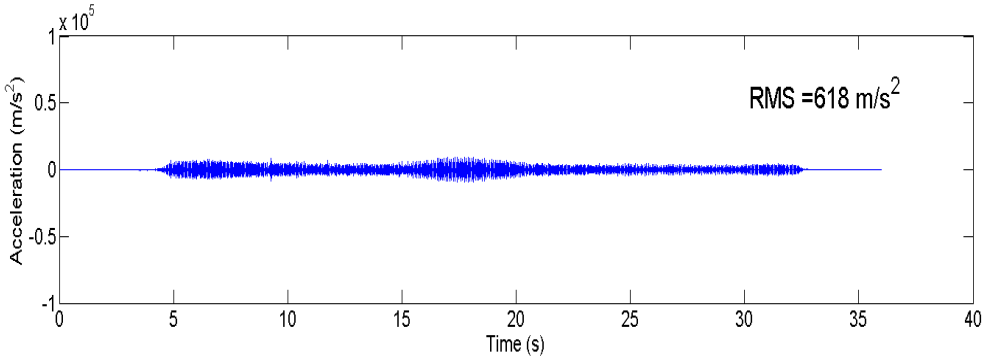

(b)

Figure 8-9 Machining acceleration signals of the casing: (a) undamped (b) with torsion spring fixture

8.4.2 Analysis of coupled interaction between tool and workpiece with torsion spring fixture

The dynamic coupled response interaction between tool and workpiece is evaluated on the machining vibration signal acquired. As explained in section 4.2, the vibration signal for one revolution of the tool is studied in time-frequency domain at equi-spaced sections. The time-frequency plot for the signal acquired with torsion spring fixture is shown in Figure 8-10. It can be noticed that all the workpiece modes are significantly damped and only tool torsional mode is present, though with reduced amplitude. The fact that there is no presence of tool bending mode indicates that there is no coupling of tool bending mode with the casing. This ensures that there will be no variation in thickness of machined thin wall. This

observation can be explained from the fact that, unlike in viscoelastic surface damper solution where tuned masses are locally mounted, the spring force is evenly spread wide across the casing periphery. Hence the casing will not behave like a cantilever in between two springs while at the same time offered improvement in stiffness and inertia due to applied spring force. This leads to exhibit behaviour of dynamically stiffened casing which offers coupling of torsional mode rather than tool bending mode.

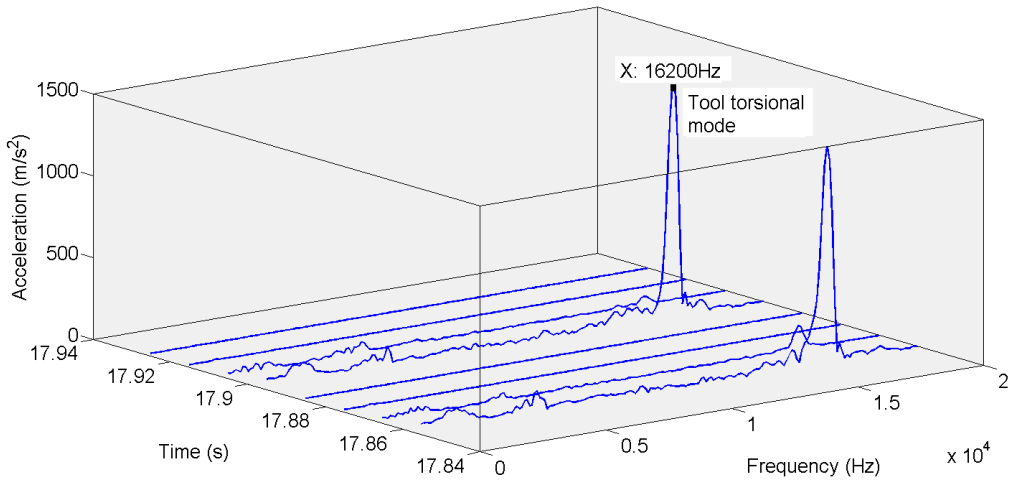

Figure 8-10 Time frequency analysis of acceleration signal acquired on casing with torsion spring fixture, a_p=2mm, a_e=1mm

8.5 Torsion spring fixture – variants

The torsion spring fixture concept discussed in section 8.2 can be used in multiple variants. For example instead of mounting the springs at the middle of connecting link as shown in Figure 8-4(a), they can be mounted at the corners so that they can be easily reconfigured for different diameter casings, as shown in Figure 8-11.

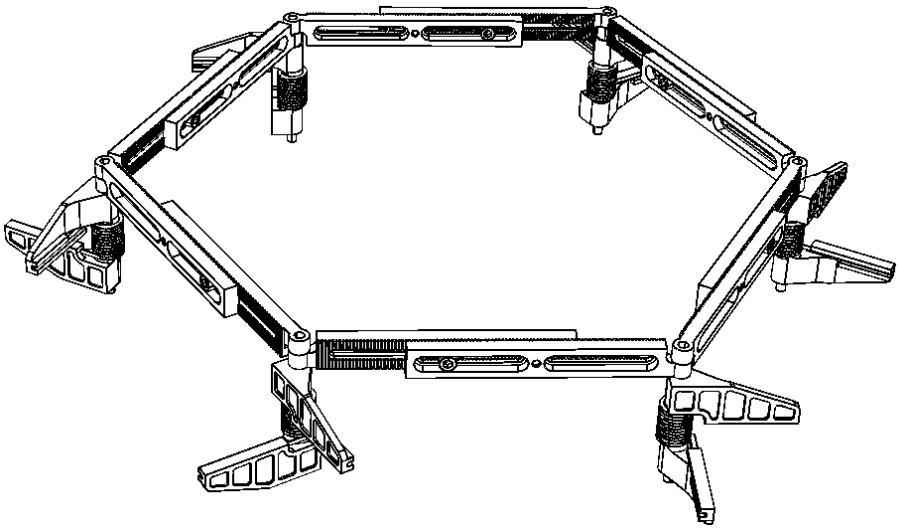

Figure 8-11 Torsion spring fixture with serrated and slotted expandable links and springs mounted at the corner of connecting links

Also using the same 270^{o} springs, the fixture can be designed to be mounted externally as shown in Figure 8-12(a) so that casings that need internal machining can be damped. Similarly the concept of using torsion springs for exerting force against the thin wall casing can be used for prismatic parts also, as shown in Figure 8-12(b).

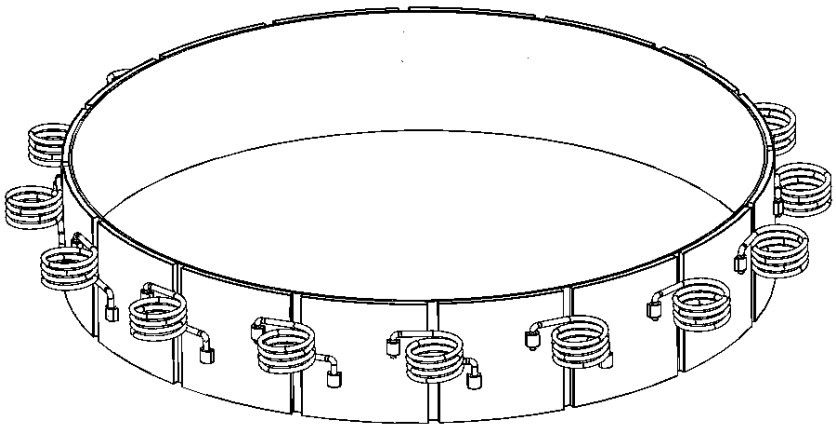

(a)

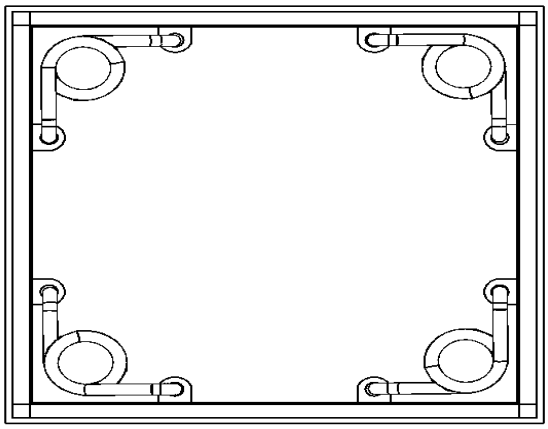

(b)

Figure 8-12 Configuration of torsion spring fixture for external mounting on casings (a) and for prismatic parts (b) – shown without connecting link

8.6 Conclusions

In this chapter a novel fixture design for minimising the vibrations in thin wall casings is proposed. The novelty of this fixture lies in the fact that it is self-actuating and hence does not require external clamps, levers, etc. This allows its easy installation. Moreover the fixture is very compact thereby providing access to the centre of casing. The fixture is completely reconfigurable for any diameter by changing the number of links and also can be used for external or internal clamping. The ability to choose different angles of torsion spring legs allows the concept to be adapted to

fixture any prismatic feature such as polygon. The design of such fixture is described in detail and dimensions of fixture and torsion spring are configured for the casing used in this research. Dynamic response tests with impact hammer showed about 65 times improvement in damping over undamped casing and about 1.3 times over viscoelastic based surface damper concept discussed in Chapter 7. This increase in damping was attributed to higher shear forces induced in the neoprene sheet due to higher spring forces – 3 times as compared to tuned masses in viscoelastic based surface damper. Milling experiments on casing showed a significant reduction of 8 times in RMS value of vibration signal. Such an increase cannot be explained only due to 1% increase in damping, especially in a forced vibration situation such as machining vibration. The increase in inertia force by 3 times and the corresponding increase in stiffness due to stretching of neoprene sheet between tighter anchoring springs is the main reason for such a reduction of vibration. Coupled dynamic response analysis of vibration signal showed presence of torsional mode of tool on casing and no major presence of tool bending mode. This is due to the distributed nature of inertia force due to spring legs rather than concentrated load such as tuned mass in surface damper. Workpiece modes are also totally damped with the installation of torsion spring fixture. Finally the possible variants of such fixture were discussed.

9 Final conclusions and future work

9.1 Conclusions

In this research, the solutions and the underlying scientific issues in minimising the machining vibrations in thin wall casings were studied. This work is driven by the requirement of minimising machining vibrations in finish machining of complex thin wall assemblies of jet engines. Being a complex assembly with internal parts and needing multiple machining operations in single set up, traditional fixturing solutions are difficult to implement. With this background, the aims and objectives of this research are stated in Chapter 1.

Chapter 2 presents an in-depth literature survey covering all aspects of thin wall machining: chatter prediction theories, machining simulation and strategies, fixturing solutions and their simulation, and damping solutions (passive and active). The research literature available till now focusses only on straight thin wall cantilever type structures, whose dynamic characteristics are different from those of thin wall casings. Moreover, surface damping solutions covering the whole area of the thin wall part being machined were not studied.

The research performed in this work initially studies the coupled dynamic interaction between tool and thin wall workpiece. Considering that the machining is dominated by forced vibrations due to tool impact, the knowledge of the combined dynamic response of the tool and workpiece is important in designing the damping solutions and also evaluating their

effectiveness. Three damping solutions were investigated in this research: (i) tuned mass dampers, (ii) viscoelastic based surface dampers (iii) an innovative reconfigurable fixture employing torsion springs.

Tuned mass dampers, which were successfully applied in other manufacturing applications such as machine tools and machining rigid blocks, were investigated for thin wall casings, presented in Chapter 6. The dampers were tuned for the workpiece fundamental mode as it is dominantly coupled with the workpiece in finish machining operations. The viscoelastic based surface damper, presented in Chapter 7, was designed to enhance not only damping, but also the mass and stiffness of the casing. The torsion spring fixture, presented in Chapter 8, was also designed to enhance mass, stiffness and damping of the casing but the inertia (mass) force was provided through springs. These three solutions were then studied based on following three aspects:

- Coupled dynamic response interaction between tool and workpiece
- Effectiveness in vibration minimisation evaluated through RMS
- Dynamic response prediction through FE analysis

The torsion spring fixture was investigated only as a proof-of-concept and hence no FE analysis was carried out. The key findings and novel contributions in each of these areas are summarised below.

9.1.1 Coupled dynamic response interaction between tool and workpiece

- When the machining vibration signal was analysed in the time-frequency domain, it was observed that the tool's modes couple

with the workpiece and this is shown as modulation of the cutting tooth harmonics near to the frequencies of the tool's modes. This is a novel finding and was experimentally verified with a range of machining tests.

- The kind of tool mode that couples depends on the dynamics of the workpiece – whether it is an open geometry (straight thin wall cantilever) or closed geometry (thin wall casing) structure. While the tool's bending mode couples when machining an open geometry structure, it is the tool's torsional mode which couples for closed geometry structures. This is due to the inherent stiffness of closed geometry structures that excites the tool's torsional mode.
- The extent of tool mode coupling was observed to depend on the depth of cut as well. At higher depths of cut, tool's torsional mode completely dominates the spectrum, whereas at lower depths of cut the workpiece fundamental mode also shows up along with tool's torsional mode. Hence, in finish machining operations both the workpiece fundamental mode and tool torsional mode are present in the spectrum.
- The coupled dynamic response was studied for different damping solutions proposed: tuned mass dampers, viscoelastic based surface damper and torsion spring fixture. It was shown that the 3D time-frequency plot generated for the machining vibration signal can be used as an indicator for defining damping effectiveness and also choosing an appropriate damping solution – by observing the extent of participation of the tool's bending mode.

As the tool's torsional mode couples with a thin wall casing, the presence of the tool bending mode in the machining spectrum indicates that a local deflection of the casing causing thickness variation, which is undesirable.

- When tuned mass dampers are mounted on the casing, the coupling of the tool's mode changed from torsional to bending in between two masses resulting in thickness variation. Hence, though tuned mass dampers are good at damping the targeted mode, they may not be successfully used in large surface area applications such as thin wall casings.
- When a viscoelastic surface based damper was mounted on the casing, the change in coupling was not as significant as that with the tuned mass dampers alone. Hence, there is a presence of both torsional and bending modes of the tool in the machining spectrum. This is due to the stiffness offered by the stretched neoprene in between the two masses.
- With the torsion spring fixture, no noticeable change in coupling was observed. Only the tool torsional mode was distinctly present after damping of all the workpiece modes. This can be attributed to the fact that the spring force is distributed over a wide surface area of the casing, and also a higher spring force (3 times) than that of the tuned mass forces resulted in better stretching of the neoprene sheet.

9.1.2 Effectiveness in minimisation of vibration

The three solutions that were investigated are evaluated for their effectiveness in minimising the machining vibrations. This evaluation was done based on the RMS content of the vibration signal.

- With tuned mass dampers, the vibration reduction in terms of RMS value is 2.29 times with reference to the undamped casing, when machining at a_p = 2mm and a_e = 1mm. At a lower depth of cut of a_p=0.5mm and a_e = 0.5mm, this improvement was noticed to be about 4 times and could be due to the lower excitation levels of the tool's forced vibration and also the dominant presence of the workpiece fundamental for which the damper masses were tuned.
- With a viscoelastic based surface damper, the reduction in vibration was 3.76 times with reference to the undamped casing at a_p = 2mm and a_e = 1mm. Such an increase was possible due to the enhancement of stiffness due to the stretching of neoprene in between the masses.
- With a torsion spring fixture, the reduction in vibration was 8 times against an undamped casing at a_p = 2mm and a_e = 1mm. This significant increase in improvement comes from the fact that the inertia forces are 3 times more than the tuned masses can offer and also the corresponding increase in stiffness due to stiffer holding of the neoprene sheet with springs. Thus this fixture demonstrates the necessity of improving the mass and stiffness of the casing in

forced vibration situations such as machining. The influence of damping is very minor in such non-resonant conditions.

9.1.3 Dynamic response prediction through FE

The FE modelling was taken up in this research with the objective of demonstrating successful modelling of damping and the ability to predict the dynamic response. Such a modelling process is not reported for any manufacturing applications earlier, for any of the damping solutions – either passive or active. Hence, the work done in this research opens up the work in this direction which has the scope of integrating into the computer aided fixture designing process. The undamped casing was modelled in FE and validated through experimental modal analysis, and the predicted frequencies are within 2% of the experimentally measured ones. Frequency response curves were obtained through harmonic analysis and compared with experimentally measured FRFs, and reasonable matching was observed thereby validating the damping factor assumed in the FE model.

The frequencies for the casing with tuned mass dampers and the viscoelastic based surface damper are predicted with maximum error of 8% and 9.5% respectively. This error was considered acceptable considering that the updating of the FE model was not performed. The predicted dynamic responses also matched satisfactorily, indicating the ability to model the damping due to the viscoelastic tape and neoprene sheet with reasonable accuracy. Hence the developed FE model can predict the damped dynamic response with the proposed damping

solution in place. Moreover, the elastic strain energy map produced during modal extraction proved the concept of stretching of neoprene sheet in between the masses, thus enhancing the stiffness of the casing during vibration.

9.2 Future work

From the research carried out and reported in this thesis, various possible future avenues of research, derived from this work, are suggested as follows:

- One of the important future directions of this work can be carried out in predicting the coupling of tool-work dynamic interaction through FE analysis or analytically. The FE model developed in this work has the capability to predict the dynamic response of the workpiece alone. If the tool is modelled and the combined dynamic response is predicted, then the actual dynamics of machining can be simulated. The tool's bending and torsional mode appearance can then be seen clearly. This also paves way for evaluating the effectiveness of different damping solutions.
- The FE model used in this work is not updated. Updating a FE model using experimental modal data improves the accuracy of prediction of natural frequencies and also the dynamic response prediction (FRF curves). However, there is no commercial software that can do the updating of the FE model if the structure has non-proportional damping. This is still of research interest and hence has to be addressed accordingly.

- The torsion spring fixture concept was validated just as a proof-of-concept and hence FE analysis was not performed to predict the dynamic response. This can be taken up as future work to predict the damped dynamic response in the presence of such fixtures with torsion springs.
- Parametric studies can be taken up to find out the effects of variations in the tuned masses and thickness of neoprene sheet. Though these effects can be intuitively predicted, a detailed parametric study results in achieving optimum values for these parameters.

10 References

[1] Airbus, "Navigating the future - Global Market Forecast 2012-2031," p. 164, 2012.

[2] "Rolls-Royce plc group 2010 full year results." [Online]. Available: http://www.rolls-royce.com/news/press_releases/2011/090211_2010_full_year_results.jsp. [Accessed: 12-Mar-2013].

[3] S. D. Antolovich and A. Saxena, "Fatigue fracture of 1040 steel splined shaft," *Fatigue failures, Failure analysis and prevention, ASM Handbook*, 1986. [Online]. Available: http://products.asminternational.org/fach/data/fullDisplay.do?database=faco&record=143&trim=false. [Accessed: 26-Apr-2013].

[4] NTSB, "Accident report of an agricultural airplane Ayres S2R-T34," 1997. [Online]. Available: http://www.ntsb.gov/aviationquery/brief2.aspx?ev_id=20001208X08110&ntsbno=FTW97FA220&akey=1. [Accessed: 26-Apr-2013].

[5] W. D. Feist, F. Niklasson, and K. M. Fox, "The Influence of Manufacturing Anomalies on Fatigue Performance of Critical Rotating Parts in the Aero-Engine."

[6] G. Quintana and J. Ciurana, "Chatter in machining processes: A review," *Int. J. Mach. Tools Manuf.*, vol. 51, no. 5, pp. 363–376, May 2011.

[7] S. A. Tobias, *Machine-Tool Vibration*, 1st ed. Blackie & Son Ltd, 1965, p. 351.

[8] "CutPro machining process simulation software." [Online]. Available: http://www.malinc.com/. [Accessed: 14-May-2013].

[9] "MetalMax - Dynamic machine tool characterisation." [Online]. Available: http://www.mfg-labs.com/. [Accessed: 14-May-2013].

[10] S. A. Tobias and W. Fishwick, "Theory of regenerative machine tool chatter," *Eng. London*, vol. 205, pp. 199–203, 1958.

[11] J. Tlusty and M. Polacek, "The stability of machine tools against self-excited vibrations in machining," *Int. Res. Prod. Eng.*, pp. 465–474, 1963.

[12] R. Sridhar, R. E. Hohn, and G. W. Long, “A stability algorithm for the general milling process,” *Trans. ASME J. Eng. Ind.*, vol. 90, pp. 330–334, 1968.

[13] I. Minis, T. Yanushevsky, R. Tembo, and R. Hocken, “Analysis of linear and non-linear chatter in milling,” *Ann. CIRP*, vol. 39, pp. 459–462, 1990.

[14] I. Minis and T. Yanushevsky, “A new theoretical approach for the prediction of machine tool chatter in milling,” *Trans. ASME J. Eng. Ind.*, vol. 115, pp. 1–8, 1993.

[15] E. Budak, “Mechanics and dynamics of milling thin walled structures,” University of British Columbia, 1994.

[16] E. Budak and Y. Altintas, “Analytical prediction of chatter stability in milling - Part I and II,” *J. Dyn. Syst. Meas. Control*, vol. 120, no. 1, pp. 22–36, 1998.

[17] U. Bravo, O. Altuzarra, L. N. Lopez De Lacalle, J. A. Sanchez, and F. J. Campa, “Stability limits of milling considering the flexibility of the workpiece and the machine,” *Int. J. Mach. Tools Manuf.*, vol. 45, no. 15, pp. 1669–1680, 2005.

[18] T. L. Schmitz, T. J. Burns, J. C. Ziegert, B. Dutterer, and W. R. Winfough, “Tool Length-Dependent Stability Surfaces,” *Mach. Sci. Technol.*, vol. 8, no. 3, pp. 377–397, Oct. 2004.

[19] J. Y. Chang, G. J. Lai, and M. F. Chen, “A study on the chatter characteristics of the thin wall cylindrical workpiece,” *Int. J. Mach. Tools Manuf.*, vol. 34, no. 4, pp. 489–498, 1994.

[20] G. J. Lai and J. Y. Chang, “Stability analysis of chatter vibration for a thin-wall cylindrical workpiece,” *Int. J. Mach. Tools Manuf.*, vol. 35, no. 3, pp. 431–444, 1995.

[21] K. Mehdi, J.-F. Rigal, and D. Play, “Dynamic Behavior of a Thin-Walled Cylindrical Workpiece During the Turning Process, Part 1: Cutting Process Simulation,” *J. Manuf. Sci. Eng.*, vol. 124, no. 3, pp. 562–568, 2002.

[22] K. Mehdi and D. Play, “Dynamic Behavior of a Thin-Walled Cylindrical Workpiece During the Turning Process , Part 2 : Experimental Approach and,” vol. 124, no. August, pp. 569–580, 2002.

[23] W. A. Kline and R. E. Devor, “Effect of runout on cutting geometry and forces in end milling,” *Int. J. Mach. Tool Des. Res.*, vol. 23, no. 2–3, pp. 123–140, 1983.

[24] E. Budak and Y. Altintas, “Modeling and avoidance of static form errors in peripheral milling of plates,” *Int. J. Mach. Tools Manuf.*, vol. 35, no. 3, pp. 459–476, 1995.

[25] E. M. Lim and C. H. Menq, “Prediction of dimensional error for sculptured surface productions using the ball-end milling process. Part 2-Surface generation model and experimental verification,” *Int. J. Mach. Tools Manuf.*, vol. 35, no. 8, pp. 1171–1185, 1995.

[26] H. Y. Feng and C. H. Menq, “Prediction of cutting forces in the ball-end milling proccess. II - Cut geometry analysis and model verification,” *Int. J. Mach. Tools Manuf.*, vol. 34, no. 5, pp. 711–719, 1994.

[27] H. Ning, W. Zhigang, J. Chengyu, and Z. Bing, “Finite element method analysis and control stratagem for machining deformation of thin-walled components,” *J. Mater. Process. Technol.*, vol. 139, no. 1–3, pp. 332–336, Aug. 2003.

[28] S. Herranz, F. J. Campa, L. N. L. de Lacalle, a Rivero, a Lamikiz, E. Ukar, J. a Sánchez, and U. Bravo, “The milling of airframe components with low rigidity: a general approach to avoid static and dynamic problems,” *Proc. Inst. Mech. Eng. Part B J. Eng. Manuf.*, vol. 219, no. 11, pp. 789–801, Apr. 2005.

[29] S. Ratchev, “Force and deflection modelling in milling of low-rigidity complex parts,” *J. Mater. Process. Technol.*, vol. 143–144, pp. 796–801, Dec. 2003.

[30] S. Ratchev, S. Liu, and a Becker, “Error compensation strategy in milling flexible thin-wall parts,” *J. Mater. Process. Technol.*, vol. 162–163, pp. 673–681, May 2005.

[31] S. Ratchev, S. Liu, W. Huang, and A. a. Becker, “Machining simulation and system integration combining FE analysis and cutting mechanics modelling,” *Int. J. Adv. Manuf. Technol.*, vol. 35, no. 1–2, pp. 55–65, Aug. 2007.

[32] M. Wan, W. Zhang, G. Qin, and Z. Wang, “Strategies for error prediction and error control in peripheral milling of thin-walled workpiece,” *Int. J. Mach. Tools Manuf.*, vol. 48, no. 12–13, pp. 1366–1374, Oct. 2008.

[33] RINGSPANN UK LTD, “RINGSPANN idea for precision clamping of cylindrical parts.” [Online]. Available: http://www.ringspann.co.uk/en/Products/Precision-Clamping-Chucks/Technology/The-RINGSPANN-Idea__755/?itid=755. [Accessed: 01-Apr-2013].

[34] Z. Geng, “Adaptive design of fixture for thin walled shell cylindrical components,” US2010/0164187 A12010.

[35] Y. Wang, X. Jainfan, K. Venkata, and W. Zhigang, “Advanced reconfigurable modular fixture design for casing family.” [Online]. Available: http://www.nottingham.ac.uk/nimrc/documents/pdfsanddocs/castingfixture.pdf. [Accessed: 02-Apr-2013].

[36] A. William, “Fluid actuated workholder with a collet driven by a soft and thin bladder,” US2010/0253015 A12010.

[37] M. Daimon, T. Yoshida, N. Kojima, H. Yamamoto, and T. Hoshi, “Study for designing fixtures considering dynamics of thin -walled plate- and box-like workpieces,” *CIRP Ann. - Manuf. Technol.*, vol. 34, no. 1, pp. 319–322, 1985.

[38] J. H. Yeh and F. W. Liou, “Contact condition modelling for machining fixture setup processes,” *Int. J. Mach. Tools Manuf.*, vol. 39, no. 5, pp. 787–803, May 1999.

[39] B. Li and S. N. Melkote, “Optimal Fixture Design Accounting for the Effect of Workpiece Dynamics,” *Int. J. Adv. Manuf. Technol.*, vol. 18, no. 10, pp. 701–707, Nov. 2001.

[40] E. Y. T. Tan, a. S. Kumar, J. Y. H. Fuh, and a. Y. C. Nee, “Modeling, Analysis, and Verification of Optimal Fixturing Design,” *IEEE Trans. Autom. Sci. Eng.*, vol. 1, no. 2, pp. 121–132, Oct. 2004.

[41] S. Satyanarayana and S. N. Melkote, “Finite element modeling of fixture-workpiece contacts: single contact modeling and experimental verification,” *Int. J. Mach. Tools Manuf.*, vol. 44, no. 9, pp. 903–913, Jul. 2004.

[42] S. Ratchev, K. Phuah, G. Lammel, and W. Huang, “An experimental investigation of fixture–workpiece contact behaviour for the dynamic simulation of complex fixture–workpiece systems,” *J. Mater. Process. Technol.*, vol. 164–165, pp. 1597–1606, May 2005.

[43] S. Liu, L. Zheng, Z. H. Zhang, and D. H. Wen, “Optimal fixture design in peripheral milling of thin-walled workpiece,” *Int. J. Adv. Manuf. Technol.*, vol. 28, no. 7–8, pp. 653–658, May 2005.

[44] I. Boyle, Y. Rong, and D. C. Brown, “A review and analysis of current computer-aided fixture design approaches,” *Robot. Comput. Integr. Manuf.*, vol. 27, no. 1, pp. 1–12, Feb. 2011.

[45] H. Wang, Y. (Kevin) Rong, H. Li, and P. Shaun, “Computer aided fixture design: Recent research and trends,” *Comput. Des.*, vol. 42, no. 12, pp. 1085–1094, Dec. 2010.

[46] R. Hahn, “Active dampers for machine tools,” *Trans. ASME*, vol. 73, p. 331, 1951.

[47] Y. . Tarng, J. . Kao, and E. . Lee, “Chatter suppression in turning operations with a tuned vibration absorber,” *J. Mater. Process. Technol.*, vol. 105, no. 1–2, pp. 55–60, Sep. 2000.

[48] E. C. Lee, C. Y. Nian, and Y. S. Tarng, “Design of a dynamic vibration absorber against vibrations in turning operations,” *J. Mater. Process. Technol.*, vol. 108, pp. 278–285, 2001.

[49] T. Alwarsamy, P. Thangavel, and V. Selladurai, “Reduction of machining vibration by use of rubber layered laminates between tool holder and insert,” *Mach. Sci. Technol.*, vol. 11, pp. 135–143, 2007.

[50] N. E. Shurtliff, “Universally damped tool holder,” 35822261971.

[51] R. W. New, “Boring bars,” 40614381977.

[52] N. E. Shurtliff, “Damped boring bar and tool holder,” 46167381986.

[53] Sandvik, “Silent Tool - Damped boring bar.” [Online]. Available: www.sandvik.coromant.com. [Accessed: 01-May-2013].

[54] H. Moradi, F. Bakhtiari-nejad, and M. R. Movahhedy, “Tuneable vibration absorber design to suppress vibrations : An application in boring manufacturing process,” *J. Sound Vib.*, vol. 318, pp. 93–108, 2008.

[55] H. Moradi, M. R. Movahhedy, and G. Vossoughi, “Tuneable vibration absorber for improving milling stability with tool wear and process damping effects,” *Mech. Mach. theory*, vol. 52, pp. 59–77, 2012.

[56] J. P. Den Hartog, *Mechanical Vibrations*, 4th ed. New York: Dover Publications, 1985.

[57] N. D. Sims, “Vibration absorbers for chatter suppression: A new analytical tuning methodology,” *J. Sound Vib.*, vol. 301, no. 3–5, pp. 592–607, Apr. 2007.

[58] Y. Yiqing, L. Qiang, and W. Min, “Optimization of the Tuned Mass Damper for Chatter Suppression in Turning,” *Chinese J. Mech. Eng.*, 2010.

[59] Y. Yang, J. Munoa, and Y. Altintas, “Optimization of multiple tuned mass dampers to suppress machine tool chatter,” *Int. J. Mach. Tools Manuf.*, vol. 50, pp. 834–842, 2010.

[60] Y. Zhang and N. D. Sims, “Milling workpiece chatter avoidance using piezoelectric active damping: a feasibility study,” *Smart Mater. Struct.*, vol. 14, no. 6, pp. N65–N70, Dec. 2005.

[61] N. D. Sims, A. Amarasinghe, and K. Ridgway, “Particle dampers for workpiece chatter mitigation,” in *IMECE2005: ASME International Mechanical Engineering Congress and Exposition*, 2005, pp. 1–8.

[62] A. Rashid and C. M. Nicolescu, “Design and implementation of tuned viscoelastic dampers for vibration control in milling,” *Int. J. Mach. Tools Manuf.*, vol. 48, no. 9, pp. 1036–1053, Jul. 2008.

[63] A. Rashid and C. M. Nicolescu, “Active vibration control in palletised workholding system for milling,” *Int. J. Mach. Tools Manuf.*, vol. 46, pp. 1626–1636, 2006.

[64] M. A. Davies and B. Balachandran, “Impact Dynamics in Milling of Thin-Walled Structures,” *Nonlinear Dyn.*, vol. 22, pp. 375–392, 2000.

[65] R. Teti, K. Jemielniak, G. O’Donnell, and D. Dornfeld, “Advanced monitoring of machining operations,” *CIRP Ann. - Manuf. Technol.*, vol. 59, no. 2, pp. 717–739, 2010.

[66] T. Segreto, a. Simeone, and R. Teti, “Multiple Sensor Monitoring in Nickel Alloy Turning for Tool Wear Assessment via Sensor Fusion,” *Procedia CIRP*, vol. 12, no. Fig 2, pp. 85–90, Jan. 2013.

[67] a. Simeone, T. Segreto, and R. Teti, “Residual Stress Condition Monitoring via Sensor Fusion in Turning of Inconel 718,” *Procedia CIRP*, vol. 12, pp. 67–72, Jan. 2013.

[68] I. Marinescu and D. Axinte, “A time–frequency acoustic emission-based monitoring technique to identify workpiece surface malfunctions in milling with multiple teeth cutting simultaneously,” *Int. J. Mach. Tools Manuf.*, vol. 49, no. 1, pp. 53–65, Jan. 2009.

[69] T. Segreto, a. Simeone, and R. Teti, “Chip form Classification in Carbon Steel Turning through Cutting Force Measurement and Principal Component Analysis,” *Procedia CIRP*, vol. 2, pp. 49–54, Jan. 2012.

[70] Sandvik, “Shoulder milling of thin deflecting walls.” [Online]. Available: http://www.sandvik.coromant.com/en-gb/knowledge/milling/application_overview/shoulder_milling/sho

ulder_milling_thin_walls/pages/default.aspx. [Accessed: 01-Jul-2013].

[71] "MatWeb Material Property Data." [Online]. Available: www.matweb.com.

[72] *Abaqus Analysis User Manual Vol.2*. .

[73] A. Leissa, *Vibration of shells*, 2nd ed. Acoustical society of America, 1993, p. 428.

[74] D. J. Ewins, *Modal testing: Theory, Practice and Application*, 2nd ed. Research Studies Press Ltd, 2000, p. 563.

[75] *LMS Test.Lab Modal Analysis Theory manual*. .

[76] P. Avitabile, "Tutorial notes: Structural dynamics and experimental modal analysis." [Online]. Available: http://higheredbcs.wiley.com/legacy/college/craig/0471430447/pdf/Tutorial_Notes.pdf. [Accessed: 20-Sep-2013].

[77] A. W. Phillips and R. J. Allemang, "Data Presentation Schemes for Selection and Identification of Modal Parameters λ," in *IMAC XXIII Proceedings*, 2005.

[78] B. Peeters, G. Lowet, H. Van Der Auweraer, J. Leuridan, and L. M. S. International, "A New Procedure for Modal Parameter Estimation," *Sound and Vibration*, no. January, pp. 24–28, Jan-2004.

[79] "LMS Test.Lab Modal Analysis." [Online]. Available: http://www.lmsintl.com/testing/structures/modal-analysis. [Accessed: 20-Sep-2013].

[80] "ME'scopeVES." [Online]. Available: http://www.vibetech.com/go.cfm/en-us/content/mescope. [Accessed: 20-Sep-2013].

[81] P. Avitabile, "Modal Space : Back to basics." [Online]. Available: http://sdasl.uml.edu/umlspace/mspace.html. [Accessed: 20-Sep-2013].

[82] P. W. Spence and C. J. Kenchington, *The role of damping in finite element analysis*. NAFEMS, 1993.

[83] C. M. A. Vasques, R. A. S. Moreira, and J. D. Rodrigues, "Viscoelastic Damping Technologies – Part I : Modeling and Finite Element Implementation ⋆," *Mech. Eng.*, vol. 1, no. 1986, pp. 76–95, 2010.

[84] S. O. Oyadiji, *How to analyse the static and dynamic response of viscoelastic components*. NAFEMS, 2004.

[85] C. M. A. Vasques, R. A. S. Moreira, and J. D. Rodrigues, "Viscoelastic Damping Technologies – Part II : Experimental Identification Procedure and," vol. 1, pp. 96–110, 2010.

[86] A. Rashid, "On passive and active control of machining system dynamics: Analysis and implementation," KTH, Stockholm, Sweden, 2005.

[87] 3M, "Polymers useful for damping: Technical bulletin," 2003.

[88] 3M, "Viscoelastic damping polymers: Technical bulletin," 2012.

[89] M. Potvin, "Comparison of time-domain finite element modelling of viscoelastic structures using an efficient fractional Voigt-Kelvin Model or Prony Series," McGill University, 2001.

[90] R. Moreira and J. D. Rodrigues, "Constrained damping layer treatments: Finite Element Modeling," *J. Vib. Control*, vol. 10, pp. 575–595, 2004.

[91] B. . Nakra, R. Singh, K. Gupta, and T. . Kundra, Eds., *Emerging trends in vibration and noise engineering*. Allied Publishers Ltd, 1996.

[92] D. Jones, *Handbook of viscoelastic vibration damping*, 1st ed. John Wiley & Sons, Inc., 2001, p. 391.

[93] R. M. Lin and J. Zhu, "Model updating of damped structures using FRF data," *Mech. Syst. Signal Process.*, vol. 20, no. 8, pp. 2200–2218, Nov. 2006.

[94] M. Link, T. Boettcher, and L. Zhang, "Computational Model Updating of Structures with Non-Proportional Damping," in *IMAC-XXIV: Conference & Exposition on Structural Dynamics - Looking Forward: Technologies for IMAC*, 2006, no. 1.

[95] R. Teti, T. Segreto, and R. Neugebauer, "Machining process acceptability for high performance materials by multiple sensor monitoring," in *International Chemnitz Manufacturing Colloquium - ICMC 2010*, 2010.

[96] B. C. Nakra, "Structural dynamic modification using additive damping," *Sadhana*, vol. 25 (3), no. June, pp. 277–289, 2000.

[97] E. Budak, a. Ertürk, and H. N. Özgüven, "A Modeling Approach for Analysis and Improvement of Spindle-Holder-Tool Assembly

Dynamics," *CIRP Ann. - Manuf. Technol.*, vol. 55, no. 1, pp. 369–372, Jan. 2006.

[98] DuPont, "Types of Neoprene," 2010.

[99] Theplasticshop.co.uk, "Rubber Selection Quick Reference Guide."

[100] "RS Components and allied Electronics." [Online]. Available: http://uk.rs-online.com/web/. [Accessed: 17-Oct-2013].

[101] "Torsion springs." [Online]. Available: www.assocspring.co.uk. [Accessed: 10-Oct-2013].

[102] PlanetSpring, "Torsion Spring Calculator." [Online]. Available: http://www.planetspring.com/pages/torsion-spring-calculator-torsion-spring-calculation.php?id=torsion. [Accessed: 12-Oct-2013].